

See discussions, stats, and author profiles for this publication at: <https://www.researchgate.net/publication/256325701>

Integrated Approach for the Assessment and Development of Groundwater Resources in Arid Lands: Applications in the Quetta Valley, Pakistan

THESIS · DECEMBER 2010

READS

53

1 AUTHOR:



Jay Sagin

Nazarbayev University

27 PUBLICATIONS 54 CITATIONS

SEE PROFILE

Integrated Approach for the Assessment
and Development of Groundwater
Resources in Arid Lands: Applications in
the Quetta Valley, Pakistan

Western Michigan University

Department of Geosciences

Kalamazoo, MI, 49008

July 21, 2010

Zhanay (Jay Sagin) Sagintayev

INTEGRATED APPROACH FOR THE ASSESSMENT AND DEVELOPMENT
OF GROUNDWATER RESOURCES IN ARID LANDS: APPLICATIONS IN
THE QUETTA VALLEY, PAKISTAN

Zhanay (Jay Sagin) Sagintayev, Ph.D.

Western Michigan University, 2010

The lack of adequate field measurements (e.g., precipitation and stream flow) and difficulty in obtaining them often hampers the construction and calibration of rainfall-runoff models over many of the world's watersheds, leaving key elements of the hydrologic cycle unconstrained. We adopted methodologies that rely heavily on readily available remote sensing datasets as viable alternatives and useful tools for assessing, managing, and modeling the water resources of such remote and inadequately gauged regions. The Soil and Water Assessment Tool was selected for continuous (1998–2005) rainfall-runoff modeling of the northeast part of the Pishin Lora basin (NEPL), a politically unstable area that lacks adequate rain gauge and stream flow data. To account for the paucity of rain gauge and stream flow gauge data, input to the model included satellite-based Tropical Rainfall Measuring Mission TRMM precipitation data. Modeled runoff was calibrated against satellite-based observations including: (1) monthly estimates of the water volumes impounded by the Khushdil Khan (latitude 30° 40'N, longitude 67° 40'E) and the Kara Lora (latitude 30° 34'N, longitude 66° 52'E) reservoirs, and (2) inferred wet versus dry conditions in streams across the NEPL throughout this period. Calibrations were also conducted against observed flow reported from the Burj

Aziz Khan station at the NEPL outlet (latitude 30°20'N; longitude 66°35'E). Model simulations indicate that (1) average annual precipitation (1998–2005), surface runoff, and net recharge are $1,300 \times 10^6 \text{ m}^3$, $148 \times 10^6 \text{ m}^3$, and $361 \times 10^6 \text{ m}^3$, respectively; (2) within the NEPL watershed, precipitation and runoff are high for the northeast (precipitation: 194 mm/year; runoff: $38 \times 10^6 \text{ m}^3/\text{year}$) and northwest (134 mm/year; $26 \times 10^6 \text{ m}^3/\text{y}$) basins compared to the southern basin (124 mm/year; $8 \times 10^6 \text{ m}^3/\text{year}$); and (3) construction of delay action dams in the northeast and northwest basins of the NEPL could increase recharge from $361 \times 10^6 \text{ m}^3/\text{year}$ up to $432 \times 10^6 \text{ m}^3/\text{year}$ and achieve sustainable extraction. The adopted methodologies are not a substitute for traditional approaches that require extensive field datasets, but they could provide first-order estimates for rainfall, runoff, and recharge in the arid and semi-arid parts of the world that are inaccessible and/or lack adequate coverage with stream flow and precipitation data.

INTEGRATED APPROACH FOR THE ASSESSMENT AND DEVELOPMENT
OF GROUNDWATER RESOURCES IN ARID LANDS: POTENTIAL
APPLICATIONS IN THE QUETTA VALLEY, PAKISTAN

by

Zhanay (Jay Sagin) Sagintayev

A Dissertation
Submitted to the
Faculty of The Graduate College
in partial fulfillment of the
requirements for the
Degree of Doctor of Philosophy
Department of Geosciences

Advisors:

Mohamed Sultan, Ph.D., Duane Hampton, Ph.D., and R.V. Krishnamurthy, Ph.D.
from Department of Geosciences, WMU:, and
Eugene Yan, Ph.D. from Argonne National Laboratory, Environmental Research
Division

Western Michigan University
Kalamazoo, Michigan
May 2010

Copyright by
Zhanay (Jay Sagin) Sagintayev
2010

ACKNOWLEDGMENTS

My great appreciation to my committee members: Drs. Mohamed Sultan, Duane Hampton, and R.V. Krishnamurthy, from the Department of Geosciences at WMU, and Dr. Eugene Yan from Argonne National Laboratory.

I am very thankful also to the colleagues and collaborators of the Remote Sensing Facility laboratory: Dr. Adam Milewski, Dr. Richard Becker, Peter Marsala, Abdou Aly Abou El-Magd, Benjamin Welton, Rajesh Balekai, Dr. Abdul Salam Khan, Dr. Khalid Mahmood, Dr. Shurab Khan, Dr. Farouk Soliman, Talal Al-Harbi, Dee Becker, Jinal Kothari, Mohamed El-Sayed Ahmed, and Swaroop Jayaprakash.

I would have not been able to complete my work without the support, patience, and understanding from my wife and partner, Elmira, who was very supportive and put up with my busy schedule, took care of our small kids, Adam and Tomiris, and kept on nourishing our relationship.

This research is funded by the U.S. Agency for International Department in cooperation with the Higher Education Commission of Pakistan, and by the Graduate College of Western Michigan University which provided Dissertation Completion Fellowship.

Zhanay (Jay Sagin) Sagintayev

TABLE OF CONTENTS

ACKNOWLEDGMENTS	ii
LIST OF TABLES	v
LIST OF FIGURES	vi
LIST OF NOTATIONS AND ABBREVIATIONS	vii
CHAPTER	
1. INTRODUCTION	1
1.1 Introduction and Problem Statement	1
1.2 The Research Objectives	5
1.3 Methodology.....	5
2. LITERATURE REVIEW AND SITE DESCRIPTION	7
2.1 Previous Studies	7
2.2 Geology and Hydrology of NEPL	10
2.3 Type of Aquifers.....	18
2.4 Temperature, Precipitation and Stream flow in NEPL.....	18
2.5 Delay Action/Storage Dams	19
3. MODEL CONSTRUCTION AND CALIBRATION	22
3.1 Model Framework	22
3.2 Data Collection	22
3.2.1 Data Processing	23
3.2.2 Digital Elevation: Watershed, Stream Delineation,	
and Reservoir Storage	25
3.2.3 Climate Datasets: Temporal and Spatial Precipitation over Watersheds	27
3.2.4 Land Use and Soil types.....	29
3.3 Model Calibration and Validation	30
3.3.1 Coarse Adjustment and Calibration of Snow Pack/Melt Parameters	33
3.3.2 Delay Action/Storage Dams and Model Calibration Against Reservoir	
Volume and Flow Versus no Flow Conditions in Ephemeral Stream.....	34

Table of Contents—Continued

CHAPTER	
3.3.3 Model Calibration against Stream Flow Data	37
3.3.4 Calibration Criteria and Model Evaluation.....	37
4. DISCUSSIONS.....	38
4.1 Novelty of Model	38
4.2 Model Applications	43
5. CONCLUSIONS.....	49
6. FURTHER RESEARCH	51
6.1 Potential Reservoir Types.....	51
6.2 Climate Changes.....	61
REFERENCES	62
APPENDICES	67
A. Hydrologic Modeling Tutorial.....	67
B. Calibration of Hydrologic Model	104
C. Using ACCESS and EXCEL for Data Management and Data Review	110

LIST OF TABLES

Table 1: Lithostratigraphy of NEPL	11
Table 2: Geologic and Hydrogeologic Data for NEPL Used in Hydrological Modeling.	17
Table 3: Significant Calibration Parameters	32
Table 4: Modeled Average Annual Values.....	44
Table 5: Scenarios.....	45

LIST OF FIGURES

Figure 1: Location, Extent and Elevations for the Pishin Lora Basin.	3
Figure 2: E-W Trending Cross Sections A-A`	4
Figure 3: Distribution of Land Use and Soil Types.....	20
Figure 4: Annual Precipitation Extracted from 3-hourly TRMM Precipitation Data.....	21
Figure 5: Distribution of Major (NE, NW, and Southern) Basins	26
Figure 6: Temperature and Precipitation Comparison.....	28
Figure 7 Time Series Calibration Results	35
Figure 8: Precipitation and Elevation for TRMM Station	40
Figure 9: Temporal Landsat Band 5 Images.....	42
Figure 10: Lithologic and Structural Features from Remote Sensing Data.....	53
Figure 11: Bedrock Reservoirs: Intersection of Shear Zones	55
Figure 12: Bedrock Reservoirs: Intersection of Shear Zones, 3D View.....	56
Figure 13: Tectonic Depressions	57
Figure 14: Bedrock Reservoirs: Nose of Plunging Fold.....	58
Figure 15: Bedrock Reservoirs: Nose of Plunging Fold 3D View	59
Figure 16: Bedrock Reservoirs: Shear Zones	60

LIST OF NOTATIONS AND ABBREVIATIONS

ACO	Agricultural Census Organization
ADB	Asian Development Bank
ARD	Arab Resources Development s.a.r.l. (Lebanon)
ASTER	Advanced Spaceborne Thermal Emission and Reflection Radiometer
AVHRR	Advanced Very High Resolution Radiometer (Satellite)
COE	Coefficient of Efficiency
CSI	Critical Success Index
EM	Electromagnetic
ESRI	Environmental Systems Research Institute
FAR	False Alarm Rates
GIS	Geographic Information System
CLASS	Comprehensive Large Array-Data Stewardship System (from NOAA)
GoB	Government of Balochistan
DAAC	Distributed Active Archive System
DEM	Digital Elevation Model
GCS	Geographic Coordinate System
GPS	Geographic Positioning System
GSP	Geological Survey of Pakistan
IEE	Initial Environmental Evaluation
IIASES	International Institute for Aerospace Survey and Earth Sciences
IPD	Irrigation and Power Department
IWRM	Integrated Water Resources Management
JICA	Japan International Cooperation Agency
Landsat TM	Landsat Thematic Mapper (Satellite)
m ³ /y	Cubic Meters per Year
Mm ³ /y	Million Cubic Meter per Year
MODIS	Moderate Resolution Imaging Spectroradiometer (Satellite)

List of Notations and Abbreviations —Continued

NASA	National Aeronautics and Space Administration
NEPL	North East part of the Pishin Lora basin
NDC	National Development Consultant
NOAA	National Oceanic and Atmospheric Administration
PCS	Projected Coordinate System
POD	Probability Of Detection
PMD	Pakistan Meteorological Department
R ²	Coefficient of Determination
RESDEM	Remote Sensing Data Extraction Model
RS	Remote Sensing
SCS	Soil Conservation Service
SRTM	Shuttle Radar Topography Mission (Satellite)
SWAT	Soil and Water Assessment Tool
TCI	Techno-Consult Internationals
TOPAZ	Topographic Parameterization (program)
TRMM	Tropical Rainfall Measuring Mission (Satellite)
UNDP	United Nation Development Program
UTM	Universal Transverse Mercator
USDA	United States Department of Agriculture
USGS	United States Geological Survey
VES	Vertical Electrical Sounding
WAPDA	Water & Power Development Authority
WASA	Water Authority & Sanitation Authority
WGS	World Geodetic System
WRS	Worldwide Reference System

CHAPTER 1

INTRODUCTION

1.1 Introduction and Problem Statement

Balochistan is the largest province in Pakistan, yet it has the smallest number of people per unit area. This is largely because of its arid to semiarid conditions (rainfall: ~100 mm/year) and the paucity of its water resources. In recent years, the indiscriminant and unplanned use of groundwater resources in Balochistan has led to water shortages, unsustainable overexploitation of groundwater, and progressive deterioration in groundwater quality and quantity (TCI et al., 2004). Water shortages in the area were exacerbated by the recent drought conditions that affected the area, causing population migration from rural to urban centers, and by war-related migrations from neighboring Afghanistan. These factors contributed to a dramatic rise in the local population of the Quetta Valley in general, and the city of Quetta in particular. Quetta Valley is part of the Pishin Lora watershed, and the city of Quetta is the capital of the Balochistan province (Figure 1); both areas are bearing the brunt of the population migration (IWRM, 2004).

Flooding events are rare but can be catastrophic. Large watersheds in mountainous areas can channel vast amounts of water into a limited number of main channels downstream, causing extreme flooding. According to the government of Balochistan, in the past decade or so, drought-flooding cataclysms affected 85% of the Balochistan population; over 2 million people migrated, 75% of the livestock died, and three major dams crashed in the flood of 2005 alone (Majeed and Khan, 2008; RedCross, 2005). Our research addresses the urgent need to assess and develop the Pishin Lora basin groundwater resources, as well as the general deficiency in understanding the hydrogeologic setting, namely the temporal and spatial partitioning of precipitation in the area; one of our goals is to develop scenarios for sustainable water extraction in the Pishin Lora basin.

I constructed a catchment-based continuous (1998–2005) rainfall-runoff model for the northeast part of the Pishin Lora basin (NEPL) watershed using the Soil and Water Assessment Tool (SWAT). The NEPL is a significant watershed that covers an area of 8,500 km²; it is subdivided into three main basins, the southern, northeast (NE), and northwest (NW) basins (Figure 1), with the majority of the precipitation occurring over the NE and NW basins. The NEPL was selected for the following reasons: (1) it has the highest elevations (up to 3500 m) in the Pishin Lora basin (Figure 1), and is thus more likely to receive substantial amounts of precipitation (Kazmi et al., 2003), (2) the Quetta Valley in general, and the city in particular, are the most popular destinations for the waves of immigrants, and (3) stream flow data needed for calibration purposes are available for the Burj Aziz Khan station (latitude 30°20'; longitude 66°35') on the West end outlet on the NEPL (Figure 1).

Given the paucity of monitoring systems (e.g., rain gauges, stream flow gauges), and the difficulty in accessing the areas of investigation because of ongoing security problems, we adopt an approach that relies heavily on observations extracted from readily available temporal remote sensing datasets. Remotely sensed data (e.g., precipitation from TRMM) were used as inputs to the model; the model outputs (e.g., runoff) were calibrated against observations (e.g., reservoir volume, wet versus dry streams) extracted from temporal satellite imagery. The adopted methodologies could potentially be applied to many of the world's watersheds that are inaccessible and lack adequate field monitoring datasets.

Figure 1: Location, Extent and Elevations for the Pishin Lora Basin.

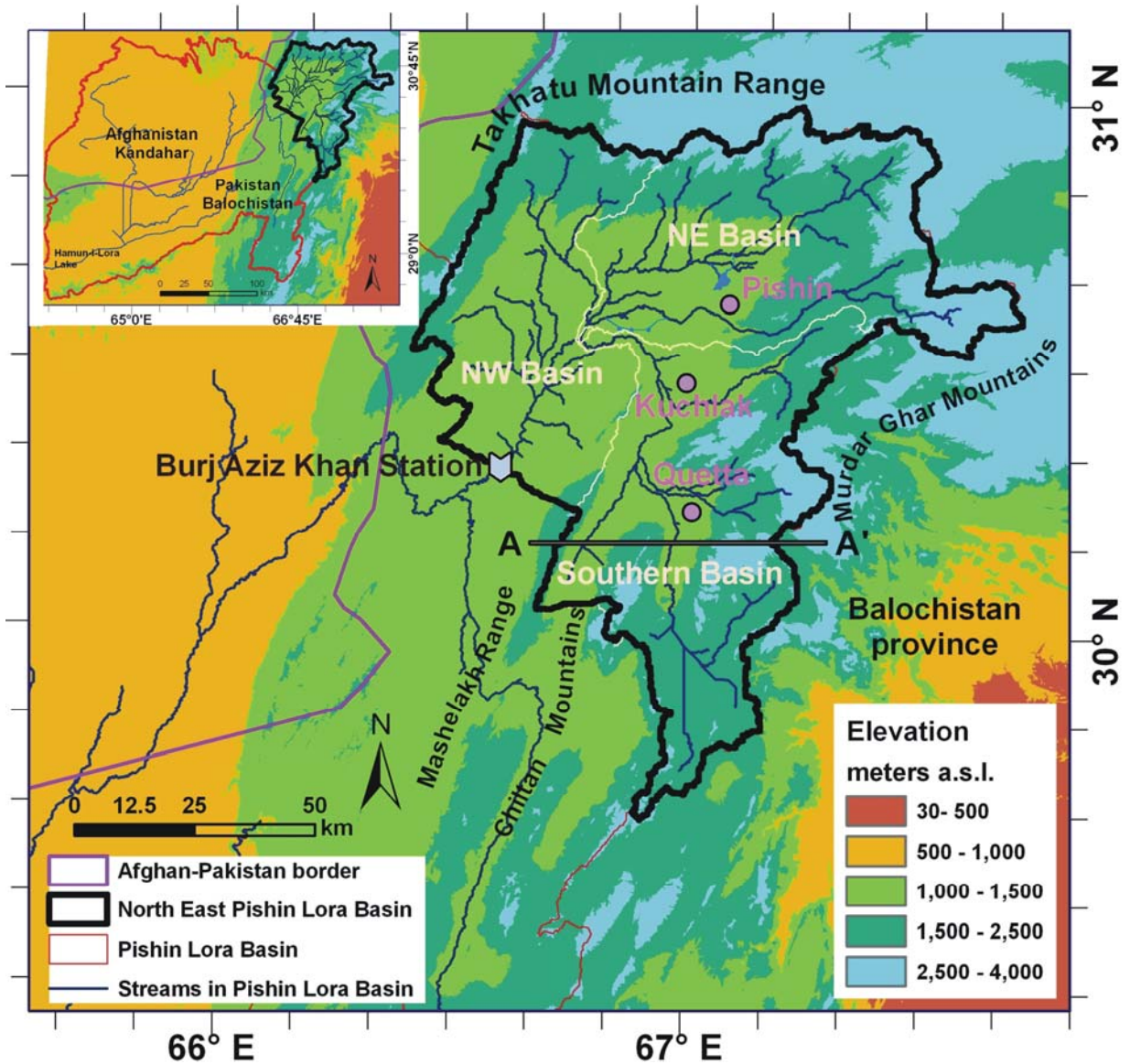


Figure 1 shows the Pishin Lora Basin on the inset in the upper left corner (outlined by red lines), the NEPL watershed (outlined by thick black lines), the NE, NW and Southern Basins inside within the NEPL (outlined by white lines). Also shown are stream networks in Pishin Lora and in the NEPL (blue lines), Afghanistan-Pakistan's border (purple line), main cities (Pishin, Kuchlak and Quetta), Burj Aziz Khan discharge station, mountain ranges, north, and the location of cross section A-A' displayed in Figure 2.

Figure 2: E-W Trending Cross Sections A-A`.

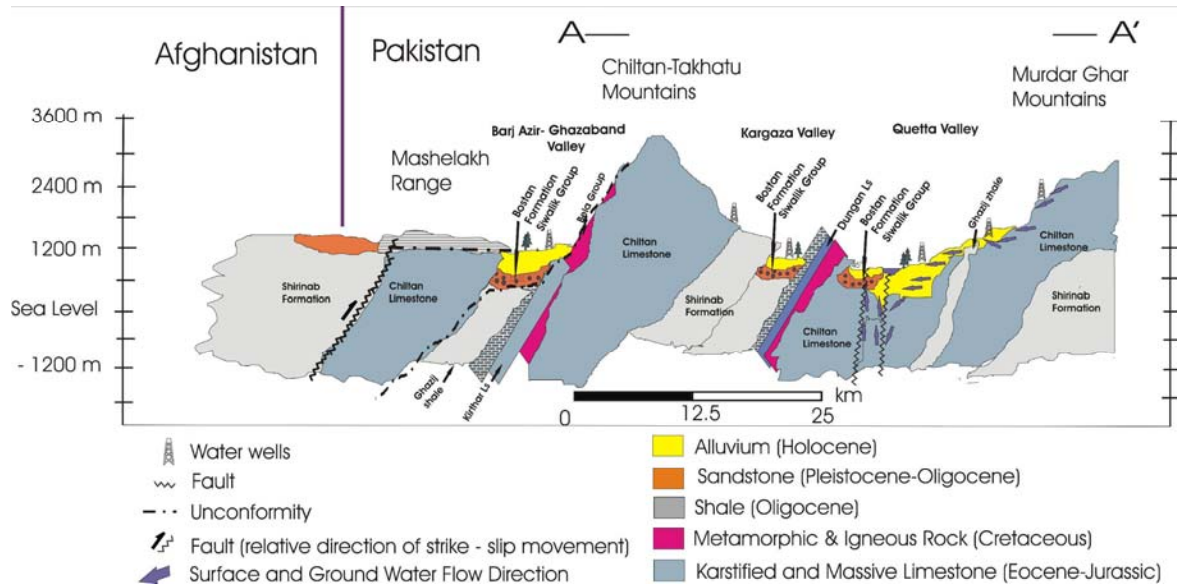


Figure 2 shows E-W trending cross sections A-A` outlined in Figure 1, showing the distribution of main valleys (Quetta, Kargaza, and Barj Aziz-Ghazaband), mountains ranges (Takhatu, Murdar Ghar, Ghiltan, Mashelakh), and the lithological and structural elements at depth.

1.2 The Research Objectives

The goals of the research are:

1. To obtain a better understanding of the overall hydrologic regime within NEPL.
2. To develop an integrated approach for the assessment and development of groundwater resources in arid lands.
3. To develop innovative methodology for calibration of hydrologic models based on the comparison of simulated data with data extracted from readily available remote sensing datasets.
4. To assess the sustainability of the water resources in meeting the water demand in the region.
5. To develop sustainable water extraction scenarios in the research area.

1.3 Methodology

An integrated and interdisciplinary approach was applied. The adopted approach integrates inferences from remote sensing data with observations extracted from other relevant data sources such as field geology and hydrologic flow modeling for a better understanding of the hydrological setting and the groundwater potentialities. To reach this goal, the following tasks were conducted:

- I. Stage one was the preliminary stage. In this stage, the following steps were taken: review of background information, collection of field data, compilation of published data, digitization of compiled data, development of a GIS to host the accumulated data sets and a web-based GIS for data distribution. An extensive web-based GIS was developed that incorporates all relevant data sets including co-registered digital geologic maps, remote sensing data, hydrologic parameters, drainage patterns, and soil maps, etc.

- II. Stage two included analysis of the accumulated data sets in a GIS environment for the purpose of development of conceptual and quantitative models.

- III. Stage three involved the construction and calibration of a hydrological rainfall runoff model, and development of sustainable water extraction scenarios for the research area using the calibrated model.

CHAPTER 2

LITERATURE REVIEW AND SITE DESCRIPTION

2.1 Previous Studies

My first activity was data collection for the Pishin Lora Basin, including reports, maps and other information relevant to the research objectives. This included previous studies on geology, hydrogeology, hydro-chemical, hydrological etc. With help from our Pakistani collaborators Dr. Salam and Dr. Mahmood, and from Western Michigan University interlibrary loans system, I collected a useful database for the research that was conducted on the geology and hydrogeology of the Pishin Lora Basin. I also collected several significant reports including those prepared by the United Nations, Japan International Corporation Agency (JICA), Water and Power Development Authority (WAPDA) and Asian Development Bank (ADB) funded projects. Additional references included reports from the Geological Survey of Pakistan (GSP), Bureau of Water Resources, Irrigation and Power Department, WAPDA Hydrogeology Directorate, and Water Authority & Sanitation Authority (WASA) as well as available data from consultant companies such as Arab Resources Development, Cameos Limited, Hunting Survey Corporation Limited, and Techno-Consult Internationals Limited.

Information on the geology and hydrology of the research area, the Pishin Lora Basin, was gathered from numerous references. The relevant and most referenced publications on this region are listed below.

Hunting Survey Corporation Limited (1961) developed the most comprehensive reconnaissance geological survey for West Pakistan, which includes the Balochistan province and the eastern part of the Pishin Lora Basin. This survey was supported by the Governments of Canada and Pakistan under a Colombo Plan Co-Operative Project. This report includes aerial and geological surveys with detailed maps, cross sections and description of the region. I used their maps as the base geological maps to study this

region. Also, I scanned, georeferenced and uploaded the most useful maps and cross sections on the Earth Science Remote Sensing Lab web site (esrs.wmich.edu).

In a study conducted by the UNDP (1982) and entitled “UNTC-Pk/73-032 Groundwater Investigations in Selected Areas of Balochistan”, the Pishin Lora basin, which is the main regional basin that encompasses the Quetta sub-basin or local basin, was investigated. The main objectives of the study were to: assess the groundwater resources; provide a basis for groundwater planning for economic development; undertake groundwater development through installation of production wells; and strengthen the Hydrogeology Directorate, WAPDA. In the UNDP study of 1982, the different geological formations were classified according to their capacity to yield water. The limestone formations of Jurassic age were classified as poor water yielding formations (i.e., aquitards). Based on the study, the alluvial deposits were identified as being by far the main aquifer that contains the main groundwater resources in the basin, with the alluvial fan deposits being the main recharge areas for the corresponding aquifer. Overexploitation of Quetta groundwater resources was also highlighted. The main recommendations of the UNDP study were to 1) implement a groundwater level monitoring plan; 2) establish a water resources board; and 3) enforce the water rights code.

JICA (1988) surveyed the groundwater resources in Quetta and Kalat districts of Balochistan in order to formulate a master plan for improving irrigation based on developing groundwater resources. The investigation undertook a helicopter-borne aerial gamma-ray spectro survey to delineate the so called groundwater “veins”.

NDC (1994) studied the feasibility of various methodologies for improving the recharge of groundwater in the Quetta valley. Detention reservoirs were found to be less favorable, whereas diversion structures were proposed as a viable alternative. Diversion structures would convey water with low silt content through feeder channels to recharge tanks avoiding the major problem of reservoir siltation. Silt free water would ultimately be recharged into the ground through injection wells located inside the recharge tanks.

Hydrological investigations were also carried out to estimate the peak flows and annual discharge in various rivers.

Kazmi et al. (1997, 2003) described the geomorphology and climate of Quetta, the geology, the hydrogeology, and the hydrology of the basin including water extraction volumes and water quality. The depth to bedrock in the northern part of Quetta city was estimated to exceed 600 m. Groundwater producing zones were assumed to be localized only in the alluvial deposits.

GKW Consultants (2000) undertook the feasibility study for Quetta Water Supply Environment Improvement Project (QWSEIP). The main objectives of the study with respect to water resources were to assess and secure new water supply sources as well as to construct and/or rehabilitate the corresponding distribution infrastructure for the city and surrounding villages. Drainage maintenance and rehabilitation was also an important objective of this study. Both surface and groundwater resources were investigated as potential water supply sources. This study revealed overexploitation of groundwater resources and particularly the alluvial aquifer.

WAPDA (2001) has been monitoring groundwater levels since 1985. They identified and assessed the impacts of groundwater mining in the valley. Significant and constant drops of groundwater level (as much as 6 meters) were observed in several areas within the valley due to overexploitation of the alluvial aquifer. In several of these areas, groundwater levels were reported to be dropping at a rate of 0.3 meters per year. WAPDA also reported daily water level changes for the year 1989 obtained from water level recorders installed as part of the Hydrogeology Project for Quetta under the program of monitoring network in Balochistan.

Techno Consult International Corporation, Cameous and Arab Resources Development (2004) carried (2002-2004) hydrological investigations for the area as part of their obligations towards their Consultancy Services Agreement with Water and Sanitation Authority (WASA), Quetta for Quetta Water Supply and Environmental Improvement

Project (QWSEIP). The main objective of this study was to assess ground water availability and productivity of the identified targeted hard rock / limestone aquifers as well as their interaction with the existing alluvial aquifer of Quetta Valley within Pishin Lora Basin. The study also aimed at assessing the sustainability of the aquifer.

2.2 Geology and Hydrology of NEPL

The Pishin Lora basin is a landlocked watershed located on the border of two provinces, Balochistan (Pakistan) and Kandahar (Afghanistan). The upstream areas are generally in the eastern highlands in Pakistan; the streams cross into Afghanistan, then flow back into Pakistan and feed the salty Hamun-i-Lora Lake (21 km², 1.1 km above mean sea level [AMSL]) in Balochistan (Figure 1). The region of the Pishin Lora is 61,300 km² and that of the NEPL is 8,470 km², approximately 15% of the Pishin Lora basin (Figure 1).

The geologic and structural history of the study region and its surroundings is complex, as it represents the western edge of the collision zone between the Indo-Pakistan and Eurasian plates. This collision consumed the Tethys Ocean that extended in the NEPL and surroundings (HSC, 1961a). It has been suggested that in this area the Indian plate did not collide with the Afghan block until the Late Pliocene (Treloar and Izatt, 1993). The study area is predominantly composed of sedimentary sequences reaching up to 11 km in thickness. The sequence is subdivided into three main groups: (1) the lower part is composed of a marine carbonate sequence, approximately 5 km thick, that was deposited before the collision; (2) the middle section is composed predominantly of thick (~3 km) sequences of mudrock with subordinate amounts of sandstone and carbonate that were deposited during or before the collision; and (3) the upper sequences are composed of thick (~3 km) clastic sediments that were eroded from the uplifted mountains. The lower sequence in the study area is largely composed of limestone of Permian to Middle Jurassic age that belongs to the Shirinab and overlying Chiltan formations. These sequences accumulated on a shallow marine shelf along the coast of Gondwana as early as the Permian period and continued to accumulate throughout the Cretaceous in a passive continental margin setting.

A brief description of the rock units (formations) in the study is given in Table 1. The data was compiled from Halcrow and Cameous (2008), Hunting (1961a), Kazmi et al. (2003), and TCI et al. (2004).

Table 1: Lithostratigraphy of NEPL

Period	Epoch	Name	Thickness (m)	Description
QUATERNARY	Holocene	Alluvium		Present day higher coarse stream channel material consisting of sub-angular to sub-rounded pebbles, gravels, sand and silt.
		Silt and clay		Silt, clay with minor sand and gravel. Deposits cover significant areas.
		Talus and scree deposits	2-6	Angular to sub-rounded boulders, cobbles and pebbles originating from surrounding rocks of high mountains
		Silt and clay deposits	3-60	Silt and clay and some gravel.
		Cultivated Silt and Clay deposits		Cultivated loess clay and silt flat plains.
		Alluvial fan and torrential wash deposits	50-90	Unconsolidated poorly sorted rounded to sub-rounded gravels, cobbles, and pebbles with silt and sand, well dissected by streams.
		Terrace gravel	20-30	Unconsolidated to semi-consolidated assemblage of gravel, sand and silt with sandy calcareous cement. Flat topped morphology and slightly sloping.

Table 1 - Continued

Period	Epoch	Name	Thickness (m)	Description
	Pleistocene	Bostan Fm.*	100-400	White light grey, brick red, maroon or apple green poorly consolidated and gypsiferous lacustrine clay; and brown, reddish brown, and gray thin bedded soft silt and sandstone. Upper contact with sub-recent deposits represents angular unconformity and at places transitional.
TERTIARY Late	Pliocene	Urak Fm.	> 4000	Mainly thick bedded, poorly sorted, and well rounded to sub-angular conglomerate; olive, khaki and maroon soft shale; brown, green and red poorly sorted, cross-bedded and pebbly sandstone; and minor ferruginous-yellow or dark gray argillaceous and sandy limestone. Lower part of group is usually shale interbedded with sandstone or thick bedded conglomerate. In Urak valley, group divided into 3 parts: sand and shale in lower part, sand and shale with increasing conglomerate towards the top in middle part, and mainly conglomerate in upper part.
		Shinmati Fm.		1500

Table 1 - Continued

Period	Epoch	Name	Thickness (m)	Description
TERTIARY	Late Eocene	Nari Fm.	80-100	Greenish gray, medium grained, calcareous, moderately to poorly cemented and cross bedded sandstone, with subordinate reddish gray and pale orange clay, and conglomerate. Lower contact with Kirthar Fm. is conformable.
		Murgha Faquirzai Fm.	460	Pale greenish gray, green, or khaki calcareous and flaky shale with subordinate grey to green, calcareous, fine grained, sandstone; and ferruginous or black and argillaceous thin bedded shelly limestone.
		Nimargh Fm.	50-60	Dark grey or black argillaceous limestone with subordinate gray or green gray shale or conglomerate.
		Kirthar Fm.	180	White to creamy white nodular and fossiliferous limestone at base; crystalline and unfossiliferous in middle portion; and highly fractured and fossiliferous in top sequence. Lower contact with Ghazij is conformable.
	Early Eocene	Upper	2,700	Red to maroon shale, and maroon moderately cemented medium to very coarse grained sandstone.
		Middle		Ghazij Fm.

Table 1 - Continued

Period	Epoch	Name	Thickness (m)	Description
TERTIARY Early	Late Paleocene	Lower		Dominantly olive green to gray fissile shale with minor beds of sandstone and siltstone. Sandstone is gray to dark gray and medium grained. Lower contact with Dungan Fm. or Karakh Fm. is conformable.
		Karakh Fm.	90-360	Consists of limestone, conglomerate, marl, shale and sandstone. Limestone is nodular to massive light brown to yellowish gray with gray calcareous shale interbeds. Conglomerate has ash gray color and comprises limestone pebbles. Lower contact with Moro Fm. is conformable. It is of the same age as Dungan Fm. and apparently related to it. Exposed only to the southeast and outside of Quetta basin.
		Dungan Fm.	30-100	Fresh gray to dark gray and weathered brown, medium to thick bedded, cliff-forming hard limestone with minor dark gray to brown shale intercalations. Lower contact with Fort Munro Fm. is unconformable.
Cretaceous Late	Senonian	Fort Munro Fm.	40	Dark gray to black, medium bedded, very hard limestone commonly sandy in upper part and argillaceous in lower part. Lower contact with Parh limestone Fm. is unconformable.
		Moro Fm.	20-30	Black to bluish black, thin to medium bedded argillaceous limestone with subordinate siltstone and shale. Lower contact with Parh limestone is unconformable.

Table 1 - Continued

Period	Epoch	Name	Thickness (m)	Description			
CRETACEOUS	Early	Parh Limestone Fm.	270	Light gray to creamish, thin to medium bedded white platy porcellaneous limestone with subordinate shale and marl intercalations. Lower contact with Goru Fm. is transitional.			
				Parh Group (undifferentiated)	500	80	Brown and green thin to medium bedded fine grained argillaceous limestone with subordinate flaky and splintery brown to green shale and brown to green siltstone. Lower contact with Sember Fm. is conformable.
						Sember Fm.	150
JURASSIC	Middle	Dogger	Chiltan Fm.	1800	Dark gray massive and thick bedded micritic and finely crystalline hard limestone, and dolomitic limestone with occasional shale layers. Limestone is at places oolitic and pisolitic, weathers into gray to brown color, and gives off fetid smell when freshly broken. Chert nodules are also occasionally present in limestone. Exposed in most mountain ranges surrounding Quetta: Murdaghar, Chiltan, Takatu, Kumblean, and Deghari in addition to Landi and Mian Ghundi hills. Lower contact with Shrinab Fm. is conformable		

Table 1 - Continued

Period	Epoch	Name	Thickness (m)	Description
Jurassic Early	Lias	Shrinab Fm.	1500	Gray to dark gray, thin to medium bedded limestone interbedded with flaky to fissile gray shale. Grades downward into more dominant shale lithology. Chert nodules varyingly present in limestone. Mainly exposed in Chiltan and Takatu mountain ranges. Lower contact of formation not exposed.

For the purpose of hydrological modeling, and guided by information from the US Department of Agriculture Soil Conservation Service methodology (SCS, 1985), Handbook of hydrology (Maidment, 1993), Hunting (1961a), Kazmi et al. (2003), and TCI et al. (2004), the formations listed in Table 1 were assigned appropriate soil group types and hydraulic conductivities.

Table 2 lists the composition and age of the investigated lithologic units in the study area, their assigned soil types, and their reported hydraulic conductivities (Hunting, 1961a; IIASES, 1992; Kazmi et al., 2003; Maidment, 1993; SCS, 1985; TCI et al., 2004).

Table 2: Geologic and Hydrogeologic Data for NEPL used in Hydrological Modeling

Lithologic units	Age	Lithology	Hydraulic conductivity SOL_K, mm/h, and soil group (A,B,C,D)	Consolidated soil types for SWAT
Unconsolidated deposit (Stream-bed and Sub-piedmont deposits)	Quaternary Holocene, 10KYA-Present	Silts, sands, gravels, boulders, cobbles	40 mm/h, A, Alluvium	Alluvium
Bostan Formation	Quaternary Pleistocene, 2 MYA-10KYA	Sandstone with partially consolidated clay, silt, sand and gravel	28 mm/h, A, Sandstone	Sandstone
Siwalik Group	Tertiary Miocene Pliocene, 20-2 MYA	Sandstone conglomerates	28 mm/h, A, Sandstone	
Gaj Formation	Tertiary Miocene, 23-20 MYA	Shale	1.9 mm/h, C, Shale	Shale
Kirthar Formation	Tertiary Oligocene, 33-23 MYA	Highly fractured Fossiliferous Limestone	20 mm/h, A, Limestone (Karstified)	Limestone
Ghazij Formation	Tertiary Eocene, 55-33 MYA	Shale interbedded with claystone, mudstone, sandstone, limestone, and conglomerate	1.9 mm/h, C, Shale	Shale
Dungan Formation	Tertiary Paleocene, 65-55 MYA	Limestone karstified with subordinate marl, shale, and sandstone	20 mm/h, A, Limestone (Karstified)	Limestone
Bela Volcanic Group	Cretaceous, 145-65 MYA	Lava flows, volcanic conglomerate, volcanic breccia, mudstone	0.01 mm/h, D, Igneous Rock	Igneous Rock
Chiltan Formation	Jurassic, 200-145 MYA	Limestone karstified	20 mm/h, A, Limestone (Karstified)	Limestone
Shirinab Formation	Permian –M. Jurassic, 270-200 MYA	Bedded Limestone and intercalated shale	1.9 mm/h, C, Limestone	

2.3 Type of Aquifers

Two main types of aquifers are reported in the study region, alluvial aquifers in the valleys and bedrock aquifers in the surrounding mountains. These two aquifers are in direct contact and are hydraulically connected (Halcrow and Cameous, 2008; Kazmi et al., 2003; Shan, 1972; TCI et al., 2004). The majority of the wells in the study area extract water from the thick (30 to 900 m) alluvial deposits in the main valleys; less groundwater is being extracted from the bedrock aquifers (Kazmi et al., 2003; TCI et al., 2004).

The thickest alluvial aquifers are found in the main valleys, the Quetta, Kargaza, and Barj Azir–Ghazaband valleys (Figure 2), which are adjacent to, and running along the foothills of, the major mountain ranges in the area (e.g., Murdar Ghar, Chiltan-Takatu, and Mashelakh; Figs. 1 and 2). The alluvial aquifers are in contact with the underlying sandstone aquifers of the Bostan Formation and Siwalik Group. The Siwalik Group, the Bostan Formation, and the overlying unconsolidated deposits cover most of NEPL, including the valleys occupied by the Pishin Lora, Chinar N., Surhab Lora, Sariab Lora, and Karak Lora rivers and their tributaries (Aftab, 1997) (Figure 3b) and are largely composed of poorly cemented conglomerate and thus provide adequate recharge zones.

The hard rock aquifers are largely found in the karstified Chiltan Formation, and to a much lesser extent in the Dungan and Kirthar Formations; the distribution of groundwater in the Dungan and Kirthar Formations is apparently structurally controlled (Kazmi et al., 2003; TCI et al., 2004). The aquifer properties of the Chiltan Formation and to a lesser extent the Kirthar and Dungan Formations, are enhanced by its karstified texture and its well-jointed and highly-fractured nature. Numerous springs of considerable discharge were reported from these formations (Aftab, 1997; Kazmi et al., 2003).

2.4 Temperature, Precipitation and Stream Flow in NEPL

Examination of the temporal and spatial distribution of precipitation, temperature, and stream flow data indicated that the amount of precipitation is quite variable from year to

year, as indicated by the average annual precipitation data extracted from TRMM (Figure 4). Figure 4 shows that in 2003 and 2005 precipitation was high, whereas precipitation from 1998 through 2002 and 2004 was negligible. The lowest temperatures (as low as -10°C) are reported for December, January, and February (Kazmi et al., 2003; PMD, 2010; Shan, 1972; TCI et al., 2004), the time period during which snow accumulates on the mountains (e.g., Chiltan-Takhatu and Murdar Ghar; Figure 2). In the spring, snow starts melting slowly and percolates down as overflow and interflow from the highlands of the Murdar Ghar and Chiltan-Takhatu Mountains toward the interleaving valleys, including Quetta Valley (Figure 2).

2.5 Delay Action/Storage Dams

A common practice in the area is to dam the melted snow coming off the highlands to increase infiltration, and recharge the alluvial aquifers in the area. Of the 292 delay action/storage dams constructed in Balochistan, 127 were implemented in the Pishin Lora (Halcrow and Cameous, 2008). The majority of the constructed dams are quite small, as are the reservoirs formed by the impounded runoff (area $<0.01\text{ km}^2$). Only two major reservoirs built near the cities of Pishin and Kuchlak, the Khushdil Khan (latitude $30^{\circ}40'$ N, longitude $67^{\circ}40'$ E) and the Kara Lora (latitude $30^{\circ}34'$ N, longitude $66^{\circ}52'$ E) reservoirs (Figures. 1, 3b), were recognizable in Landsat TM scenes. The former collects runoff from the Chinar N. River and from the Pishin Lora Rivers; the latter is from the Surkhab Lora River (Figure 3b).

Figure 4: Annual Precipitation Extracted from 3-hourly TRMM Precipitation Data.

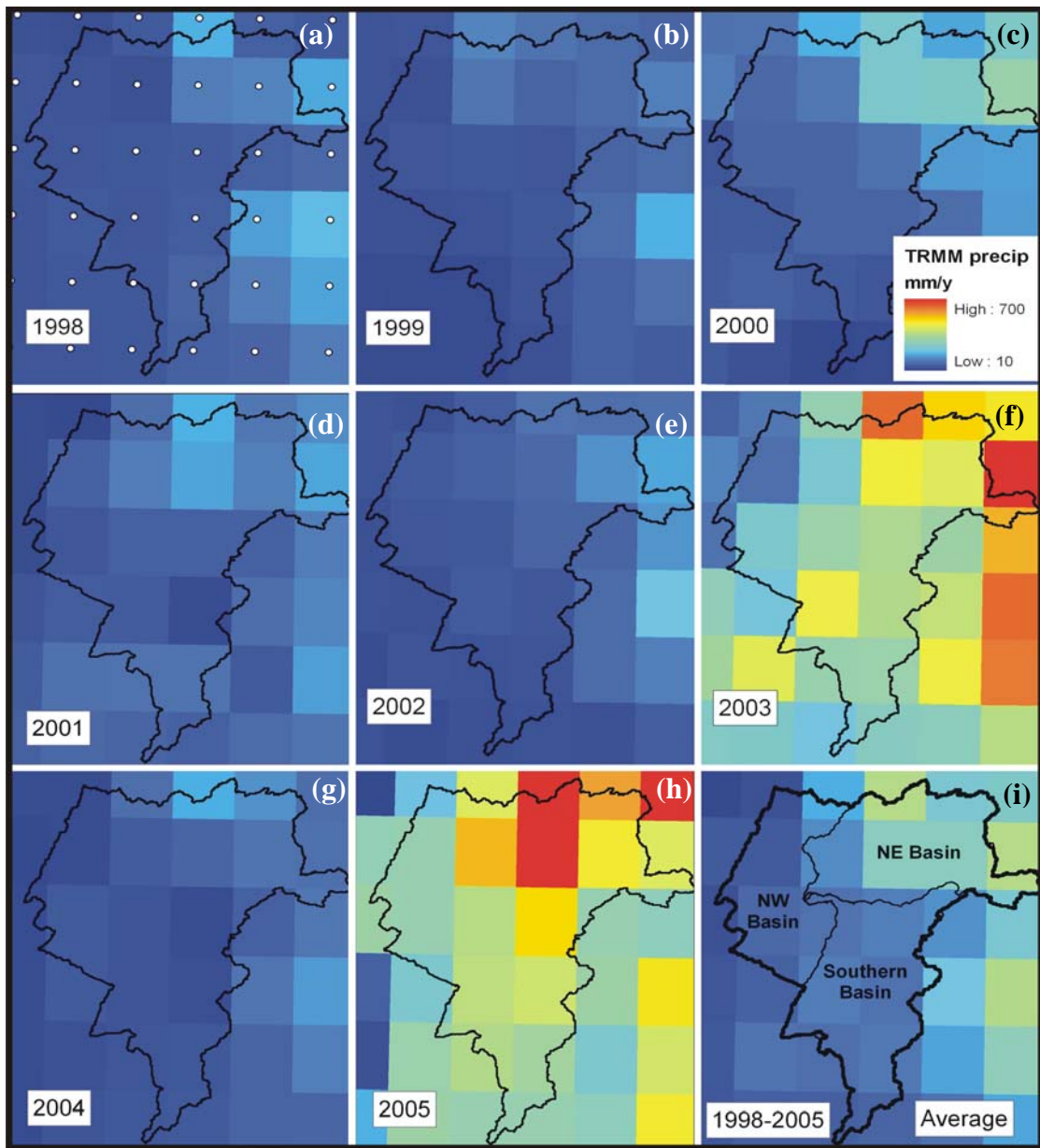


Figure 4 shows annual precipitation extracted from 3-hourly TRMM precipitation data over NEPL and surroundings for years 1998 through 2005 (a–h) showing large variations in precipitation amounts. (i) Average annual precipitation (1998-2005). Also shown are locations of TRMM stations (white circles; a) and the outlines of the major basins within NEPL. The highest precipitation rates are observed in the northeastern part of NEPL.

CHAPTER 3

MODEL CONSTRUCTION AND CALIBRATION

3.1 Model Framework

A continuous rainfall-runoff model for the NEPL was constructed within the SWAT framework to simulate the hydrologic processes using its physically based formulations. SWAT is a semi-distributed continuous watershed simulator that computes long-term water flow over large basins using daily time steps. The NEPL was divided into a number of subbasins, which were further subdivided into small groups called hydrologic response units (HRUs) that possess unique land cover, soil, and management attributes. The water balance of each HRU was calculated through four water storage bodies (snow, soil profile, shallow aquifer, and deep aquifer). Flows generated from each HRU were then summed and routed through channels, ponds, and/or reservoirs to the outlets of the watershed (DiLuzio et al., 2001; Srinivasan et al., 1998). A linear areal depletion curve (Anderson et al., 1976) was used to estimate the seasonal growth and recession of snow pack and to determine snowmelt. A modified Soil Conservation Service (SCS) curve number (CN) method (SCS, 1972), adjusted according to soil moisture conditions, was used to calculate direct surface runoff. The Penman-Monteith method (Monteith, 1981) was used to estimate evaporation on bare soils and evapotranspiration on vegetated areas. We developed a Geographic Information System (GIS) database encompassing all relevant datasets for the NEPL basin; these data served as input for the SWAT rainfall-runoff model. The ArcGIS 9.3 interface for SWAT2005 software (DiLuzio et al., 2001) was used for data input.

3.2 Data Collection

A large number of digital datasets were generated for modeling and calibration purposes: (1) Digital Elevation Model (DEM; spatial resolution: 90 m) was constructed from the Shuttle Radar Topography Mission (SRTM) data. (2) Temporal and spatial distributions of

temperature, relative humidity, wind speed, and solar radiation were generated from the available climatic stations. (3) Temporal (1998 – 2005) and spatial daily distribution maps for precipitation and snow accumulation were generated from 3-hourly TRMM (3B42.v6) precipitation data (spatial resolution: $0.25^\circ \times 0.25^\circ$); data was extracted from the National Aeronautics and Space Administration (NASA) Distributed Active Archive System (DAAC). (4) Spatial distribution of landuse and soil types were extracted from published data sources (Abbas et al., 1987; ACO, 2004; Hunting, 1961b; IIASES, 1992; Mirza, 1995). (5) Daily distribution maps for clouds were constructed for verification of TRMM-derived precipitation events (Milewski et al., 2009a); data was extracted from the Advanced Very High Resolution Radiometer (AVHRR) scenes acquired (2003 - 2005) from the National Oceanic and Atmospheric Administration Comprehensive Large Array-Data Stewardship System (NOAA CLASS, spatial resolution: 1.09 km) and from the Moderate Resolution Imaging Spectroradiometer (MODIS) scenes (spatial resolution: 250 m). (6) Landsat Thematic Mapper (Landsat TM) scenes (spatial resolution: 28.5 m), acquired (1998 – 2005) from U.S. Geological Survey (USGS) database were used to refine the DEM-derived stream networks, to extract reservoir volumes, and to examine whether streams were wet or dry.

The Remote Sensing Data Extraction Model (RESDEM) was used to preprocess large remote sensing datasets (e.g., TRMM, AVHRR). RESDEM allows users to extract user-defined subsets from the global satellite datasets and process the selected subsets in ways that unify projections, eliminate spectral variations related to differences in sun angle elevations, and verify TRMM-based precipitation events while applying verification procedure modules connected to cloud detection (Milewski et al., 2009b).

3.2.1 Data Processing

Most of the collected data, including maps and satellite images, were scanned if necessary and geo-referenced. The satellite imageries were acquired based on the Worldwide Reference System (WRS) path 153-154 and pan 38-39 of the Landsat -7 and ASTER, and latitude 29-31 North and longitude 66-68 East for the TRMM, SRTM,

AVHRR, MODIS data. The required satellite imageries were processed and geo-referenced by using ENVI software from ITT Visual Information Solutions. Various band compositions were developed with image enhancement, image sharpening and false color compositions techniques to develop a better visualization and understanding of the research area. All preliminary digitized and geo-referenced images were transformed from ENVI to Geographic Information System, ArcGIS 9.3 format. ArcGIS was developed by Environmental Systems Research Institute (ESRI) and consists of Arc Map, Arc Internet Map Server (ArcIMS), ArcCatalog and ArcTools. Soil Water Assessment Tools (SWAT), which was developed by the US Department of Agriculture (USDA), was incorporated into ArcTools of ArcGIS 9.3.

There were two main purposes for generating the GIS:

- All data could be viewed by our collaborators from Pakistan with ease and could be downloaded from the web site (<http://esrs.wmich.edu>).
- Data was to be imported from the GIS into the SWAT domain and used for the construction of rainfall runoff models

Since all the information which is maintained in the GIS represents some part or feature of the earth, the orientation of this information in the space must be in real world coordinate systems and must satisfy research requirements.

There were a number of features in the GIS:

- Two types of Coordinate Systems with uniform Datum and Projection were used for the data processing: (1) Geographic Coordinate Systems (GCS) with World Geodetic System (WGS) 1984 GCS, and (2) projected Coordinate Systems (PCS), WGS 1984 Datum, and Universal Transverse Mercator (UTM), zone 42N
- Custom tools for analysis and visualization were constructed

3.2.2 Digital Elevation: Watershed and Stream Delineation, and Reservoir Storage

The DEM mosaic covering the entire Pishin Lora watershed was used to delineate the watershed boundaries and stream networks using the Topographic Parameterization (TOPAZ) program (Garbrecht and Martz, 1995). The NEPL watershed was subdivided into 104 subbasins, with sizes ranging from 0.14 to 650 km² (Figure 5). Dam storage parameters (e.g., reservoir surface area and volume) were extracted on a monthly basis from temporal (1998–2005) Landsat images and SRTM data and used for calibration purposes (Section 3.3).

Figure 5: Distribution of Major (NE, NW, and Southern) Basins

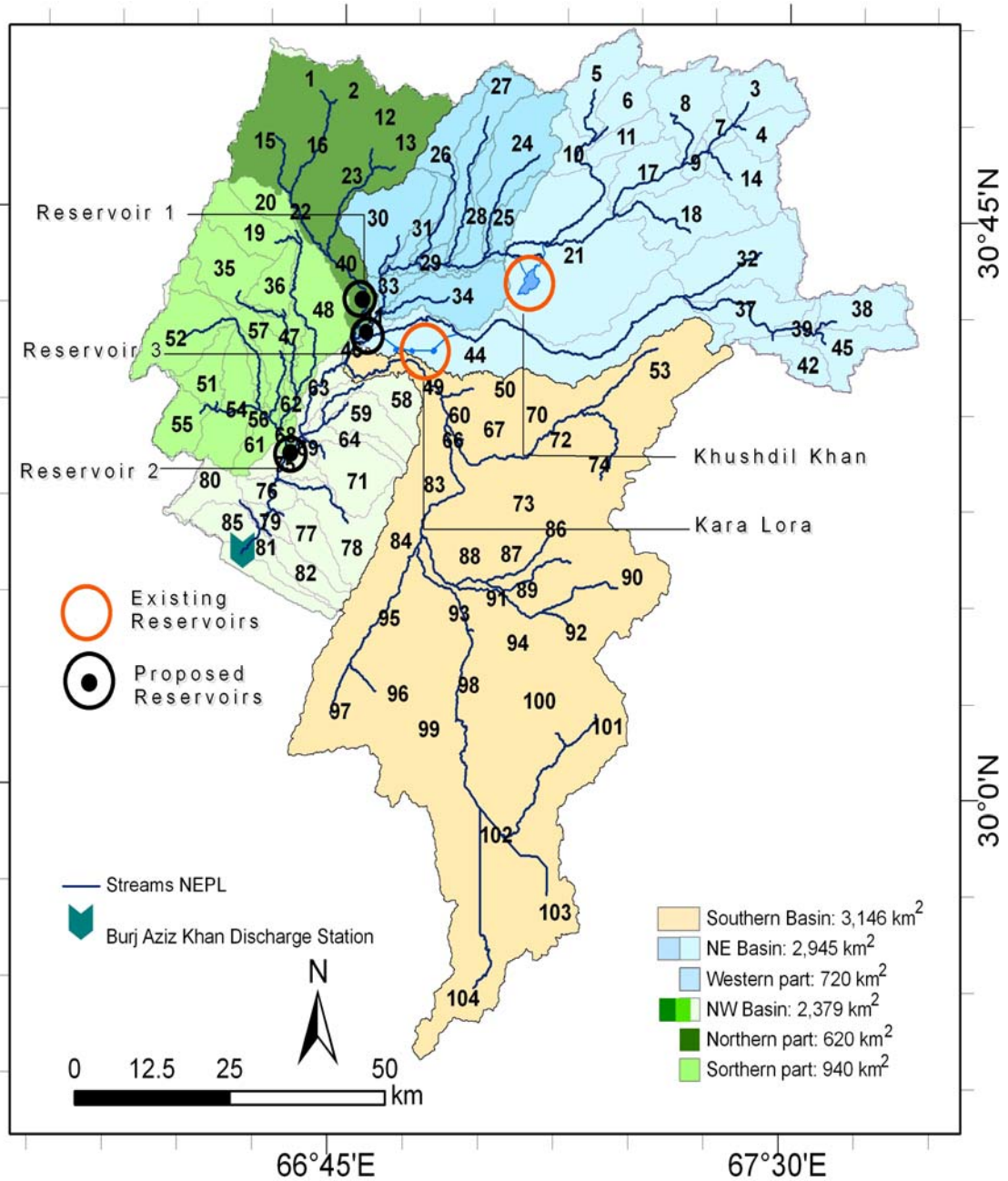


Figure 5 shows distribution of major (NE, NW, and Southern basins) and minor (104) subbasins within the NEPL watershed. Also shown are the locations of Burj Aziz Khan Discharge Station, the Khushdil Khan and Kara Lora reservoirs, in subbasins # 21 and 44, respectively, and the location of the proposed additional reservoirs: reservoir 1 (subbasin # 40), reservoir 2 (subbasin # 41), and reservoir 3 (subbasin # 68).

3.2.3 Climate Datasets: Temporal and Spatial Precipitation over Watersheds

Climatic datasets were imported to constrain the spatial distribution of precipitation, to determine onset of snow pack growth and melting, compute evapotranspiration, and constrain surface runoff and groundwater contributions. I chose to extract precipitation information from the TRMM data because of the limited and uneven distribution of precipitation gauges in the study area and the general correspondence between the TRMM and the precipitation reported from the Quetta Meteorological Station. Only one precipitation data station, the Quetta Meteorological Station, is located within the NEPL, and none are located on the Takhatu Mountain Range in the north, the highlands that receive the highest amount of precipitation in the NEPL (Figures. 1 and 4).

We used the data available from the Quetta Meteorological Station to evaluate the quality of the TRMM-based precipitation. A general correspondence (R^2 : 0.88) was observed between the average monthly (1998–2005) precipitation measured in the field and that derived from TRMM data over the same area (Figure 6a). One should not expect a 1:1 correspondence between TRMM and field-derived measurements because TRMM integrates observations over a large area ($0.25^\circ \times 0.25^\circ$), whereas rain gauges provide local measurements. The 3B42.v6 TRMM dataset was selected because it has lower false-alarm rates (FAR), higher probability of detection (POD) rates, and a greater overall critical success index (CSI) compared to the other TRMM products, including 3B42.v5 and 3B43.v5 (Chokngamwong and Chiu, 2006).

Figure 6: Temperature and Precipitation Comparison

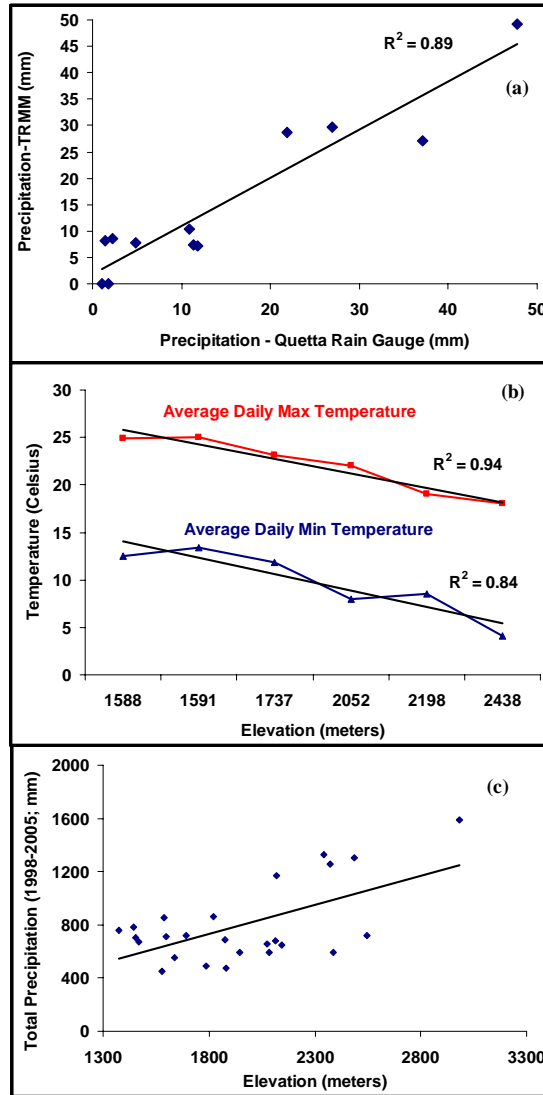


Figure 6 shows (a) Comparison between average monthly (1998-2005) precipitation reported from the Quetta Meteorological Station and TRMM-derived average monthly precipitation for the picture element covering the Quetta Meteorological Station. (b) Elevation-dependant variations in temperature revealed from a plot of average maximum and minimum temperatures extracted from six stations against their respective elevations (c) Elevation-dependant variations in precipitation revealed from a plot of annual precipitation extracted for individual TRMM stations within NEPL against station elevation.

Examination of daily maximum and minimum temperatures from the six stations in the NEPL and its surroundings revealed large elevation-dependant variations in temperature. The higher the station elevation, the lower the temperature (PMD, 2010). This relationship is displayed in Figure 6b, which shows significant correlations (R^2 : 0.84–0.94) between average daily maximum and minimum temperatures and station elevation. For modeling purposes, and to increase the accuracy of the SWAT-derived spatial distributions of precipitation (rain and snow), daily minimum and maximum temperatures were computed at fictitious stations using linear regressions with temperatures and elevations as variables. Data used in the regression analysis were extracted from the six temperature gauges (Figure 3a, red crosses), four of which are located within the NEPL. The remaining two stations are from areas proximal to the NEPL. The elevations of these stations ranged from 1600 to 2400 m AMSL. The locations of the fictitious stations were distributed across the NEPL so as to provide a more or less even distribution, laterally and vertically, and temperatures at these fictitious stations (Figure 3a, black crosses) were estimated using regression relationships derived from daily temperature datasets.

3.2.4 Land Use and Soil types

Three major land use units were mapped throughout the watershed, Agricultural, Pasture, and Mixed Forest (Figure 3a), using the agricultural census land use data prepared by Pakistan's Agricultural Census Organization (ACO) and by the Agricultural Research Council of the Agricultural Department of Balochistan (ACO, 2004; Mirza, 1995). The highlands surrounding the Quetta Valley are largely composed of Mixed Forest and Pasture, whereas the remaining lowlands are dominated by the Agricultural and Pasture land use types (Figs. 1 and 3). Using the SWAT land use library, we selected the land use types that closely resemble the mapped units. For example, the mapped Agricultural land use type was modeled as SWAT's AGRC—Agricultural Land-Close-grown. Similarly, Mixed Forest and Pasture land use types were modeled as Mixed Forest, and Pasture, respectively, in SWAT.

Five main soil types were identified and mapped in the NEPL using published soil surveys (Abbas et al., 1987; HSC, 1961b; IIASES, 1992) (Figs. 2 and 3b). These are (1) Alluvium, (2) Sandstone, (3) Shale, (4) Limestone (Karstified or Massive), and (5) Metamorphic and Igneous Rocks. The saturated hydraulic conductivities for these soil types were extracted from published sources (IIASES, 1992; TCI et al., 2004; WAPDA, 2001). The reported range of hydraulic conductivities for the five soil types are as follows: Alluvium, 28.8–324 mm/hr; Sandstone, 0.1–100 mm/hr; Limestone, 0.4–76 mm/hr; Shale 0.004–10 mm/hr; and Metamorphic and Igneous Rocks, 0.004–5 mm/hr.

I compared the reported ranges for hydraulic conductivities for the five soil types in the study area to those listed (A: >7.6 mm/hr; B: 3.8 to 7.6 mm/hr; C: 1.3 to 3.8 mm/hr; and D: 0.0 to 1.3 mm/hr) for the SCS soil hydrologic groups (SCS, 1985) and classified them accordingly. The Alluvium, Sandstone, Shale, Massive Limestone, Karstified Limestone, and Metamorphic/Igneous soil types were assigned to groups A, A, C, C, A, and D, respectively (Table 2). Table 2 also lists the composition and age of the investigated lithologic units in the study area, their assigned soil types, and their reported hydraulic conductivities (HSC, 1961a; IIASES, 1992; Kazmi et al., 2003; Maidment, 1993; SCS, 1985; TCI et al., 2004).

Digital maps depicting distributions of soil hydrologic groups, together with the generated land use digital maps, were imported into the model and used to define multiple HRUs for each of the 104 subbasins (Figure 5). With threshold levels of 20% and 10% for land use and soil, respectively, recommended by SWAT (DiLuzio et al., 2001), 4 to 12 HRUs were defined for each of 104 subbasins, resulting in a total of 798 HRUs for the watershed. The integration of the information contained in the soil type and land use coverage allowed the extraction of CN distribution maps for each of the soil horizons across the entire watershed.

3.3 Model Calibration and Validation

Conventional calibration using stream flow data has limited application in our study area because only one flow gauge is available at Burj Aziz Khan Field Discharge Station in

subbasin 85 (IPD, 2006) (Figs. 1 and 5). Because of the paucity of stream flow data, we explored the utilization of satellite data to improve model calibration. In addition to the traditional approaches to model calibration (e.g. manual and automatic calibrations, observed/simulated stream flow hydrographs), we developed methods that take advantage of observed changes in the volumes of the Khushdil Khan and Kara Lora reservoirs, which are located in subbasins 21 and 44, respectively (Figure 5).

Model calibration was conducted in three major steps via a stepwise, iterative process by adjusting the key snow pack/melt and soil/groundwater parameters. SWAT's default values were adopted as our initial parameter values, and the implemented adjustments were constrained by the ranges of parameter variation provided by SWAT. Table 3 defines the key parameters and lists the adopted value and SWAT's default value, range, and data source for each of them.

The first step is a coarse adjustment step for the snow pack/melt parameters (see Section 3.3.1) to calibrate the simulated flow rates with the observed peaks in the Burj Aziz Khan Field Discharge Station. Throughout the second step, we calibrated the simulated runoff reaching the Khushdil Khan and the Kara Lora Reservoirs against reservoir volumes extracted from temporal satellite imagery by adjusting key soil/groundwater parameters (Section 3.3.2). The third step involved calibrating simulated flow against discharge flow from the Burj Aziz Khan Field Discharge Station by adjusting key soil/groundwater parameters and channel routing parameters (see Section 3.3.3). Fine-tuning was then performed manually by repeating the calibration adjustments described in Sections 3.3.1 through 3.3.3 until a best fit was achieved between modeled and observed reservoir volume and between modeled and observed flow values (Figure 7). The values for the parameters that achieved the optimum calibration are given in Table 3.

Table 3: Significant Calibration Parameters

Parameter ^a	SWAT Default Range (Value)	Final Value	Definition
SFTMP	(-)5 - 5 (1.0) ^{a,b}	-2.0	Snowfall Temperature (°C)
SNOCOVMX	0-500 (1.0) ^b	500.0	Minimum snow water content that corresponds to 100% snow cover, SNO ₁₀₀ (mm H ₂ O)
SNO50COV	0-1 (0.5) ^a	0.5	Fraction of snow volume represented by SNOCOVMX that corresponds to 50% snow cover
TIMP	0-1 (1.0) ^a	1	Snow pack temperature lag factor
SMTMP	(-)5 - 5 (0.5) ^a	3.0	Snow melt base temperature (°C)
SMFMX	0-10 (4.5) ^c	10	Melt factor for snow on June 21 (mm H ₂ O/ °C-day)
SMFMN	0-10 (4.5) ^c	0.0	Melt factor for snow on December 21 (mm H ₂ O/ °C-day)
SOL_AWC	Varies ^a	Varies (0.01-1)	Available water capacity of the soil layer (mm/mm soil)
ESCO	0-1 (0.95) ^a	0.0	Soil Evaporation Compensation Factor
GWQMN	0-5000 (0) ^a	Varies (100-600)	Threshold depth of water in the shallow aquifer required for return flow to occur (mm H ₂ O)
REVAPMN	0-500 (1.0) ^a	500	Threshold depth of water in the shallow aquifer for "revap" to occur (mm H ₂ O)
GW_REVAP	0.2-1.0 (0.2) ^a	0.2	Groundwater "revap" coefficient
GW_DELAY	0-500 (31) ^e	0	Groundwater delay time (days)
ALPHA_BF	0-1 (.048) ^f	Varies (0.048, 1)	Baseflow alpha factor (days)
RCHRG_DP	0-1 (0.05) ^a	0.05	Deep aquifer percolation fraction
CH_K1	0-150 (0.50) ^g	100.0	Effective hydraulic conductivity in tributary channel alluvium (mm/hr)
CH_K2	0-150 (0.0) ^g	0.5	Effective hydraulic conductivity in main channel alluvium (mm/hr)
CH_N1	0-0.3 (0.014) ^h	Varies (0.014)	Manning's "n" value for the tributary channels
CH_N2	0-0.3 (0.014) ^h	Varies (0.014)	Manning's "n" value for the main channel
RES_K	0-150 (0.50) ⁱ	Varies (5, 15)	Hydraulic conductivity of the reservoir bottom (mm/hr)

Table 3 shows significant calibration parameters (20 parameters) grouped in three main categories: snow, groundwater, and soil parameters, where a-i references:

- a Neitsch et al. (2002), Maidment (1993), TCI and ARD (2004).
- b Anderson et al. (1976).
- c Huber and Dickison (1988).
- d USDA, NRCS (1999).
- e Sangrey et al.(1984).
- f Smedema and Roycroft (1983).
- g Lane (1983).
- h Chow (1959).
- i Halcrow and Cameous (2008), IIASES (1992), TCI and ARD (2004).

3.3.1 Coarse Adjustment and Calibration of Snow Pack/Melt Parameters

Several main parameters related to snow formation/pack and melt were adjusted to calibrate the modeled flow rates against the observed peaks in the hydrographs. The SWAT model classifies precipitation as snow or rain depending on the mean daily air temperature (SFTMP). The observed peaks in the hydrographs coincided with the flooding periods in February and March, the snow melting period; the largest of these peaks occurred in 2003 and 2005 (Figure 7). The seasonal growth and recession of the snow pack was defined using an areal depletion curve (Anderson et al., 1976). The snowmelt is constrained by the minimum snow water content that corresponds to 100% snow cover (SNOCOVMX) and a specified fraction of snow volume represented by SNOCOVMX that corresponds to 50% snow coverage (SNO50COV). SWAT assumes a nonlinear relationship between snow water content and snow pack. Because of the lack of snow pack/melt data, we assumed a linear relationship and assigned the SNOCOVMX a value of 0.5, which correlates to 50% of SNOCOVMX. The areal depletion curve affects snowmelt if the snow water content is below SNOCOVMX. In addition to the areal coverage of snow, snowmelt is also controlled by the snow pack temperature and melting rate. The former is influenced by a lagging factor (TIMP) and threshold temperature for snow melt (SMTMP). The melting rate is controlled by the maximum snowmelt factor (SMFMX) and the minimum snowmelt factor (SMFMN), estimated at 10 and 0, respectively, values that can account for the observed rapid snow melting during

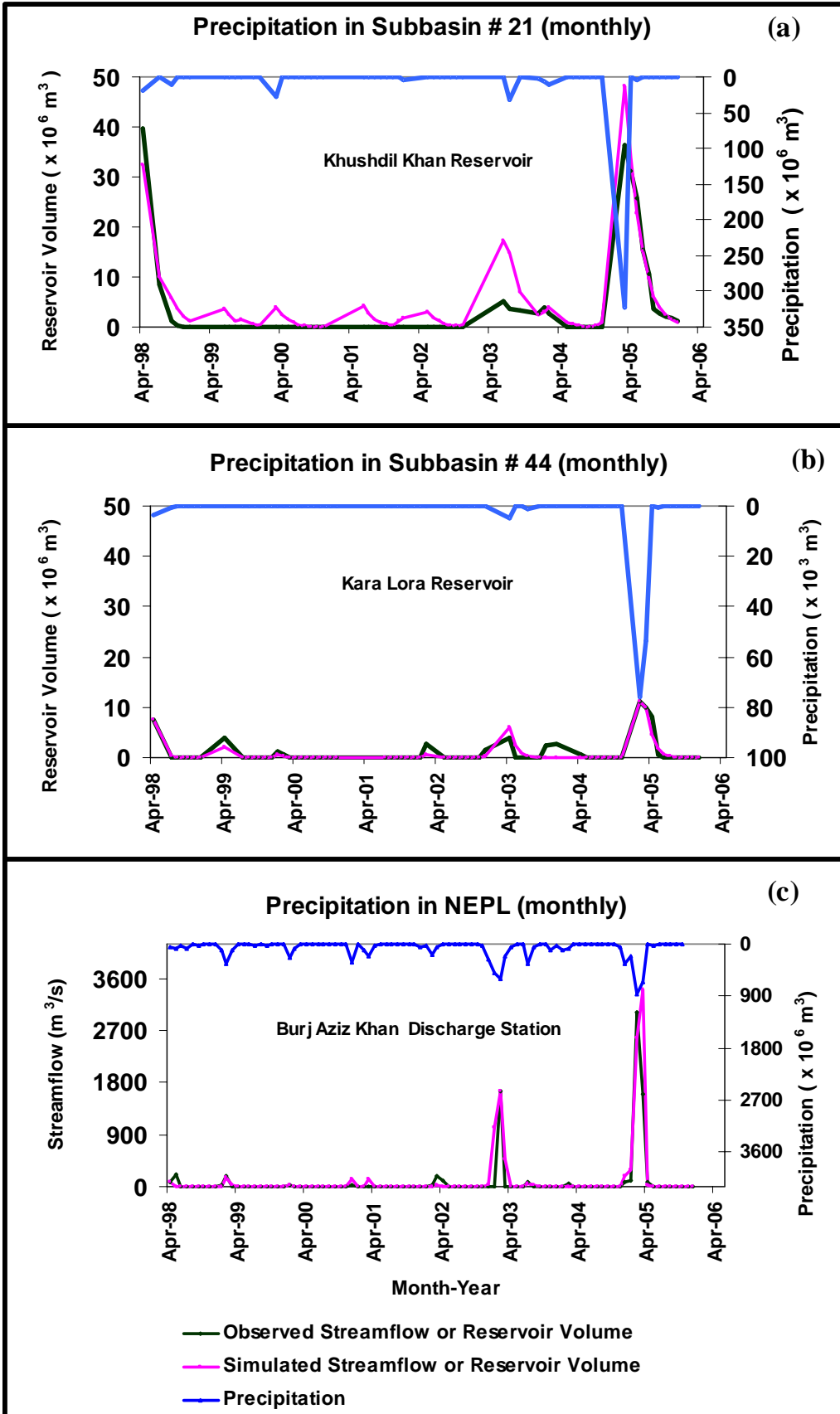
relatively short periods of time. The adjustments for the seven parameters (SFTMP, SNOCOVMX, SNO50COV, TIMP, SMTMP, SMFMX, and SMFMN) were made heuristically to achieve a general agreement between simulated and observed monthly hydrographs, particularly the large flood-induced peaks of 2003 and 2005. The characteristics of the simulated hydrograph were found to be more sensitive to the SNOCOVMX, SFTMP, and SMTMP parameters.

3.3.2 Delay Action/Storage Dams and Model Calibration against Reservoir Volume and Flow versus No Flow Conditions in Ephemeral Streams

The next step in the calibration process was to calibrate the flows in two of the major subbasins, taking advantage of the observed changes in reservoir volumes in these two areas. The reservoir volumes were calculated for each month using temporal Landsat scenes and SRTM data, except for the months reservoir areas were difficult to discern due to cloud coverage and/or poor-quality images. Reservoir volumes were calculated using the Three-Dimensional Analyst's Surface Volume Tool in ArcGIS 9.3.

Figure 7 shows time series calibration results (April 98-April 2006). (a) Time series for the simulated and observed (from satellite data) reservoir volume for the Khushdil Khan Reservoir. (b) Time series for simulated and observed reservoir volume for the Kara Lora Reservoir. (c) Time series for simulated and observed stream flow at the Burj Aziz Khan station. Also shown are TRMM-derived monthly precipitation values over subbasin #21 (a), subbasin #44 (b), and the NEPL watershed (c).

Figure 7 Time Series Calibration Results



The Landsat images were also used to extract first-order estimates of the reservoir storage parameters required for modeling reservoir storage and routing in SWAT. For the Khushdil Khan and Kara Lora reservoirs (Figure 5), these parameters include (1) RES_PVOL, the volume of water that fills the reservoir to the principal spillway, assumed to be the volume of the reservoir at its largest observed areal extent and estimated at $53.7 \times 10^6 \text{ m}^3$ and $11 \times 10^6 \text{ m}^3$ for the Khushdil Khan and Kara Lora reservoirs, respectively; (2) RES_PSA, the surface area of the impounded water body that fills the reservoir to the principal spillway, assumed to be the largest observed areal extent for the reservoir and estimated at $5.2 \times 10^6 \text{ m}^2$ and $0.8 \times 10^6 \text{ m}^2$; (3) RES_EVOL, the volume of water that fills the reservoir to the emergency spillway, estimated at $59 \times 10^6 \text{ m}^3$ and $12 \times 10^6 \text{ m}^3$; and (4) RES_ESA, the surface area of the impounded water that fills the reservoir to the emergency spillway, estimated at $5.7 \times 10^6 \text{ m}^2$ and $0.9 \times 10^6 \text{ m}^2$. Because RES_ESA has to be larger than RES_PSA, the former was estimated by multiplying the latter by an arbitrary multiplier (1.1). The same arbitrary multiplier was used to estimate RES_EVOL from RES-PVOL. The use of temporal satellite imagery for calibration purposes was not solely restricted to monitoring reservoir volumes; the images were also used to examine whether the main rivers were dry or wet (i.e., flowing or not flowing), and the model was calibrated to account for such types of observations.

Soil and groundwater parameters were adjusted to achieve finer fitting with estimated reservoir volumes. The groundwater parameters include soil available water capacity (SOL_AWC), soil evaporation compensation coefficient (ESCO), threshold water levels in shallow aquifer for base flow (GWQMN), re-evaporation/deep aquifer percolation (REVAPMN), re-evaporation coefficient (GW_REVAP), delay time for groundwater recharge (GW_DELAY), and base flow recession constant (ALPHA_BF). These parameters dictate the amount of water flow through the soil zone and underlying aquifer to the stream channel as well as the timing (Table 2). The GWQMN, SOL_AWC, and hydraulic conductivity of reservoir bottom (CH_K) were found to be the major parameters affecting the reservoir volume.

3.3.3 Model Calibration against Stream Flow Data

The next step in the calibration process was to calibrate the modeled flow against the observed hydrograph at the Burji Aziz Khan station. All calibration parameters (Table 3) were used for the calibration in this step with emphasis on those related to channel routing. Transmission losses through channels were calculated for both tributary and main channels. The key parameter for losses is the effective hydraulic conductivity (CH_K). Most tributary channels are ephemeral or intermittent, receiving little groundwater, and are thus likely to lose water to bank storage or to the underlying aquifer, whereas the main channels receive groundwater through lateral flow from soils, and thus the transmission losses for these channels are minimal (Lane, 1983). The initial hydraulic conductivity (CH_K1) values (0.5 mm/hr) were adjusted (adopted value: 100.0 mm/hr). A small transmission loss for the main channels was simulated by setting effective hydraulic conductivity (CH_K2) close to the SWAT default value (0.5 mm/hr) (Table 3).

3.3.4 Calibration Criteria and Model Evaluation

The model parameters were adjusted in a SWAT domain using the procedures outlined above until the overall simulated values for stream flow were similar to the observed values. Two statistical measures, coefficient of determination (R^2) and coefficient of efficiency COE (Nash and Sutcliff, 1970), were used to quantify the achieved levels of calibration and evaluate the overall performance of the model. Figure 6 compares the simulated reservoir volumes to those extracted from satellite data, and simulated stream flow to observed stream flow over the calibration period (1998–2005). Visual inspection of Figure 6 shows a close agreement between simulated and observed monthly reservoir volumes and flow rates throughout the calibration period. High degrees of correlation were achieved between satellite-derived reservoir volumes and simulated reservoir volumes (R^2 : 0.85 and 0.86; COE: 0.89 and 86; Figure 7), as well as a good correlation between observed and simulated stream flow values at the watershed outlet (R^2 : 0.78, COE: 0.69; Figure 7).

CHAPTER 4

DISCUSSIONS

4.1 Novelty of Model

The NEPL, like the majority of the world's basins, lacks adequate field data for the construction and calibration of reliable rainfall-runoff models. With daily precipitation extracted from a single precipitation gauge (Quetta Station) in the NEPL, and with simulated flows calibrated against stream flow from the only gauge at the outlet of the watershed, any constructed rainfall-runoff model for the basin will undoubtedly yield unreliable results. Because of the lack of adequate field data in the NEPL, previous attempts (e.g., Kazmi et al., 2003; Shan et al., 2002; TCI et al., 2004; WAPDA, 2001) to assess water resources in the NEPL in particular, and the Pishin Lora basin in general, were based largely on simplified water balance calculations in which the essential parameters (e.g., evapotranspiration, runoff, and groundwater recharge) were extracted locally from limited observations from few field gauging stations in the Quetta Valley and the surrounding area. The uncertainties associated with such water-balance calculations in the NEPL basin and its surroundings are reflected in the large variations in the reported mean annual rainfall (150 to 300 mm/year, or 1.3 to 2.6 10^9 m³/year) and in the estimated partitioning of the rainfall into runoff (5– 20%), evapotranspiration (38– 78%), and infiltration/recharge (20–40%) (e.g., Kazmi et al., 2003; Shan et al., 2002; TCI et al., 2004; WAPDA, 2001). The results from such studies should be regarded with caution because of the extreme temporal and spatial variability in precipitation, surface water, and the hydrologic parameters across the examined area (Kazmi et al., 2003; Tareen et al., 2008).

My approach addresses these problems by complementing the limited existing field data with observations derived from readily available remote sensing datasets. The remote sensing data are used as input to the model and for calibration purposes. Precipitation was derived from TRMM data covering the entire NEPL area and surroundings with 36

picture elements (i.e., stations; Figure 4a). Earlier studies (Chiu et al., 2006; Chokngamwong and Chiu, 2006; Milewski et al., 2009a; Turk et al., 2003) cautioned against uncertainties in TRMM-derived precipitation, but our comparisons showed a good correspondence (R^2 : 0.89; Figure 6a) between precipitation from the Quetta rain gauge and that derived from TRMM data over the same area.

The use of satellite-based precipitation data provided adequate spatial coverage with uninterrupted data for some 8 years and captured topography-related variations in precipitation in the area. It has been shown in many mountainous areas worldwide that precipitation over the mountains far exceeds that in the surrounding valleys (Death Valley: Osterkamp et al., 1994; Saudi Arabia: Sorman and Abdulrazzak, 1993). Similar trends were observed in the study area; a positive correlation is observed between the average elevation and TRMM-derived average annual (1998–2005) precipitation over the Takhatu mountain ranges and the surrounding valleys and lowlands (Figs. 1 and 6c). The average annual TRMM-derived precipitation over the NEPL is 155 mm/year, or 1.31×10^9 m³/year, approximately 30% more than the estimates (125 mm/year, or 1.06×10^9 m³/year) that assume the same reported precipitation from the Quetta station across the entire NEPL basin.

Average annual precipitation for the NE (area: 2,945 km²), NW (2,379 km²), and southern basins (3,146 km²) of the NEPL were estimated from TRMM data at 194 mm/year (570×10^6 m³), 134 mm/year (320×10^6 m³), and 124 mm/year (390×10^6 m³), respectively (Figure 8c). As expected, the NE basin, which has the highest elevation (average elevation: 2700 m a.m.s.l), receives the highest amount of precipitation; the southern basin, the basin with the lowest elevation (average elevation: 1600 m a.m.s.l), receives the least amount of precipitation; and the NW basin, with intermediate average elevation (average elevation: 2200 m a.m.s.l), receives intermediate amounts of precipitation (Figs. 1, 4i, and 8ab).

Figure 8: Precipitation and Elevation for TRMM Station

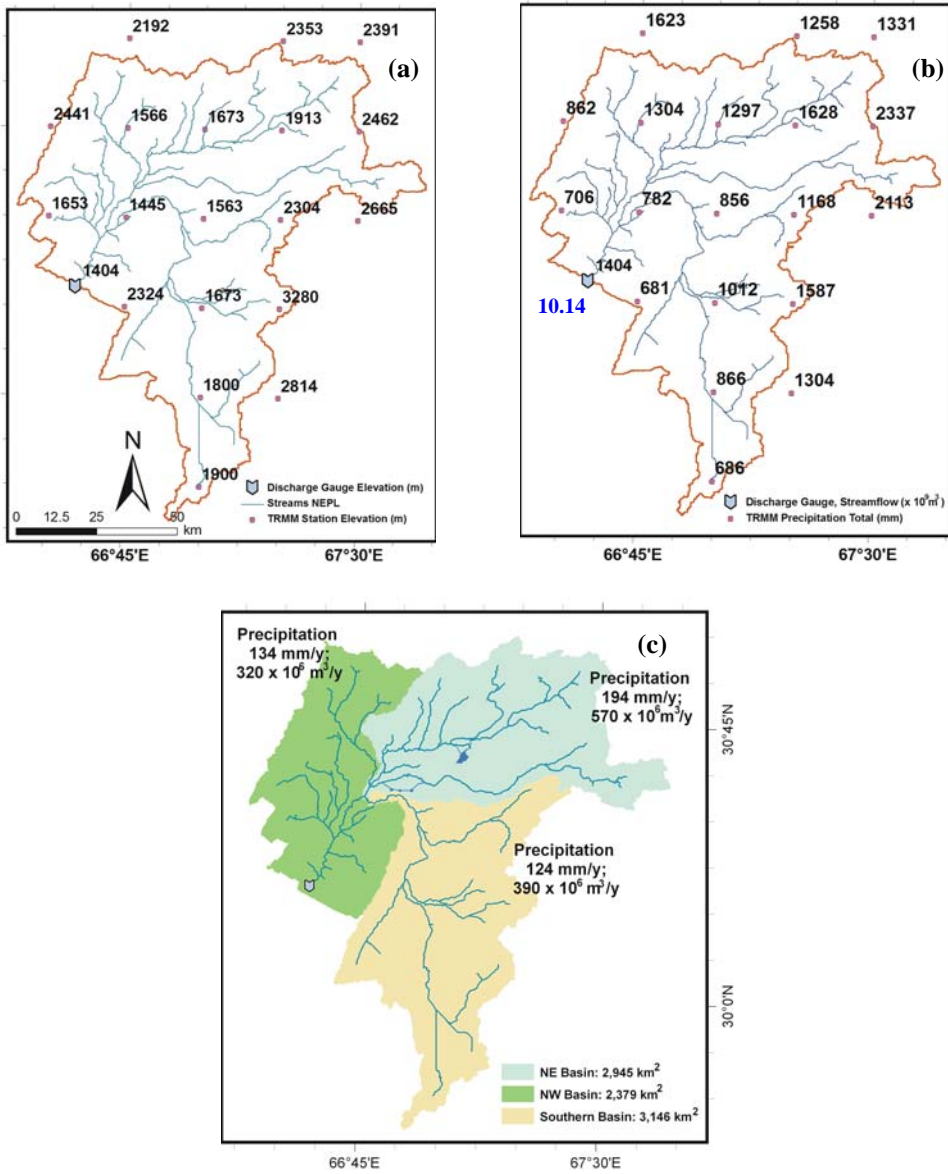


Figure 8 shows precipitation and elevation for TRMM stations in the NEPL and its major basins. (a) Elevations for each of the TRMM picture elements within NEPL measured at its center. (b) Cumulative precipitation (1998 to 2005) for each of the TRMM stations within NEPL. Also shown is the cumulative simulated stream flow for the same duration at the Burj Aziz Khan station. (c) Average Annual TRMM precipitation over the three major basins in the NEPL, namely the NE, NW and Southern basins.

Calibrating each of the basins is an important step toward the calibration of the entire watershed. To compensate for the lack of adequate stream flow gauge data coverage for the NEPL, we took advantage of temporal changes in the areal extent of the reservoirs—such as those observed on temporal satellite imagery for the months of March 2000 (Figure 9d), March 2003 (Figure 9e), and March 2005 (Figure 9f)—to calibrate the simulated flow. The estimated volumes of impounded water for these three periods are 0.0 m^3 , $7.2 \times 10^6 \text{ m}^3$, and $53.7 \times 10^6 \text{ m}^3$, respectively. The use of temporal satellite imagery for calibration purposes was not solely restricted to monitoring the temporal variations in reservoir volumes, but the images were also used to examine whether the main rivers were dry or wet. For example, our examination of cloud-free, temporal satellite images (64 images; one to two images/month on average) acquired over the Rokhi Lora River at the outlet of the southern subbasin 49 (Figs. 3b and 5) between 1998 and 2005 indicated that the river remained dry throughout the examined period except in the springs of 2003 and 2005 (Figs. 9b and 9c). These observations were accounted for in the calibrated model. The calibrated model yielded no flow at this location except for the months of February and March in 2003, when the simulated flow was 39.8 and $19.4 \text{ m}^3/\text{s}$, and in the months of February, March, and April 2005, when the simulated flow was 58.8 , 114.1 , and $7.4 \text{ m}^3/\text{s}$, respectively. Similar observations that pertain to the presence or absence of water in the main ephemeral streams across the NEPL watershed throughout the calibration period were made from temporal satellite data and used to calibrate the model as described above.

Figure 9: Temporal Landsat Band 5 Images

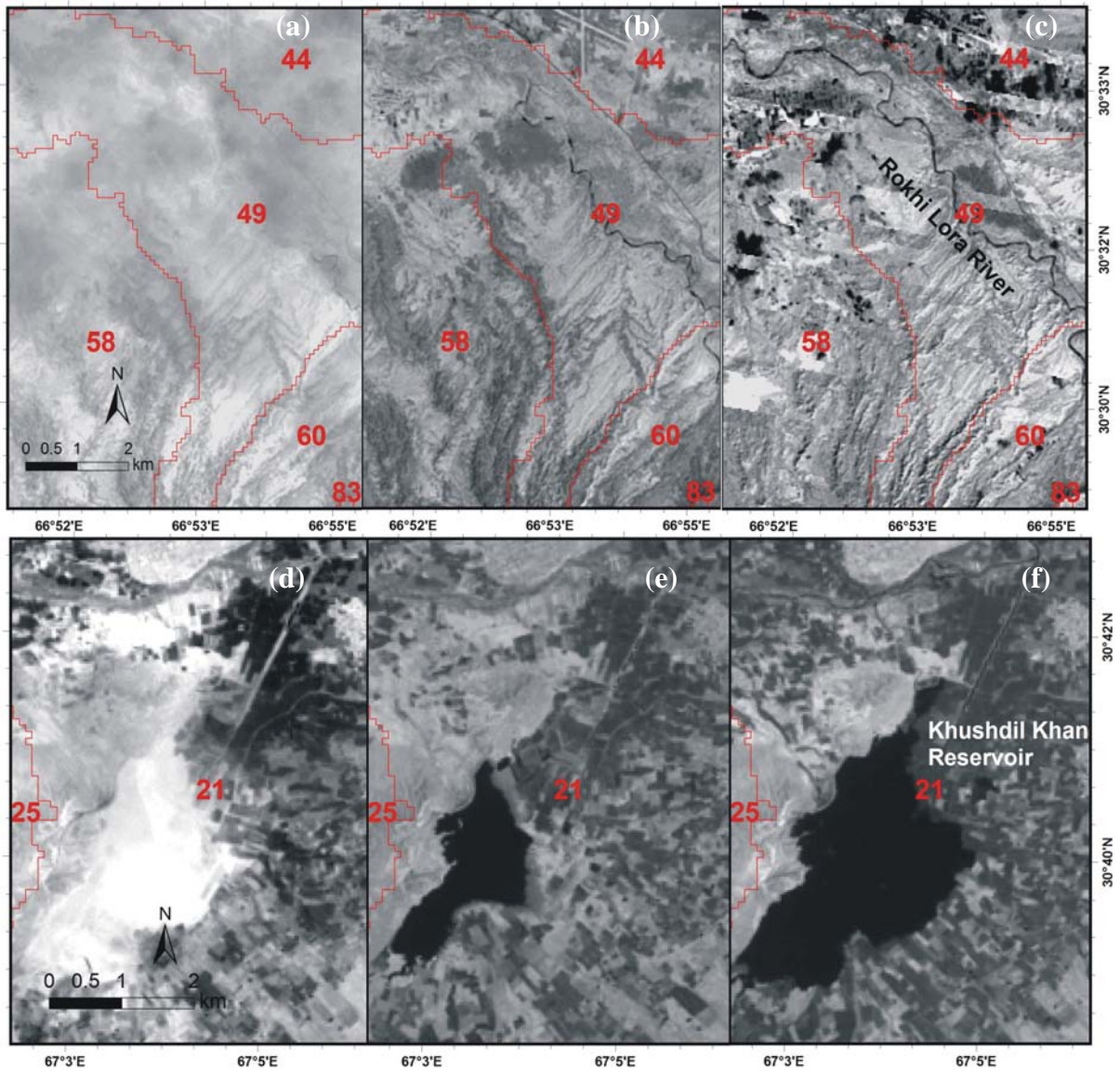


Figure 9 shows temporal Landsat band 5 images over the ephemeral Rokhi Lora River and the Khushdil Khan reservoir under flowing and non-flowing conditions. In wet periods, streams appear as dark lines (b, c) and reservoirs filled by impounded waters appear as dark polygons (e, f), whereas in dry periods streams and reservoirs appear in bright shades making them indistinguishable from their surroundings (a, d).

4.2 Model Applications

The calibrated model serves a number of purposes, the most important of which include (1) providing an understanding of the spatial and temporal partitioning of precipitation into runoff, recharge, and evapotranspiration, and (2) utilizing the model to simulate various water management scenarios. In Table 4, we provide model results for the entire basin and for each of the three major basins within the NEPL watershed, namely the NE, NW, and southern basins (Figs. 1, 4i, and 5), to better understand spatial variations in the partitioning of precipitation from one part to another in the NEPL with such an understanding we use the calibrated model to examine various potential scenarios for water management across the NEPL.

The average annual precipitation ($1,280 \times 10^6 \text{ m}^3$; 151.1 mm/year) in the NEPL (Table 4) is partitioned as follows: (1) runoff is estimated at the Burji Aziz Khan station at $72 \times 10^6 \text{ m}^3/\text{year}$ (6% total precipitation), (2) recharge is estimated at $361 \times 10^6 \text{ m}^3/\text{year}$ (28% total precipitation), and (3) evapotranspiration (initial losses) estimated at $847 \times 10^6 \text{ m}^3/\text{year}$ (66% total precipitation). The recharge reported in Table 5 includes contributions from transmission losses ($22.8 \times 10^6 \text{ m}^3/\text{year}$; 2% total precipitation), reservoir seepage ($74.6 \times 10^6 \text{ m}^3/\text{year}$; 6% total precipitation), percolation out of soil ($280 \times 10^6 \text{ m}^3/\text{year}$; 22% total precipitation), and water moving out of the soil ($16 \times 10^6 \text{ m}^3/\text{year}$; 1%). Earlier attempts did not fully account for large variability (of precipitation, elevation, hydrologic properties, etc.) across the watershed.

Table 4: Modeled Average Annual Values

Basin	Basin Area		Average Precipitation Depth	Annual Precipitation Volume		ET		Recharge		Surface Runoff	
	km ²	% of NEPL	mm/y	x 10 ⁶ m ³ /y	Basin Precip (%)	x 10 ⁶ m ³ /y	Precip (%)	x 10 ⁶ m ³ /y	Precip (%)	x 10 ⁶ m ³ /y	Precip (%)
NE	2945	35%	194	571	45%	364	64%	172	30%	38	7%
NW	2379	28%	134	320	25%	208	65%	84	26%	26	8%
Southern	3146	37%	124	389	30%	275	71%	105	27%	8	2%
NEPL	8,470	100%	151	1280	100%	847	66%	361	28%	72	6%

Table 4 shows modeled average annual (1998–2005) values of hydrologic variables for the NEPL watershed and its three major basins (NE, NW and Southern basins).

Table 5: Scenarios

Proposed Delay Action Dams		Average Annual Recharge				Stream flow	
Scenarios	Location	Reservoirs seepage		Net Recharge		Runoff on Burj Aziz Khan Discharge Station	
		x 10 ⁶ m ³ /y	%	X 10 ⁶ m ³ /y	%	x 10 ⁶ m ³ /y	%
1: Reservoirs 1 and 2	Subbasins # 40, # 68	107	8%	393	31%	47	4%
2: Reservoir 3	Subbasin # 41	120	9%	404	32%	37	3%
3: Reservoirs 1, 2 and 3	Subbasin # 40, 68, 41	155	12%	432	34%	8.5	1%

Table 5 shows scenarios for increasing recharge by constructing reservoirs.

As described earlier, the highest precipitation rates are observed in the NE basin (194.0 mm/year), the lowest were observed in the southern basin (123.6 mm/year), and intermediate values (134.3 mm) were observed over the NW basin (Figure 8c; Table 4). The southern basin receives the lowest amount of precipitation and is largely covered by alluvial deposits (50.3% of total area) and karstified limestone (29.3% of total area) (Figure 3b). These features could explain the reduced runoff in the southern basin compared to the NW and NE basins (NW runoff: $26.4 \times 10^6 \text{ m}^3/\text{year}$; NE runoff: $37.8 \times 10^6 \text{ m}^3/\text{year}$; South runoff: $7.7 \times 10^6 \text{ m}^3/\text{year}$). The northern sections of the NW basin on the other hand, are largely covered (23.3% of total area) by outcrops of shale, a rock type that promotes runoff and inhibits recharge (Figure 3b). Indeed, the NE basin has the highest runoff ($37.8 \times 10^6 \text{ m}^3/\text{year}$), followed by the NW basin ($26.4 \times 10^6 \text{ m}^3/\text{year}$). The NE basin experiences the largest amounts and proportions of recharge ($172 \times 10^6 \text{ m}^3/\text{year}$) compared to the NW ($84 \times 10^6 \text{ m}^3/\text{year}$) and southern basins ($105 \times 10^6 \text{ m}^3/\text{year}$). This is largely related to the infiltration of the runoff impounded behind the two major reservoirs and the presence of extensive outcrops of alluvial deposits (34.2% of total area) and sandstone (52.8%) that facilitate infiltration within the basin (Figure 3b).

The position of the two reservoirs, the Khushdil Khan and the Kara Lora (Figure 5), were carefully selected; they collect runoff from watersheds that cover a large area (Khushdil Khan: 1320 km^2 ; Kara Lora: 960 km^2), with source areas that receive large amounts of precipitation in the high Takhatu mountain range (Figure 1). Runoff at the dam locations is substantial; using the calibrated model, we estimate that the average annual (1998–2005) stream flows at Khushdil Khan and Kara Lora are $65 \times 10^6 \text{ m}^3$, and $35 \times 10^6 \text{ m}^3$, respectively. Moreover, the reservoirs are floored by thick (up to 900 m) and extensive alluvial deposits that enhance recharge (Kazmi et al., 2003; TCI et al., 2004).

The delay action dams were constructed for one main purpose, to increase infiltration. Currently, water consumption in the NEPL is about $400 \times 10^6 \text{ m}^3/\text{year}$ (Halcrow and Cameous, 2008; TCI et al., 2004), which exceeds our estimates for recharge ($361 \times 10^6 \text{ m}^3/\text{year}$; Table 4), even with the Khushdil Khan and the Kara Lora reservoirs in place. The difference is substantial, approximately $40 \times 10^6 \text{ m}^3/\text{year}$. Currently, population is

concentrated in the southern part of the NEPL, and so are the delay action dams; over 100 small dams were constructed in the southern basin of the NEPL (Halcrow and Cameous, 2008). The concentration of the population in the southern basin and the reduced precipitation in this area contributed to the reduced runoff from the southern basin (Table 4). No additional delay action dams are proposed in the southern basin; instead, we suggest that such dams be created in the NE and NW basins. Using criteria similar to those noted above for the Khushdil Khan and Kara Lora reservoirs, we suggest three locations for the construction of delay action dams, two in the NW basin and a third in the NE basin (Figure 5). One of the two proposed dams (reservoir 1) in the NW basin is on the Arambi Manda River (Figs. 3b and 5) at the outlet of subbasin 40 and the other (reservoir 2) is on the outlet of subbasin 68. The latter impounds runoff from the Loe Kandil Chul and the Loe Dara Rivers (Figs. 3b and 5). The size of the drained subbasins is large (reservoir 1: 620 km²; reservoir 2: 940 km²); their source areas are in the surrounding Takhatu mountain range, which receives substantial precipitation. The average annual runoff impounded by the dams is large (reservoir 1: 14 × 10⁶ km³; reservoir 2: 10 × 10⁶ km³), and the area over which the reservoir will be developed is covered by thick (up to 900 m) alluvium with high infiltration rates (Kazmi et al., 2003; TCI et al., 2004).

Despite the fact that two major reservoirs were constructed on the NE basin and a considerable fraction of the recharge in this basin is attributed to the construction of the two dams, the runoff at the outlet of the NE basin is still the highest (37.8 × 10⁶ m³) of the three basins (Table 4). We propose an additional reservoir (reservoir 3) at the outlet of subbasin 41 (Figure 5). The size of the drained area is large (720 km²; Figure 5); its source area is in the Takhatu mountain range, with elevations reaching up to 4000 m AMSL (Figure 1) and precipitation rates of up to 700 mm/year (Figure 4). As is the case with all the existing and suggested dam locations, alluvial deposits are widespread (34% of the NE basin) and thick (up to 900 m) (Kazmi et al., 2003; TCI et al., 2004).

Three scenarios were considered. The first calls for the construction of reservoirs 1 and 2, the second for the construction of reservoir 3, and the third for the construction of

reservoirs 1, 2, and 3 (Figure 5). Reservoir parameters were assumed to be similar to those assigned for the existing reservoir in subbasin 21 (Figure 5). The results of these simulations are given in Table 5. The table shows a progressive increase in reservoir seepage and recharge for scenarios 1 through 3 (scenario 1: 107×10^6 m³/year, 393×10^6 m³/year; scenario 2: 120×10^6 m³/year, 404×10^6 m³/year; and scenario 3: 155×10^6 m³/year, 432×10^6 m³/year). If we were to implement scenarios 1, 2, or 3, we could achieve sustainable to near-sustainable systems in which the recharge (393 to 432×10^6 m³/year; Table 5) approximates or exceeds consumption (400×10^6 m³/year) (Halcrow and Cameous, 2008; TCI et al., 2004). This would come at the expense of decreased runoff at the Burji Aziz Khan station. Annual flow is estimated to decrease from 72×10^6 m³/year to 47×10^6 m³/year with the implementation of scenario 1. If scenarios 2 and 3 were to be implemented, the flow will be reduced to 37×10^6 m³/year, and 8.5×10^6 m³/year, respectively. A cost-effective alternative to the construction of a limited number of large dams (e.g., reservoirs 1, 2, and 3) would be to develop tens of smaller delay action dams in the NE and NW basins over areas covered by alluvial deposits. Such small dams could be constructed in the NW basin in subbasins 23, 40, 48, 54, 56, 57, 61, 62, and 68 and in the NE basin in subbasins 25, 28, 29, 31, 33, 41 (Figure 5).

CHAPTER 5

CONCLUSIONS

The NE part of Pishin Lora (NEPL) is one of the poorest and most disadvantaged provinces in Balochistan; it is currently facing severe water shortages that are largely related to migration from neighboring war-infested Afghanistan and drought-related population migration from the rural areas to urban centers. Given the difficulty of accessing the region and the paucity of field data, we adopted methodologies that rely heavily on readily available remote sensing technologies as viable alternatives and useful tools for the assessment and management of the water resources of these remote regions. We constructed a catchment-based continuous (1998–2005) rainfall-runoff model for the NEPL watershed and calibrated the model against stream flow data and observations extracted from temporal satellite imagery. Inputs to the model included satellite-based 3-hourly TRMM precipitation data, and modeled runoff was calibrated against (1) estimates of water volumes impounded behind the Khushdil Khan and the Kara Lora reservoirs, where the reservoir volumes were extracted from digital topography and temporal satellite images, and (2) satellite-based observations pertaining to the presence or absence of water in streams across the NEPL within the investigated period. Finally, the simulated runoff at the outlet of the watershed was calibrated against observed flow as reported from the Burj Aziz Khan station.

Using the calibrated model, the average annual precipitation (1998–2005), runoff, and net recharge were estimated at $1,300 \times 10^6 \text{ m}^3$, $148 \times 10^6 \text{ m}^3$, and $361 \times 10^6 \text{ m}^3$, respectively. The calibrated model was also used to characterize the spatial and temporal variations in water partitioning within the various basins, namely the NE, NW, and southern basins. The highest precipitation rates (194 mm/year) and runoff ($37.8 \times 10^6 \text{ m}^3/\text{year}$) are in the NE basin, and the lowest rates (123.6 mm/year) and runoff ($7.7 \times 10^6 \text{ m}^3/\text{year}$) in the southern basin, whereas the NW basin experiences intermediate precipitation rates (134.3 mm/year) and runoff values ($26.4 \times 10^6 \text{ m}^3/\text{year}$). The calibrated model was also used to

examine scenarios for sustainable management of the water resources of the NEPL. Results indicate that the construction of delay action dams in the NE and NW basins of the NEPL could increase recharge from $361 \times 10^6 \text{ m}^3/\text{year}$ to up to $432 \times 10^6 \text{ m}^3/\text{year}$ and achieve sustainable extraction.

The developed methodologies can be applied to many parts of the less-studied watersheds of the world, especially in areas where field data is inadequate and accessibility is limited. One of the main features of our methodology is the utilization of global datasets that are readily available for most of the world's land surface. The adopted methodologies are not a substitute for traditional approaches that require extensive field datasets, but they could provide first-order estimates for rainfall, runoff, and recharge over large areas that lack adequate coverage with stream flow and precipitation data.

CHAPTER 6

FURTHER RESERACH

6.1 Potential Reservoirs Types

Currently, the main water source for the local population in NEPL, including the most populated area of the Quetta Valley, is from alluvial aquifers collecting runoff from surrounding mountains. Over-pumping in this region has caused the water table to drop. There is a need to look for other settings (reservoir types) if we were to satisfy the increasing demand for groundwater in the study area.

The hydrological model developed in this study is useful for one of the main tasks when it comes to water management. That is the estimation of the partitioning of precipitation into runoff, recharge, and evapo-transpiration. Another important task that should be attended to is the identification of potential reservoir types. Investigating the types of reservoirs to be found in fold and thrust belts in general, and in the Pishin Lora area in particular, is an important direction of research.

One of the advantages of the generation of digital datasets and their incorporation into a web-based GIS is to enable the analysis of spatial data sets for a better understanding of the hydrologic settings in the study area. Regional and detailed geological maps, remote sensing data, and topographic maps could be used in a GIS environment to identify lithologic and structural controls on existing wells locations. We then use the acquired understanding of such settings to look for locations that portray similar geologic and hydrogeologic settings. The idea is that the location of productive wells give us clues as to where should we be looking for groundwater elsewhere.

An extensive web-based GIS that incorporates all relevant data sets including co-registered digital geologic maps, remote sensing data, hydrologic parameters, drainage patterns,

structural elements, well locations, soil maps, was generated. The web-based GIS incorporates the following categories of data sets:

- Geophysics (e.g., Earthquakes)
- Topography (e.g., Topo maps, SRTM)
- Remote Sensing (e.g., ASTER, TRMM)
- Hydrology (e.g., Streams, Soils, Wells)
- Geology (e.g., Tectonics)

Examples of the digital data sets in web-based GIS:

- Mosaic of Geologic Maps
- Coverage of faults extracted from geologic maps
- Mosaics of individual Landsat TM bands 1 through 7
- Mosaic of Landsat TM bands 2, 4, and 7
- 3 TM band ratio mosaic ($5/4 \times 3/4$, $5/1$, $5/7$)(Fig. 10)
- DEM (Digital Elevation Model) generated from ASTER
- Coverage of stream networks derived from DEM data
- Watershed boundaries derived from DEM data
- TRMM (5 years) precipitation data
- Well data (field, geochemical, and isotopic data)

Each of such images can portray information that could be useful in the identification of potential well locations. For example, the 3 TM band ratio image could be useful for lithologic and structural interpretations. Specifically, the band ratio images are useful for the identification of rock/soil types, fold/faults, shear zones. For example, band ratio $5/4$ is sensitive to mafic Fe-bearing aluminosilicates. Band Ratio $5/1$ is sensitive to felsic (Si) rocks, spectrally opaque minerals as magnesium (Mg). Band Ratio $5/7$ is sensitive to hydroxyl (OH) - bearing minerals (Sultan et al., 1987).

In Figure 10 serpentinites appear in shades of red, rocks rich in Fe-bearing aluminosilicates in shades of blue, and granitic rocks in shades of green. The same products could be used to identify folds and to map thrust and strike slip faults.

Figure 10: Lithologic and Structural Features from Remote Sensing Data

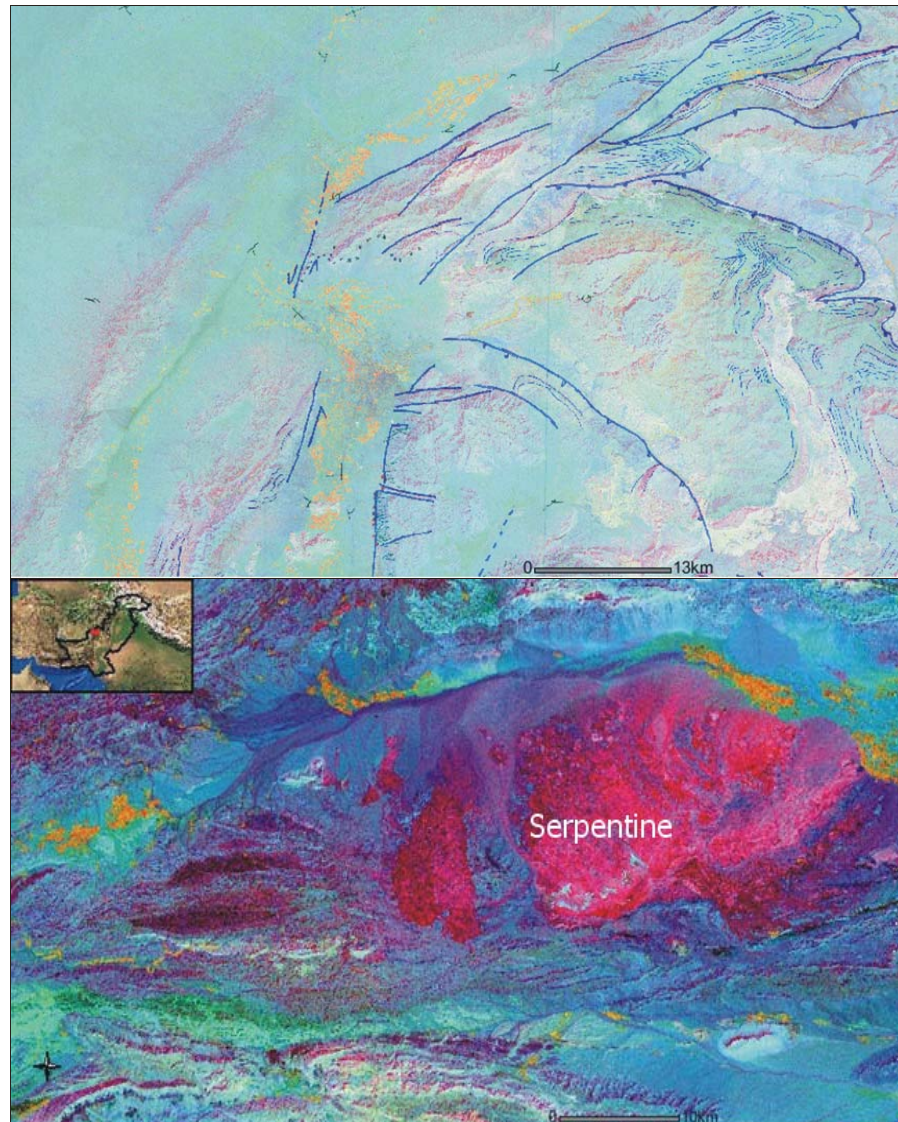


Figure 10 Color composite of Landsat TM band ratio image that could be used for lithologic and structural interpretations

Our preliminary analysis indicated the following types of reservoirs within NEPL:

- (A) Alluvial aquifers collecting runoff from surrounding mountains
- (B) Intersection of shear zones
- (C) Fractured bedrock
- (D) Intersection of fractured bedrock with folded bedrock
- (E) Folded bedrock

Alluvial aquifers are overexploited in NEPL. Water supply in the area is largely dependant on groundwater extracted from alluvial aquifers. Over-pumping from this reservoir type for domestic and irrigation caused a gradual depletion of this aquifer over the years. The aquifers in the bedrock, on the other hand, have not been well utilized. I will briefly show examples for a number of these reservoir types. Figure 11 shows one of bedrock aquifer types identified in the area. Successful wells (green circles) are located at the intersection of N-NE and S-SW shear zones (white arrows). Area outlined by an E-W trending oval at the area of intersection of these two shear zones is the area suggested for detailed geophysical work for drilling productive wells.

Figure 11: Bedrock Reservoirs: Intersection of Shear Zones

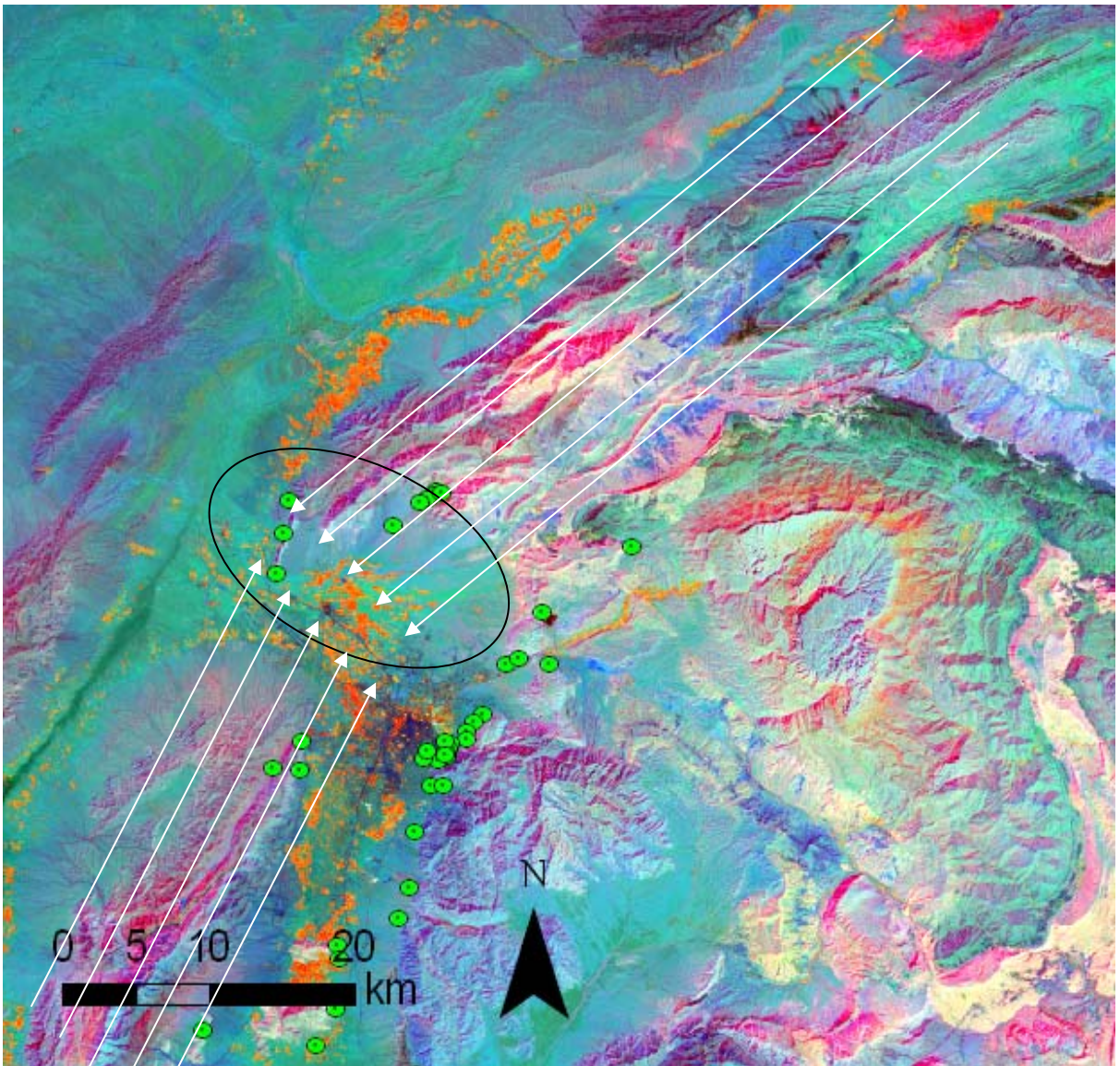


Figure 11 Potential bedrock reservoirs at the intersection of shear zones (area outlined by an ellipsoid). Green circles represent successful well locations and the image is a Landsat band ratio image: Red 5/4 Blue 5/1 Green 5/7

Figure 12: Bedrock Reservoirs: Intersection of Shear Zones, 3D View

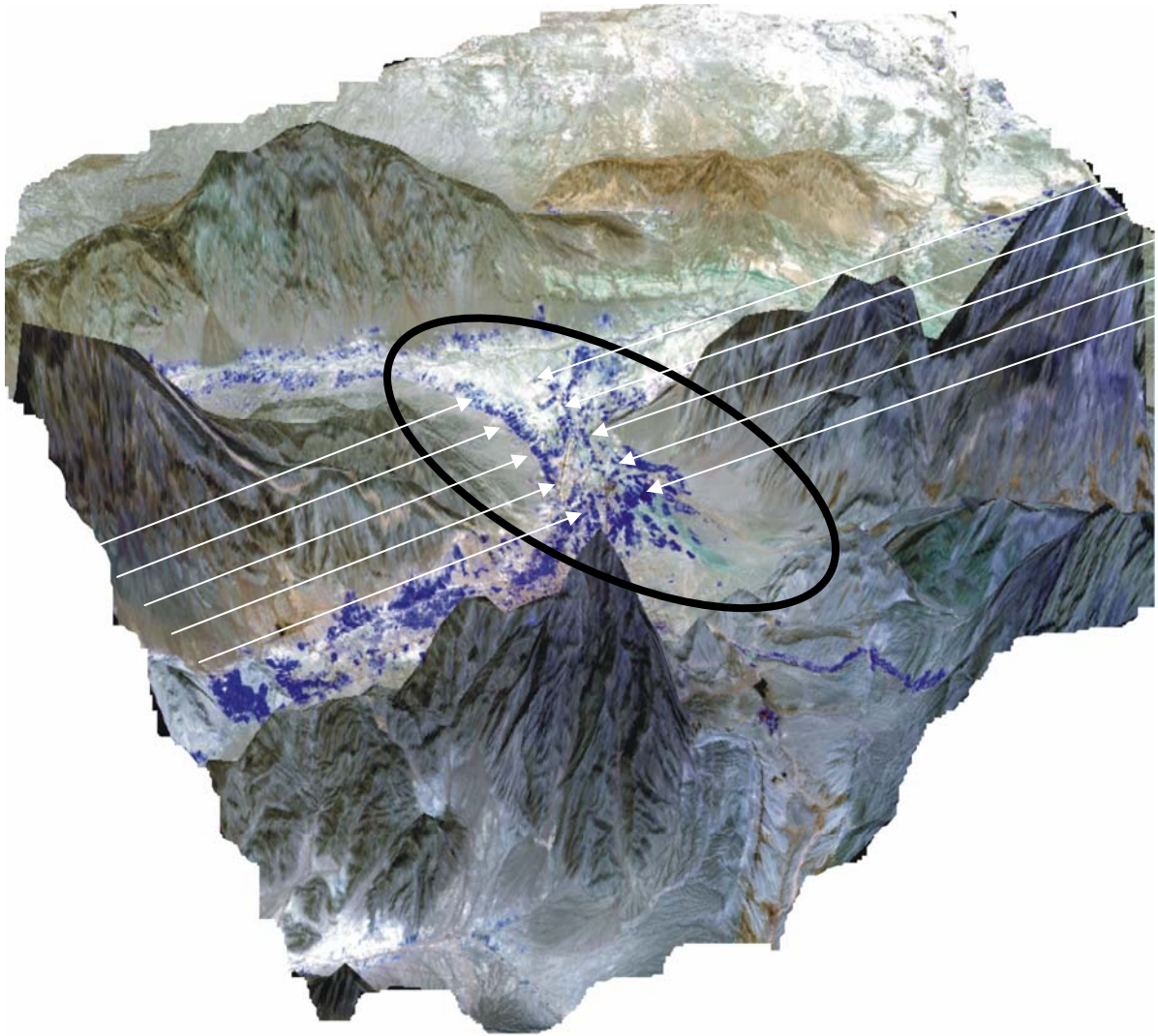


Figure 12 represents 3D view showing potential bedrock reservoirs at the intersection (area outlined by ellipse) of the shear zones shown in Fig. 11. ASTER band composite Bands 1, 2, 3 draped onto SRTM DEM.

The study area is a part of a folded fold-thrust belt. The extensive folding in the area that is manifested in many areas as plunging synclines (tectonic depressions) could offer opportunities for groundwater storage and transport (Figure 13). Ground water accumulation, aquifer development, water migration are largely controlled by structures in the NEPL. Layering of permeable fissured limestone and impermeable compact shale strata are the basis of the geologic structure of the area (Shan, 1972). Tectonic depressions can form an aquifer (Figure 13)

Figure 13: Tectonic Depressions

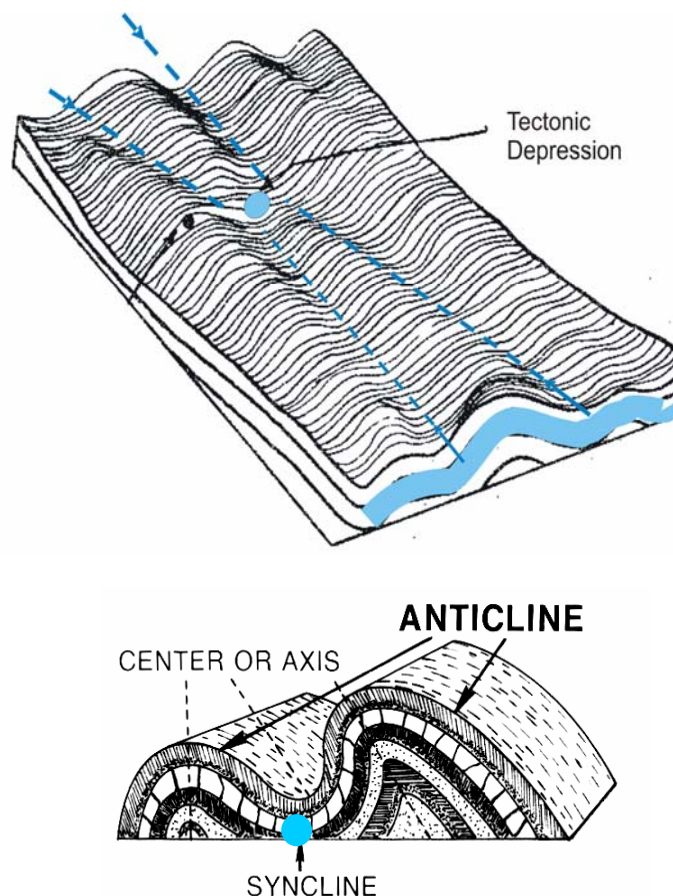


Figure 13 shows plunging anticline and syncline with folded permeable bed (karstified limestone) sandwiched between impermeable beds, where productive reservoirs can be located (modified from Shan, 1972)

Figure 14: Bedrock Reservoirs: Nose of Plunging Fold

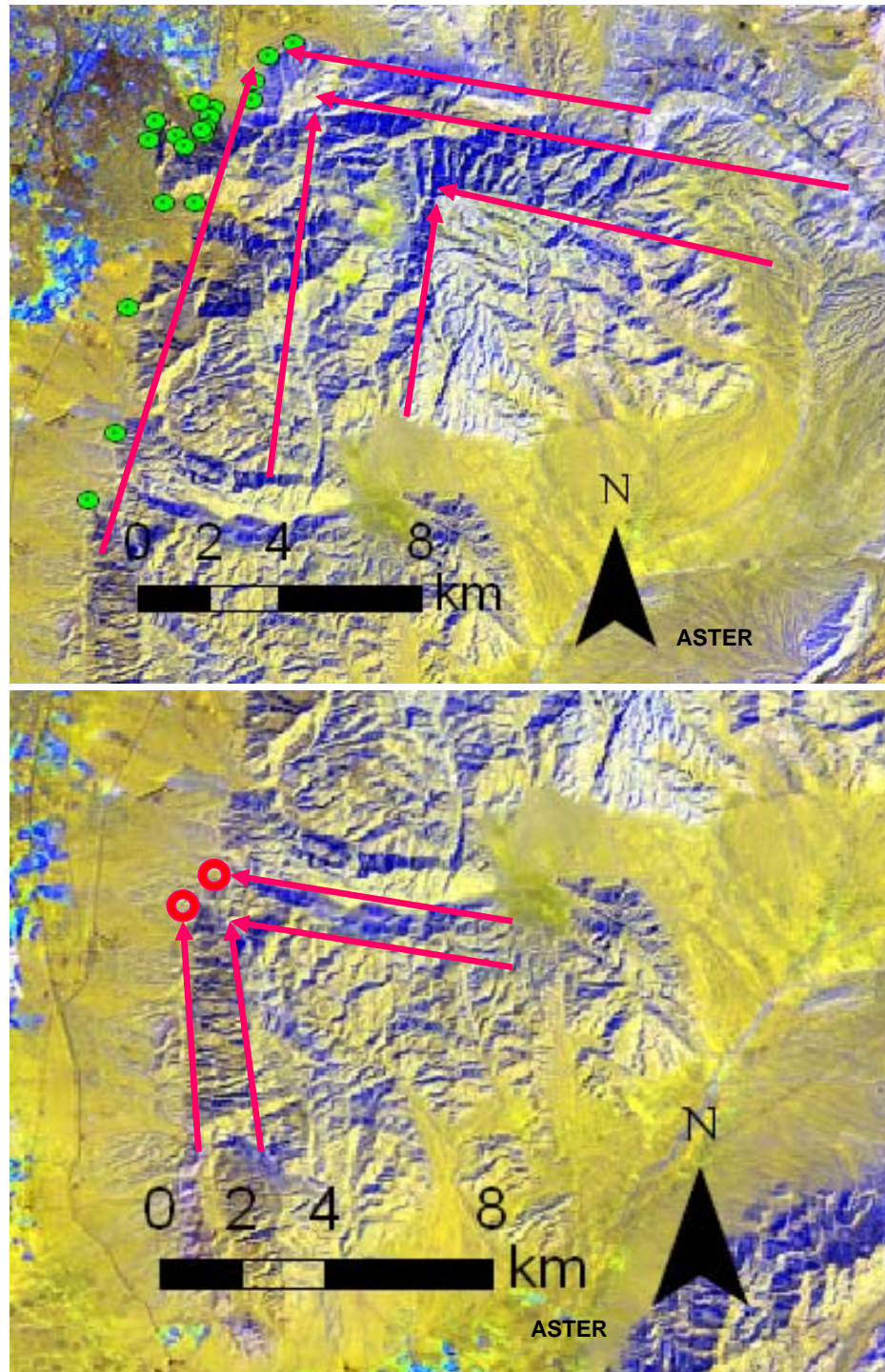


Figure 14 shows successful wells (green circles) at the nose of a plunging fold. The red lines are added to highlight the plunging nature of the fold. Suggested drilling locations (red circles) are at the nose of plunging fold. ASTER image

Figure 15: Bedrock Reservoirs: Nose of Plunging Fold 3D View

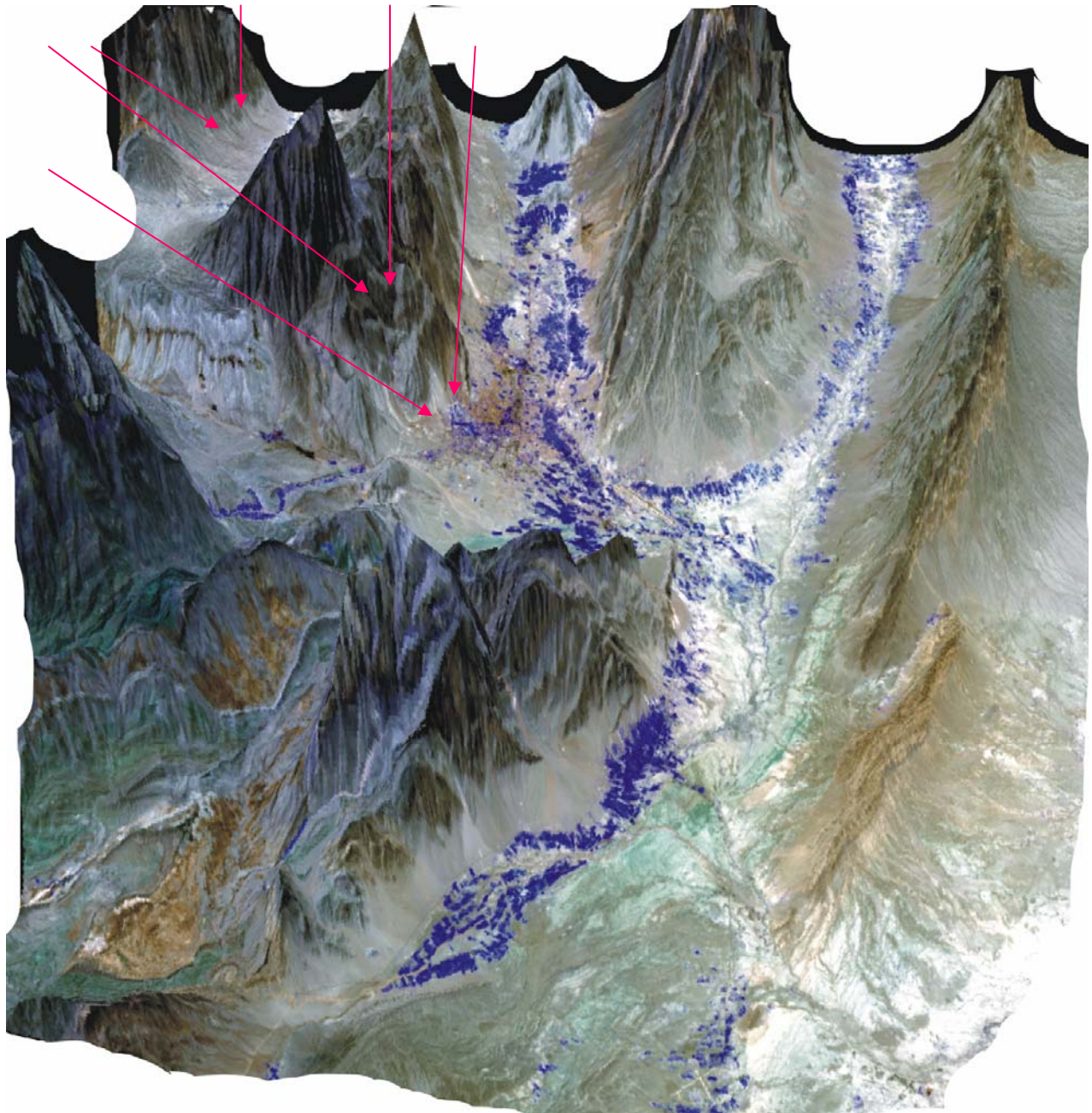


Figure 15 is 3D view of the intersection of nose of a plunging fold. ASTER band composite Bands 1, 2, 3 and DEM SRTM.

Figure 16: Bedrock Reservoirs: Shear Zones

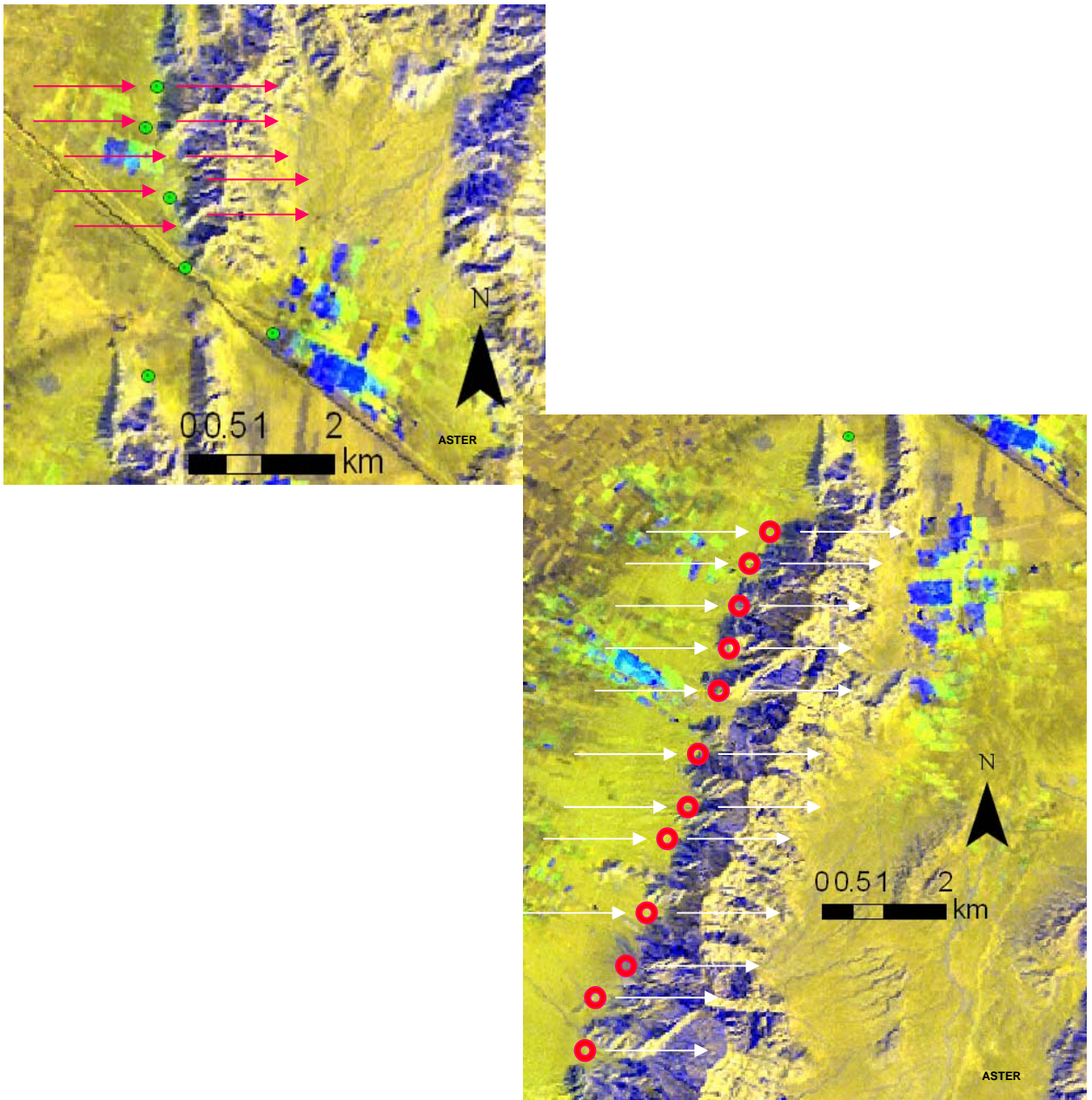


Figure 16 shows successful wells (green circles) along E-W trending shear zones (red arrows), potential productive well location (red circles) along E-W trending shear zones (white arrows). ASTER image

6.2 Climate Changes

As described earlier, water is scarce in the study area and thus the area is quite sensitive to climatic changes. For example, such changes could give rise to drought conditions where precipitation becomes less frequent and dry conditions prevail. If we were to predict climatic changes in the area, one can use such information to assess how the area will behave under such conditions.

The Intergovernmental Panel on Climate Change (IPCC) is the leading body for the assessment of climate change, established by the United Nations Environment Programme (UNEP) and the World Meteorological Organization (WMO) to provide the world with a clear scientific view on the current state of climate change and its potential environmental and socio-economic consequences. One of the IPCC achievements is the development of a database describing the projected climatic changes, specifically the temperature and precipitation in different parts of the world. Many researchers around the world are actively engaged in the construction and validation of Global Circulation Models that also provide climatic projections under various scenarios.

It would be good to put into use my model to assess the hydrologic conditions under various projected climatic conditions.

REFERENCES

- Abbas, G., Mureed, S., Saris, M., Ahmad, S., and Mehmood, S, 1987. Urban Geologic Map of Pakistan, Balochistan series. Scale 1:100,000. In: Geological Survey of Pakistan (Editor), Quetta.
- ACO, 2004. Agriculture Census 2002: Landuse in Balochistan, Agricultural Department, Balochistan, Pakistan.
- Aftab, S., 1997. Hydrogeology and groundwater resources of Balochistan, Pakistan; an overview. *Acta mineralogica Pakistanica*, 8: 30-38.
- Anderson, J.R., Hardy, E.E., Roach, J.T., and Witmer, R.E., 1976. A land use and land cover classification system for use with remote sensor data. U.S. Geological Survey Professional Paper 964: 28pp.
- Chiu, L., Liu, Z., Vongsaard, J., Morain, S., Budge, A., Neville, P., and Bales, C., 2006. Comparison of TRMM and Water District Rain Rates over New Mexico. *Advances in Atmospheric Sciences*, 23(1): 1-13.
- Chokngamwong, R., and Chiu, L., 2006. TRMM and Thailand Daily Gauge Rainfall Comparison, American Meteorological Society, Atlanta, Georgia, pp. 10.
- Chow, V.T., 1959. *Open Channel Hydraulics*. McGraw-Hill Inc., New York.
- DiLuzio, M., Srinivasan, R., Arnold, J.G., and Neitsch, S.L., 2001. *Arcview Interface for SWAT2000 User's Guide*. US Department of Agriculture-Agricultural Research Service, Temple, TX.
- Garbrecht, J., and Martz, L., 1995. *TOPAZ: An Automated Digital Landscape Analysis Tool for Topographic Evaluation, Drainage Identification, Watershed Segmentation, and Sub-Catchment Parameterization: Overview*. Agricultural Research Service, NAWQL 95(1).
- GKW, 2000. GKW Consultants. Feasibility study for Quetta Water Supply Environment Improvement Project. Water and Sanitation Authority through a grant by Asian Development Bank, Balochistan, Quetta.
- Halcrow, and Cameous, 2008. Halcrow and Cameous Consultant Companies. Effectiveness of the Delay Action/Storage Dams in Balochistan. TA-4560(PAK) Project, Asian

- Development Bank, Quetta.
- HSC, 1961a. Hunting Survey Corporation. Reconnaissance Geology of part of West Pakistan, Balochistan, A Colombo Plan cooperative project, Toronto (A report published for the Government of Pakistan by the Government of Canada).
- HSC, 1961b. Hunting Survey Corporation. Reconnaissance Geology of part of West Pakistan, Geologic Map series. Scale 1:253,440. In: Gov. of Canada (Editor), A Colombo Plan cooperative project, Toronto (A report published for the Government of Pakistan by the Government of Canada).
- Huber, W.C., and Dickinson, R.E., 1988. Storm water management model, version 4: user's manual, Athens, GA.
- IIASES, 1992. International Institute for Aerospace Survey and Earth Sciences. Soil Survey of Pakistan, Land Resources and Urban Sciences Department, Balochistan, Quetta.
- IPD, 2006. Irrigation and Power Department. Assessment of Water Resources Availability and Water Use for Balochistan, Stream Gauges database, Government of Balochistan, Quetta.
- IWRM, 2004. Integrated Water Resources Management. Balochistan Resource Management Programme, Balochistan, Pakistan. September 2004, component #3, Quetta.
- JICA, 1988. Japan International Cooperation Agency. Master plan for improving irrigation Quetta and Kalat districts of Balochistan, JICA/WAPDA, Quetta.
- Kazmi, A.H., Jan, Q., 1997. Geology and tectonics of Pakistan: Graphic Publishers, Karachi.
- Kazmi, A. H., Abbas, G., and Younas, S., 2003. Water Resources and Hydrogeology of Quetta Basin, Balochistan, Pakistan, Geological Survey of Pakistan, Quetta.
- Lane, L.J., 1983. Chapter 19: Transmission Losses, SCS–National Engineering Handbook, Section 4: Hydrology. U.S. Government Printing Office, Washington, D.C., pp. 19.1-19.21.
- Maidment, D. R., 1993. Handbook of hydrology. McGraw-Hill, Austin, TX.
- Majeed, Z., and Khan, A, I, 2008. Dam failures due to flash floods and it's review for Mirani Dam project Water and Power Development Authority, Balochistan, Quetta, pp.1-10.
- Milewski, A., Sultan, M., Yan, E., Becker, R., Abdeldayem, A., Soliman, F., and Abdel Gelil, K., 2009a. A remote sensing solution for estimating runoff and recharge in arid

- environments. *Journal of Hydrology*, 373: 1-14.
- Milewski, A., Sultan., M., Jayaprakash, S. M., Balekai, R., and Becker, R., 2009b. RESDEM, a tool for integrating temporal remote sensing data for use in hydrogeologic investigations. *Computers & Geosciences*, 35(10): 2001-2010.
- Mirza, S.N., 1995. Four wing saltbush—A multipurpose shrub for arid highlands of Balochistan, Arid zone Research Institute, Pakistan Agricultural Research Council, Quetta, pp.1-18.
- Monteith, J.L., 1981. Evaporation and Surface Temperature. *Quarterly Journal of the Royal Meteorological Society*, 10(451): 1-27.
- Nash, J. E., and Sutcliffe, J. V., 1970. River flow forecasting through conceptual models. Part-1 a discussion of principles. *Journal of Hydrology*, 10: 282-290.
- NDC, 1994. National Development Consultants. Feasibility study for improve the recharge of groundwater in Quetta Valley. Irrigation and Power Department, Balochistan, Quetta.
- Neitsch, S.L., Arnold, J.G., Kiniry, J.R., Srinivasan, R., and Williams, J.R., 2002. Soil and Water Assessment Tool: User Manual, Version 2000, Grassland, Soil and Water Research Laboratory, Temple, TX.
- Osterkamp, W., Lane, L., and Savard, C., 1994. Recharge Estimates Using A Geomorphic Distributed-Parameter Simulation Approach. *Amargosa River Basin*, 30(3): 493-507.
- PMD, 2010. Pakistan Meteorological Department. Climate Data: Daily Temperature in Balochistan, Climate Data Processing Centre, Quetta, <http://pakmet.com.pk>.
- RedCross, 2005. Pakistan: floods in Balochistan. Information bulletin # 1, February 2005, Pakistan Red Crescent Society, Federation's Disaster Relief Emergency Group, Quetta, <http://ifrc.org>.
- Sangrey, D.A., Harrop-Williams, K.O., and Klaiber, J.A., 1984. Predicting groundwater response to precipitation. *ASCE Journal of Geotechnical Engineering*, 110(7): 957-975.
- SCS, 1972. Soil Conservation Service. Section 4: Hydrology, *National Engineering Handbook*. U.S. Department of Agriculture, Engineering Division, Washington, D.C., USA.
- SCS, 1985. Soil Conservation Service. Section 4: Hydrology, *National Engineering Handbook*. U.S. Department of Agriculture, Engineering Division, Washington, D.C., USA.
- Shan, S.H.A, 1972. The geological structure as a guide in search for ground water in higher

- region of Balochistan. *Geonews, Geological Survey of Pakistan*, 2(2): 21-22.
- Shan, X. J., Song, X. Y., Liu, J. H., and Wang, C. L., 2002. Obtaining digital elevation data in different terrain and physiognomy regions with spaceborne InSAR and its application analysis. *Chinese Science Bulletin*, 47(10): 868-873.
- Smedema, L.K., and Roycroft, D.W., 1983. *Land drainage—planning and design of agricultural drainage systems*, Cornell University Press, Ithaca, New York.
- Sorman, A. U., and Abdulrazzak, M. J., 1993. Infiltration-Recharge through Wadi Beds in Arid Regions. *Hydrological Sciences Journal-Journal Des Sciences Hydrologiques*, 38(3): 173-186.
- Srinivasan, R., Ramanarayanan, T. S., Arnold, J. G., and Bednarz, S. T., 1998. Large area hydrologic modeling and assessment. Part II: model application. *Journal of American Water Resource Association*, 34(1): 91-101.
- Sultan, M., Arvidson, R. E., Sturchio, N. C., and Guinness, E. A., 1987. Lithologic Mapping in Arid Regions with Landsat Thematic Mapper Data - Meatiq Dome, Egypt. *Geological Society of America Bulletin*, 99(6): 748-762.
- Tareen, S., Sani, B., Babar, K., and S., Ahmad, 2008. Re-assessment of Water Resource Availability and Use for the Major River Basins of Balochistan – Study Findings, Policy Issues and Reforms. *Water for Balochistan*, 4(7).
- TCI, Cameous, and ARD, 2004. Techno Consult International Corporation, Cameous and Arab Resources Development. Research for water and sanitation authority, Quetta. Quetta water supply and environmental improvement project. 2008/2.
- Treloar, P.J., and Izatt, C.N., 1993. Tectonics of the Himalayan collision between the Indian Plate and the Afghan Block—A synthesis. *Geological Society Special Publications*, in Treloar, P.J., and Searle, M.P. (editors), *Himalayan tectonics*: 69–87.
- Turk, J., Eber, E. , Oh, H.J. , Sohn, B.J., Levizzani, V., Smith, E., and Ferraro, R., 2003. Validation of an Operational Global Precipitation Analysis at Short Time Scales, 12th Conference on Satellite Meteorology and Oceanography and 3rd Conference on Artificial Intelligence Applications to Environmental Science, Seattle, Washington.
- UNDP, 1982. United Nations Development Program, UNTC-Pk/73-032 Groundwater Investigations in Selected Areas of Balochistan, UNPD/WAPDA, Quetta.
- USDA, NRCS, 1999. US Department of Agriculture, Natural Resources Conservation Service.

Soil Taxonomy: A Basic System of Soil Classification for Making and Interpreting Soil Surveys.

WAPDA, 2001. Water and Power Development Authority. Individual Basinal Reports of Balochistan, Hydrogeology Project, Quetta, 1982-2000, Pakistan, Water and Power Development Authority, Pakistan, Quetta.

Appendix A

Hydrological Modeling Tutorial

This tutorial that I developed was based on the research work that I conducted for the Pishin Lora (PL) Basin, Pakistan. I constructed the tutorial for two reasons: (1) train our Pakistani collaborators, and (2) train the ESRS visitors and the Geosciences students taking the Remote Sensing class on how to conduct rainfall-runoff models. In this exercise, the students are trained on the construction of a rainfall-runoff model that simulates the partitioning of high-intensity rainfall into initial losses, evaporation, recharge, and transmission losses. These are the major processes that influence the flooding events in arid areas. The inputs to the model were extracted from Tropical Rainfall Measuring Mission (TRMM) 3-hourly precipitation data, lithologic and hydrologic parameters from soil and land use maps, and digital terrain elevation from the Shuttle Radar Topography Mission (SRTM) data to enable recharge and runoff calculations.

Objectives:

Learn how to use Soil Water Assessment Tools (SWAT) in ArcGIS 9.3

Learn how to use Remote Sensing data, including USGS DEM files in GIS

Learn how to delineate watersheds from a DEM

Learn how to construct the hydrological model

Learn how to apply Access and Excel to calibrate the hydrological model

Training Target:

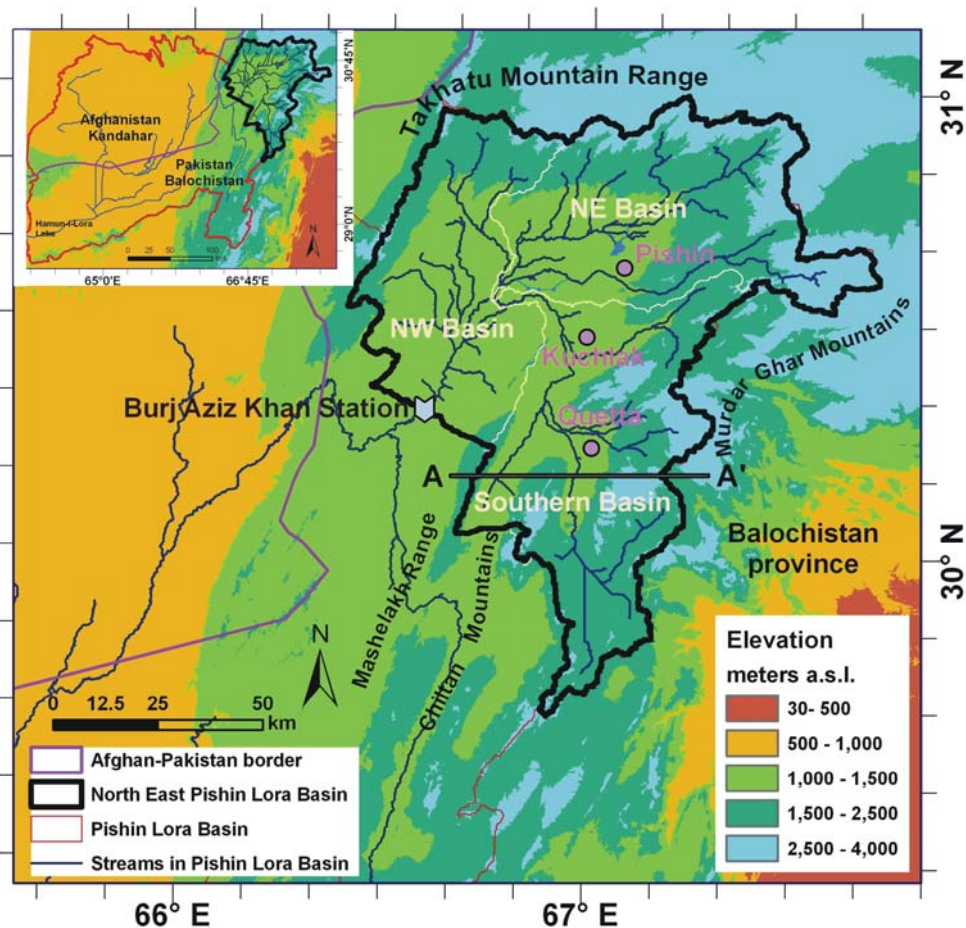
The target of this training is to help you to get preliminary skills in hydrologic model construction and calibration by using SWAT in ArcGIS 9.3

Background:

The SWAT was selected for continuous (1998-2005) rainfall-runoff modeling of the PL basin, located in Balochistan province, Pakistan. The only precipitation data available in PL region are data from a Quetta rain gauge station. This was the main reason why we

are using the satellite-based, TRMM 3-hourly precipitation data, which are available for every $0.25^\circ \times 0.25^\circ$ degrees (1998 till present). Additional model inputs include: (1) Soil types from geologic maps; (2) Land use types (Pakistani Agricultural Department); (3) Hydraulic parameters (published data); (4) Elevation data from the SRTM; (5) Meteorological data (e.g., solar radiation, temperature, humidity) from the Quetta climatic station.

The PL is located on the border of two provinces Balochistan (Pakistan) and Kandahar (Afghanistan). See image below.



The PL basin is a land lock watershed. The upstream areas are generally in the eastern highlands in Pakistan; the streams cross into Afghanistan, then return back into Pakistan and feed the seasonal non perennial salty Hamun-i-Lora Lake (21 km^2 , 1.1 km above mean sea level (a.m.s.l.)) in Balochistan. The area of the PL is $61,300 \text{ km}^2$, whereas, the

NEPL area is 8,470 km², approximately 15% of the PLB area. The Quetta Valley and the city of Quetta, capital of Balochistan province, are located approximately at latitude 30°10'N, and longitude 67°E, it is part of the NEPL. Groundwater accumulation, aquifer development, water migration are characterized by the geological structure in the PL. Layering of permeable fissured limestone and impermeable compact shale strata are the basis of the geologic structure of the area (Shan, 1972). Precipitations in and around the PL area are collected in a number of plunging folds. Folds are widespread in this tectonically depressed region on the edge of collision between the Indian and Eurasian plates. Precipitation increases on the higher peaks from December to March. Snow melts and water percolates down from the area of the tectonic culmination, which is the highest point of the surface, through joints, bedding planes and fissures along the axial dip to the zone of tectonic depression where it gets trapped in the plunging noses of the folds (Shan, 1972).

The PL is the principal stream. PL has its sources in the NEPL. PL meanders SW, then flows abruptly to the NW, at the Afghan frontier it turns again to the SW, flowing across the Afghan territory, and debouches into the Hamun-i-Lora of Balochistan, Pakistan. NEPL, which has highest elevations, up to 3500 meters with PL upstream, is better situated for receiving a water supply than any other area in Balochistan (Kazmi et al., 2003). However, the low rainfall, evaporation, and the loss by surface run-off because of deforestation makes the water supply precarious (Aftab, 1997). Groundwater abstraction for irrigation represents probably 90%-96% of the total withdrawal (WAPDA, 2001). Groundwater monitoring of the PL basin from 1989-2002 indicate a continuous decline of the water table in range 0.2-3.5 m/y (meters per year) in PL (TCI et al., 2004). Groundwater in the shallow alluvial aquifers and in the karstified limestone aquifers underlying the alluvial aquifers could potentially provide an alternative renewable water resource in Balochistan Province, Pakistan.

The hydrologic soil group with Runoff Curve Numbers, which was developed by the US Agricultural Department, are in use for this modeling. The table is shown below.

Table of Runoff Curve Numbers (SCS, 1986)

Description of Land Use	Hydrologic Soil Group			
	A	B	C	D
Paved parking lots, roofs, driveways	98	98	98	98
Streets and Roads:				
Paved with curbs and storm sewers	98	98	98	98
Gravel	76	85	89	91
Dirt	72	82	87	89
Cultivated (Agricultural Crop) Land*:				
Without conservation treatment (no terraces)	72	81	88	91
With conservation treatment (terraces, contours)	62	71	78	81
Pasture or Range Land:				
Poor (<50% ground cover or heavily grazed)	68	79	86	89
Good (50-75% ground cover; not heavily grazed)	39	61	74	80
Meadow (grass, no grazing, mowed for hay)	30	58	71	78
Brush (good, >75% ground cover)	30	48	65	73
Woods and Forests:				
Poor (small trees/brush destroyed by over-grazing or burning)	45	66	77	83
Fair (grazing but not burned; some brush)	36	60	73	79
Good (no grazing; brush covers ground)	30	55	70	77
Open Spaces (lawns, parks, golf courses, cemeteries, etc.):				
Fair (grass covers 50-75% of area)	49	69	79	84
Good (grass covers >75% of area)	39	61	74	80
Commercial and Business Districts (85% impervious)	89	92	94	95
Industrial Districts (72% impervious)	81	88	91	93
Residential Areas:				
1/8 Acre lots, about 65% impervious	77	85	90	92
1/4 Acre lots, about 38% impervious	61	75	83	87
1/2 Acre lots, about 25% impervious	54	70	80	85
1 Acre lots, about 20% impervious	51	68	79	84

*From Chow et al. (1988).

The general equation for the SCS curve number method is as follows:

$$Q = \frac{(P - I_a)^2}{(P - I_a) + S} \quad (1)$$

Q = runoff (in)
P = rainfall (in)
S = potential maximum retention
after runoff begins
I_a = initial abstratctions

$$I_a = 0.2 S \quad (2)$$

$$Q = \frac{(P - 0.2 S)^2}{(P + 0.8 S)} \quad (3)$$

$$S = \frac{1000}{CN} - 10 \quad (4)$$

The initial equation (1) is based on trends observed in data from collected sites; therefore it is an empirical equation instead of a physically based equation. After further empirical evaluation of the trends in the database, the initial abstractions, I_a, could be defined as a percentage of S (2). With this assumption, the equation (3) could be written in a more simplified form with only 3 variables. The parameter CN is a transformation of S, and it is used to make interpolating, averaging, and weighting operations more linear (4).

Initial Losses: Evapotranspiration + Infiltration + Canopy Interception

SWAT is a semi-distributed continuous watershed simulator that computes long-term water flow over large basins using daily time steps. Major model components include: flow generation, stream routing, pond/reservoir routing, erosion/sedimentation, plant growth, nutrients, pesticides, and land management. In SWAT, a large-scale watershed can be divided into a number of subbasins, which are further subdivided into small groups called hydrologic response units (HRUs) that possess unique land cover, soil, and management attributes. The water balance of each HRU is calculated through four water storage bodies: snow, soil profile, shallow aquifer, and deep aquifer. Flows generated from each HRU in a subbasin are then summed and routed through channels, ponds and/or reservoirs to the outlets of the watershed. The detailed descriptions of formulation used in modeling hydrologic processes in HRUs/subbasins and routing can be found in SWAT tutorials.

Tasks

You are to work on the following subtasks.

Task 1

Construct the hydrological model: Delineate watershed and input meteorological data.

(Detailed steps for the model constructions is presented after the Tasks requirements)

Answer the following questions:

- What is HRU?
- What is the difference between HRU and subbasin?
- Are they the same?
- How many HRU's does each sub basin have, give range from smallest number to the biggest number?

Task 2

Run the hydrological model.

(Detailed steps for the model constructions is presented after the Tasks requirements)

Answer the following questions:

- Given Table of Runoff Curve Numbers (SCS, 1986), what do you think are the approximate curve numbers for the five soil types?
- Using the output.std file located in your project folder, what are the area, surface runoff, initial losses, evapotranspiration, and recharge?
- What hydrologic factors would increase these numbers to achieve the maximum amount of groundwater resources?

Task 3

Calibrate the model.

(Detailed steps for the calibration are described in Appendix B and C)

The basic type of calibration is calibration against field data, discharge gages.

You are to calibrate your model against outlet of the NEPL basin at Burj Aziz Khan Station (Lat: 30⁰20'; Long: 66⁰35'). See map above for the period of time from 1998 to 2005. You are required to work on this type of calibration. You have to work on the calibration and to have COE and R² in the range 0.7-0.9. You may change hydrological

parameters to calibrate your model, but your parameters have to be in the required ranges. All physical soil parameters have to be in the range of specific soil type and based on the previous findings by researchers. Review *Handbook of Hydrology* by David R. Maidment and SWAT tutorials to get more data.

You may improve the quality of your calibration by involving additional calibration against reservoir volume changes by comparing datum in reservoir volumes measured from satellites (LandSat and SRTM) with the simulated reservoir volumes datum on a monthly basis. This level of calibration is more time consuming, so you may just study general methodology of how to work on this task.

Appendix B (Calibration of Hydrological Model) and appendix C (Using ACCESS and EXCEL for Data Management and Data Review) can be helpful in your calibration task.

Answer the following:

- Present sensitivity analysis with description and definition of each parameter.
- Describe your strategy to calibrate SWAT model.
- What are some ways that we could check the validity of our model outputs?
- Does the proposed method of utilizing renewable water resources in this area seem like a viable one?
- What other Remote Sensing datasets do you think we can use in this model to offset the lack of *insitu* data?

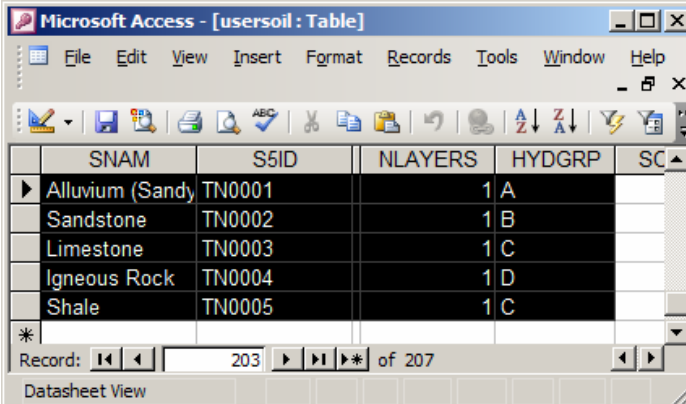
Watershed Modeling in ArcGIS 9.3, 2010

Soil Water Assessment Tool (SWAT)

Task 1

Model construction

- This tutorial is to use SWAT in ArcMap 9.3.
- Copy to your folder SWAT input database.
- All user files MUST be in the same directory. All SWAT data has to be in one folder. Keep your files in C folder, or flash card. SWAT may not work properly if you save on network folder, for example.
- SWAT has to be installed in ArcGIS 9.3 prior to use and show up in tools extensions.
- This file SWAT2005.mdb, in ACCESS format has to have the following soil types

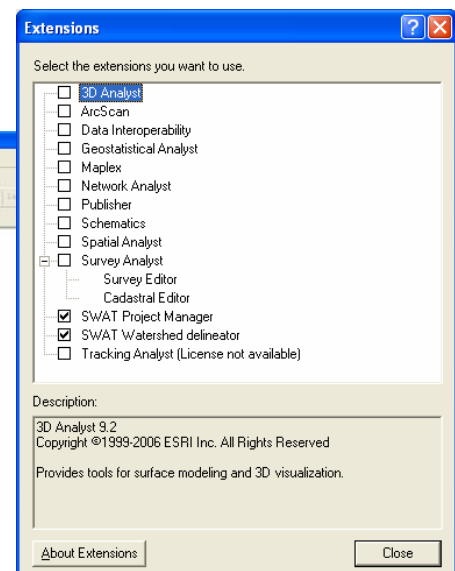
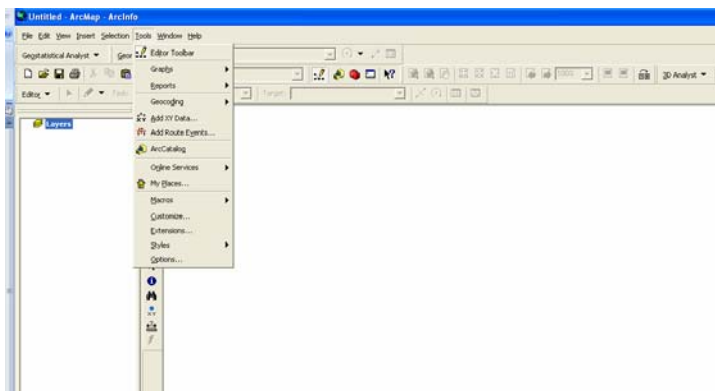


The screenshot shows a Microsoft Access window titled "Microsoft Access - [usersoil : Table]". The window displays a table with the following data:

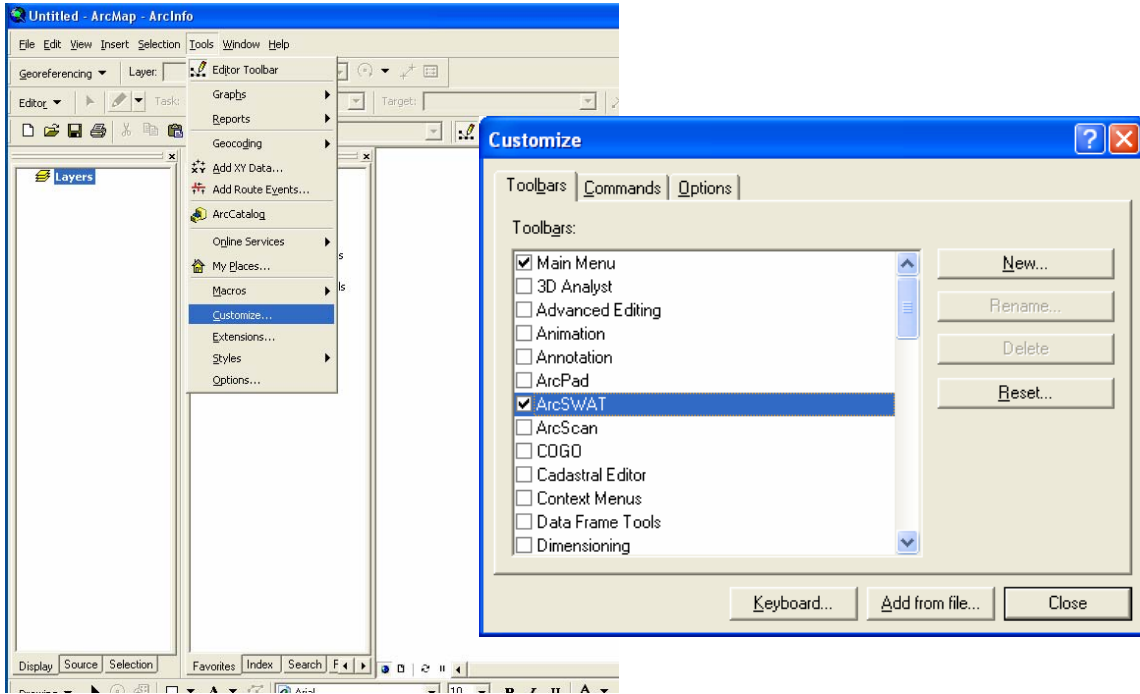
SNAM	S5ID	NLAYERS	HYDGRP	SC
Alluvium (Sandy	TN0001	1	A	
Sandstone	TN0002	1	B	
Limestone	TN0003	1	C	
Igneous Rock	TN0004	1	D	
Shale	TN0005	1	C	

The status bar at the bottom indicates "Record: 203 of 207" and "Datasheet View".

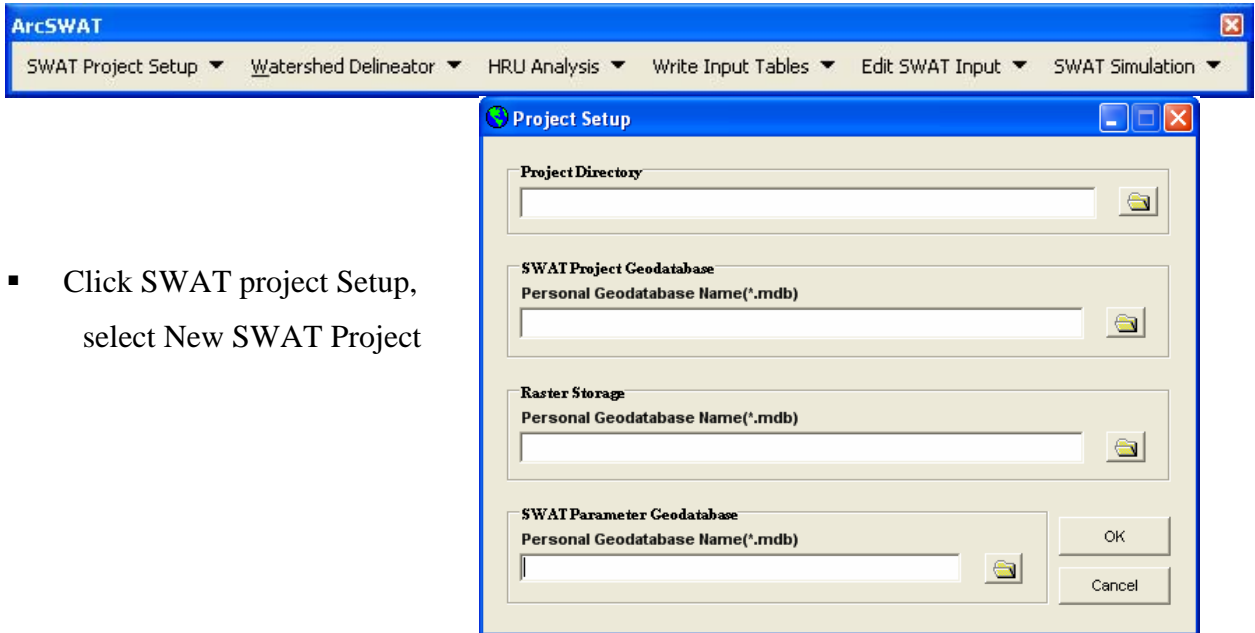
- Check these soils before moving to the next steps.
- Start ArcMap 9.3 and check, if SWAT appears.



Customize your Tools – Mark ArcSWAT

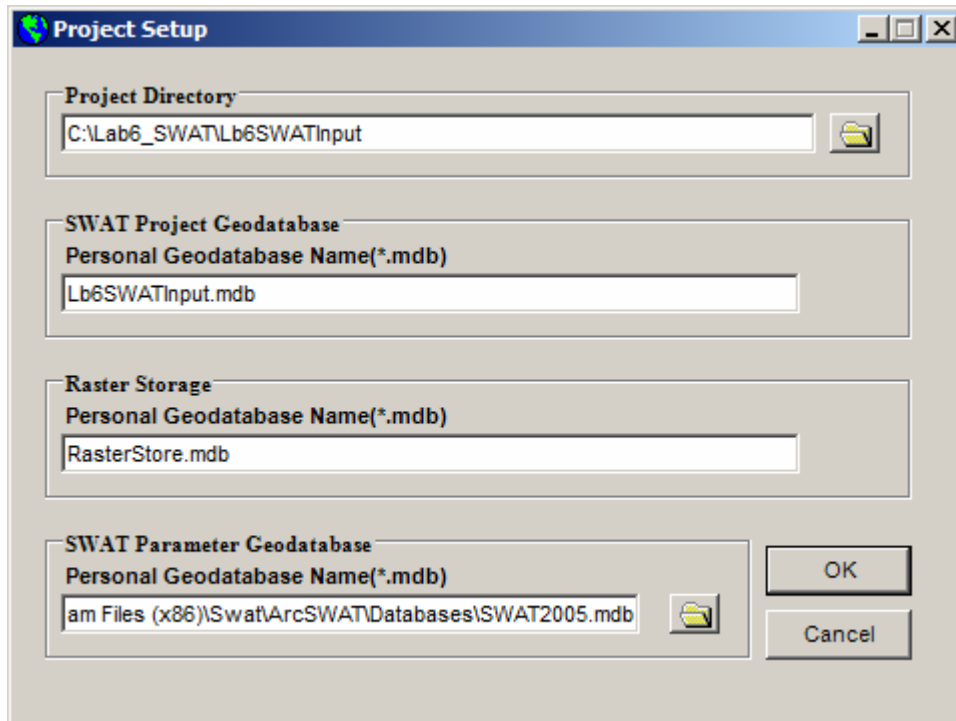


- Now it should appear on your computer in the following toolbar

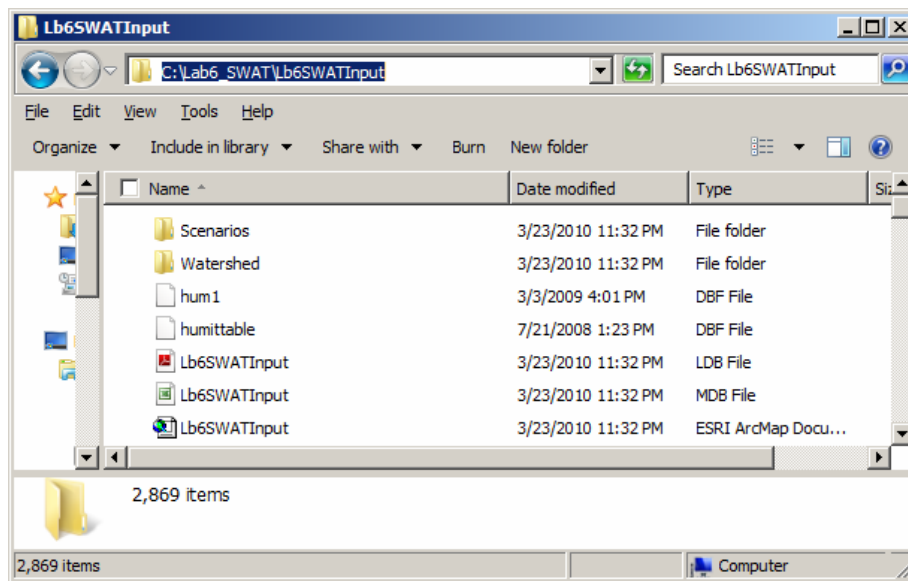


- Click SWAT project Setup,
select New SWAT Project

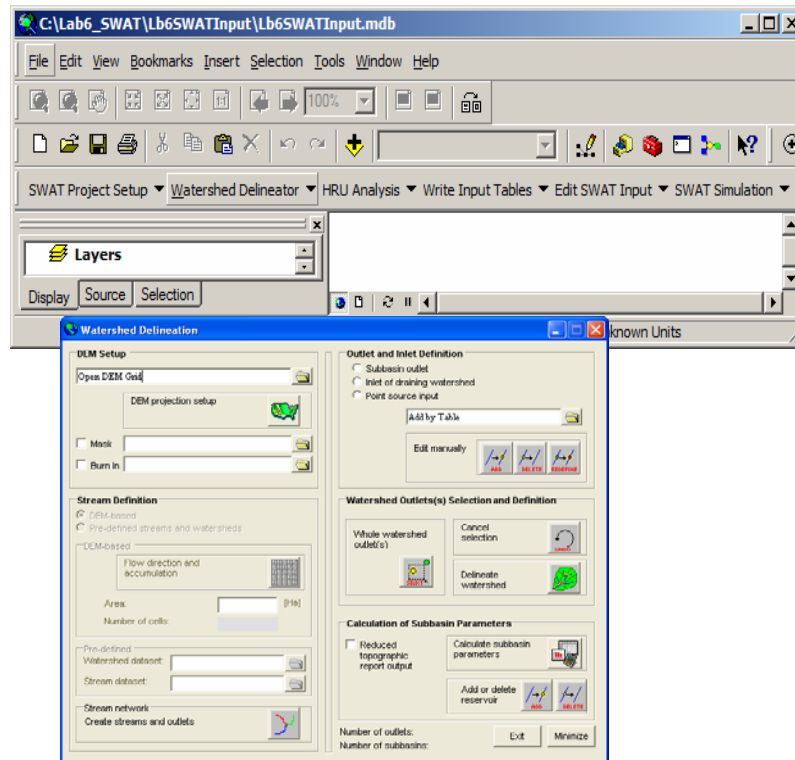
- Fill in spaces in your Project directory in your folder directory, SWAT Project Geodatabase, Raster Storage, and SWAT Parameters Geodatabase.



- When you filled out the project setup, Click “ok”.
- A similar data folder should be created in your place

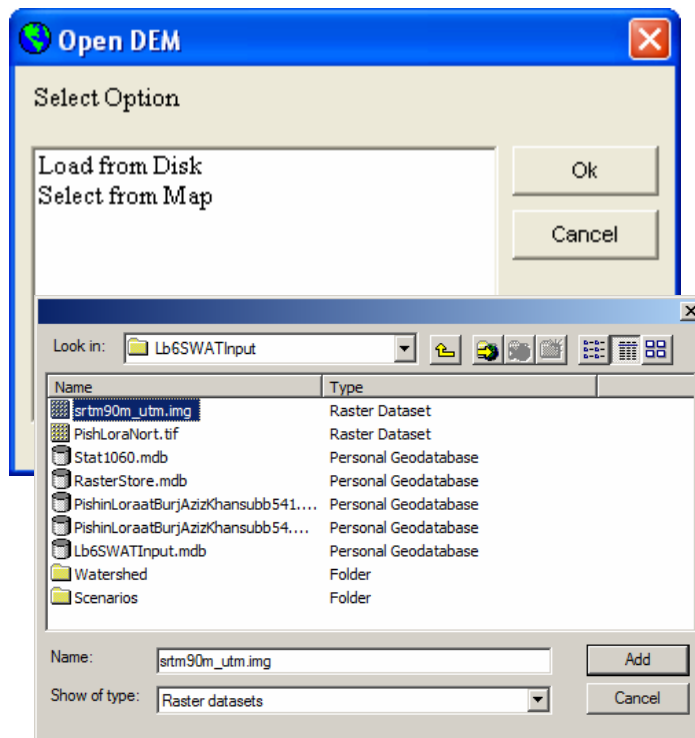


- Select from the main menu the Watershed Delineator.



- Select the DEM input grid...“Load from Disk”.

- Select file:
SRTM90m_utm.img.

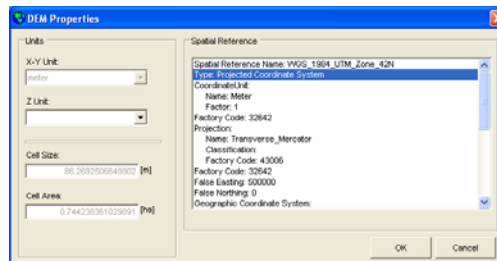
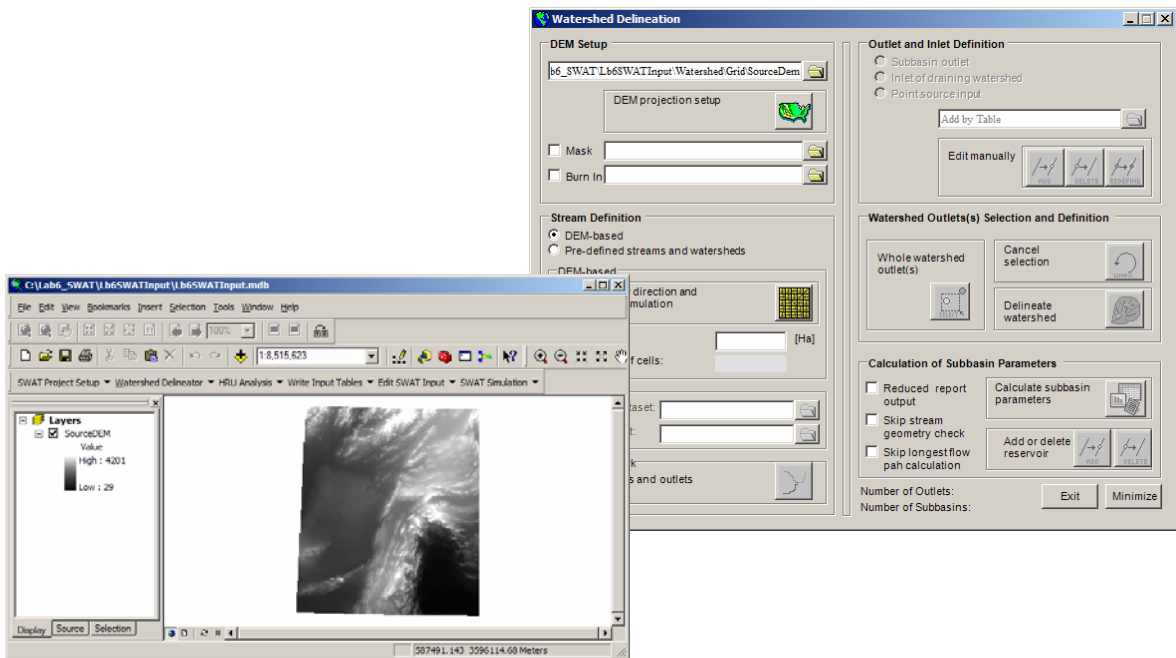


You have to use the file with the UTM projected coordinate system; otherwise you will get the following notice

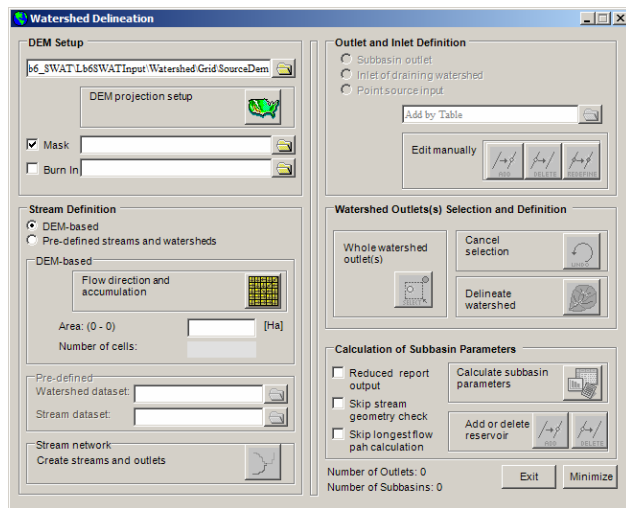


- Review the DEM projection Setup.

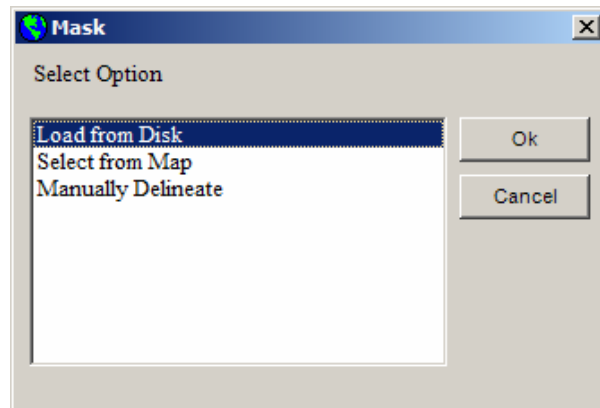
For Quetta, Pakistan region it should be WGS_1984_UTM_Zone_42N



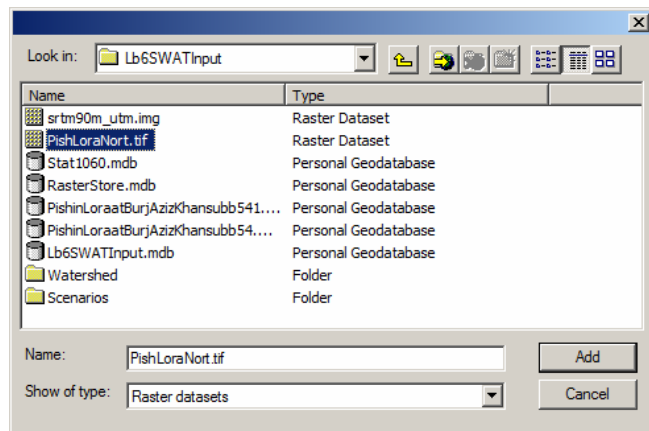
- Mark Mask and Click on the folder symbol on the right sight of the Mask



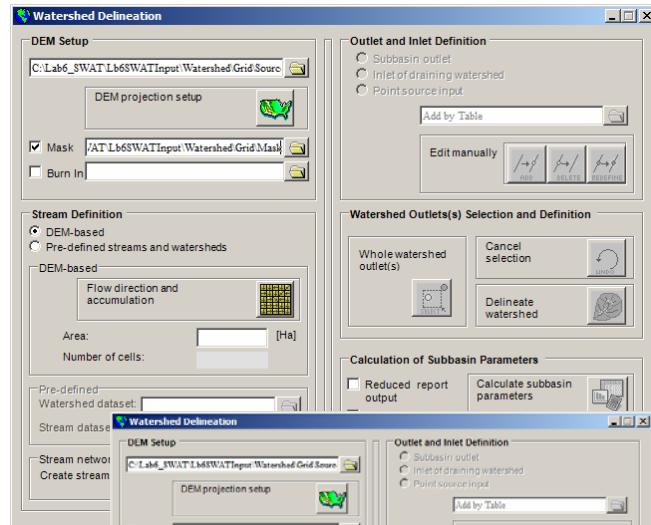
- Select Option: Load from Disk.
(You may Manually Delineate, if you wish, instead of using my Mask)



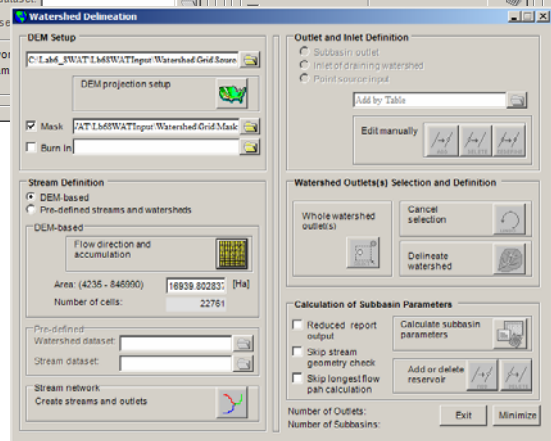
- Click "Ok".
- Select PishLoraNorth.tif



- Click on the yellow square on the right of Flow direction and accumulation.

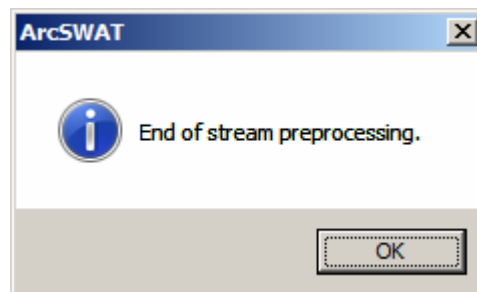
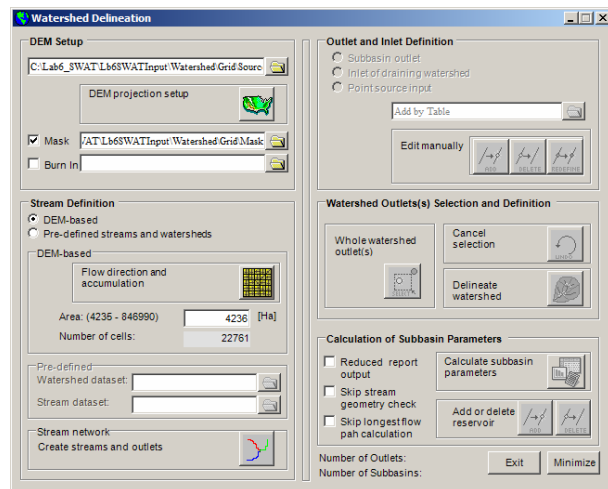


- Choose smallest available area size 4236
(Your number can be different; using same way for selection, choose smallest area)

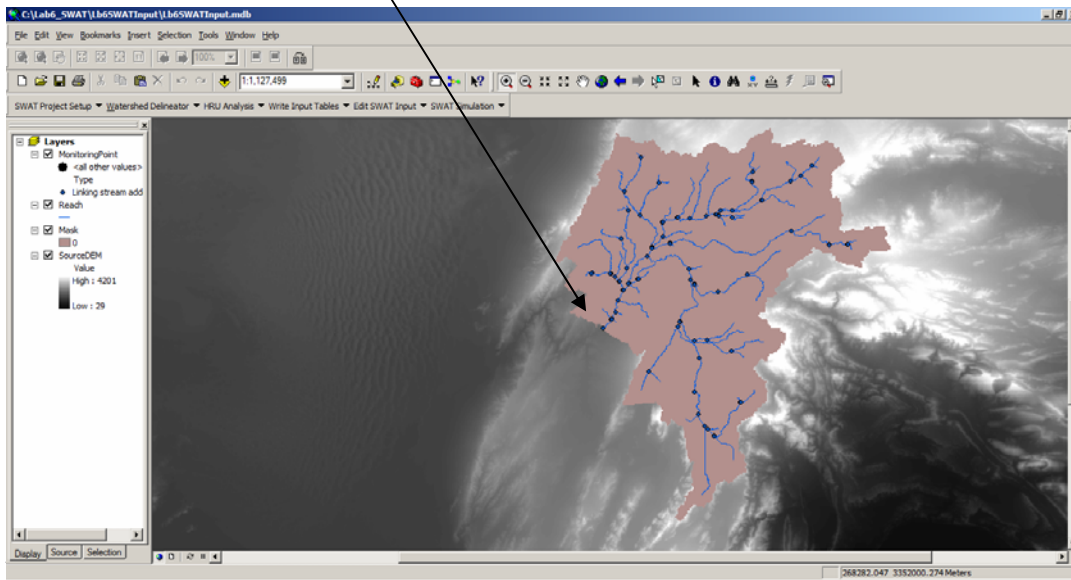


- Click on the square with green, red, blue color lines on the right of Stream network
“Create streams and outlets”

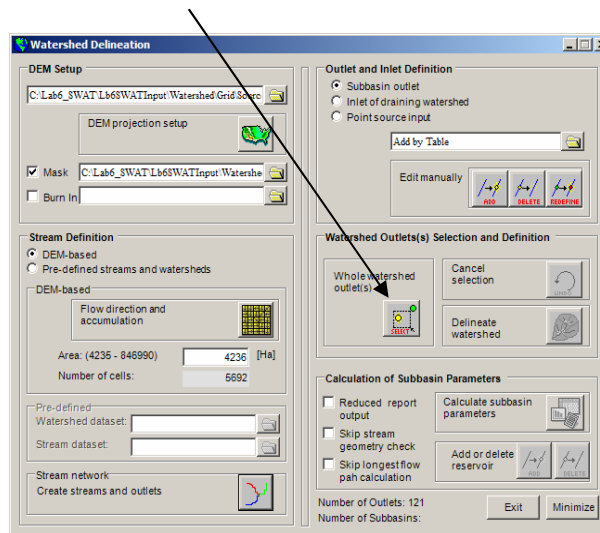
Comments: Selection of small area will give more details and smaller flow accumulation data; the bigger gives less details, for big flow accumulation data without small details.



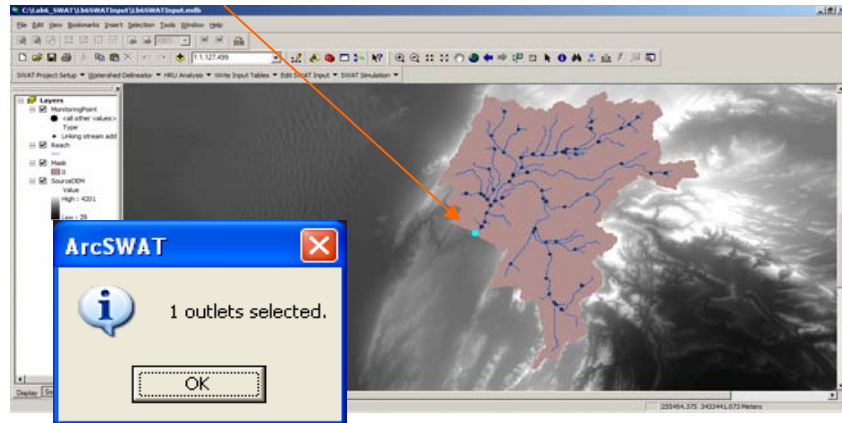
- Zoom to the stream discharge outlet



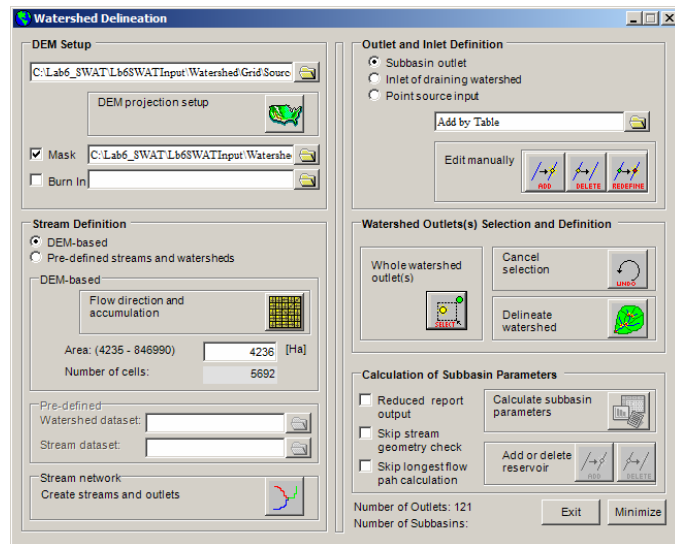
- Click on the “Whole watershed outlet(s)” –
On the “Watershed Outlet(s) Selection and Definition”



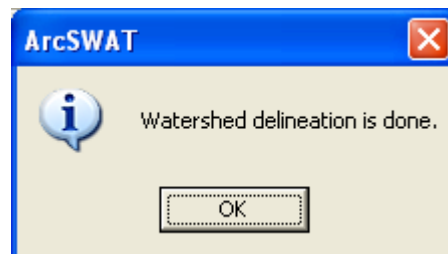
- By holding the left mouse button, drag square on the outlet point – you should get a light blue dot on the top of the outlet point. By doing so you are selecting this outlet point.



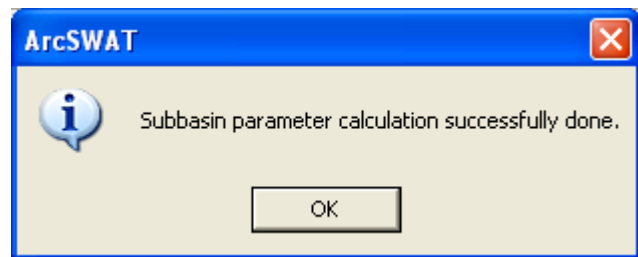
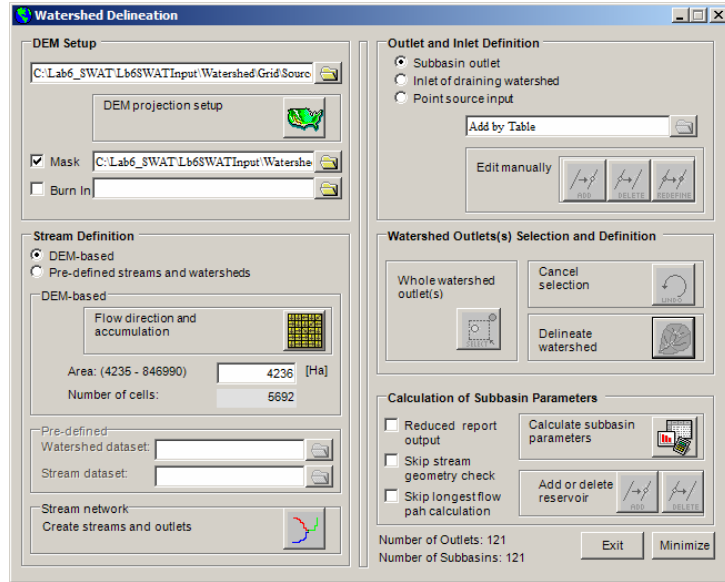
- Click on the “Delineate watershed”
(It may take some time to do this operation, be patient)



You should get this confirmation.

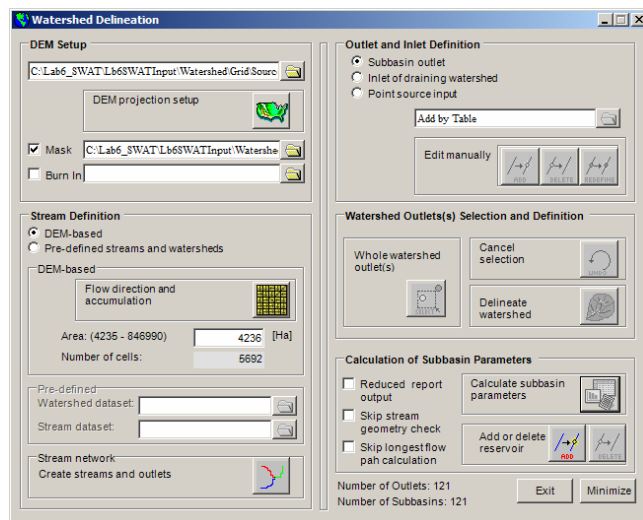


- Click on the “Calculate subbasin parameters” button (Be patient, it takes some time to finish this step)

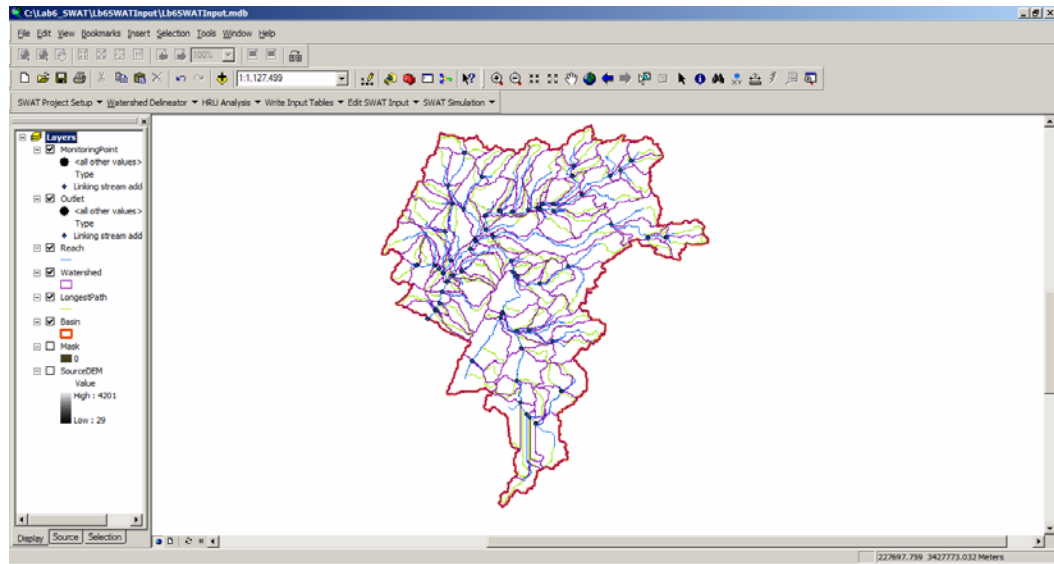


Comments: the reservoirs may be added also on this step.

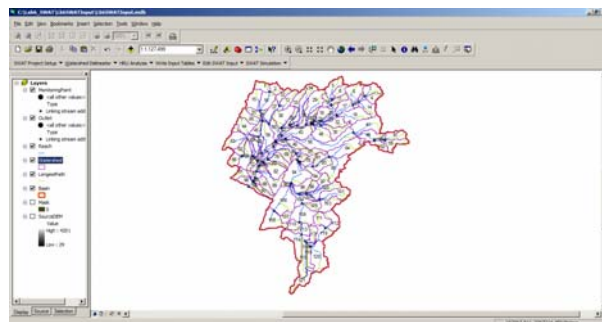
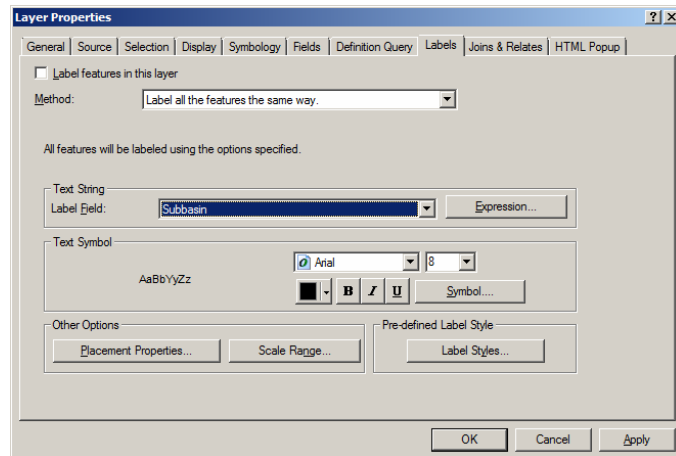
- Click on “Exit”, SWAT will make resuming parts in watershed delineations.



Your resulting watershed should look like this image.



- Click on Watershed and Select in “Layer Properties” – “Labels”
- Select in “Label Field” – Subbasin
- Click “Apply”



- Review the watershed report



TopoRep - Notepad

File Edit Format View Help

Elevation report for the watershed 1/1/0001 12:41:20 AM 3/24/2010 12:00:00 AM

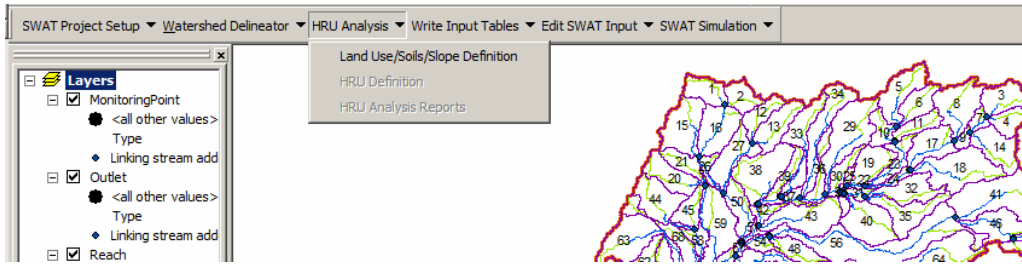
Statistics:: All elevations reported in meters

Min. Elevation: 1397
 Max. Elevation: 3537
 Mean. Elevation: 1872.90616872162
 Std. Deviation: 349.837809867876

Elevation	% Area Below Elevation	% Area Watershed
1397	0	0
1399	0	0
1400	0	0
1401	0	0
1402	0	0
1403	0	0
1404	.01	0
1405	.01	0
1406	.01	0
1407	.02	0
1408	.02	0
1409	.03	.01
1410	.03	.01
1411	.04	.01
1412	.05	.01
1413	.06	.01
1414	.07	.01
1415	.08	.02
1416	.1	.02
1417	.12	.02
1418	.14	.02
1419	.16	.02
1420	.18	.02
1421	.21	.03

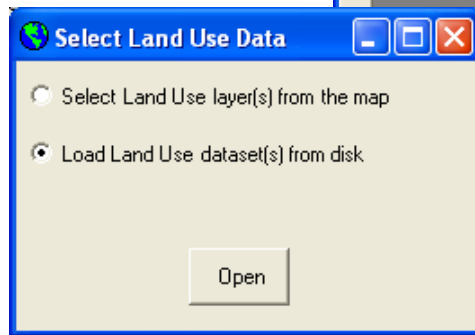
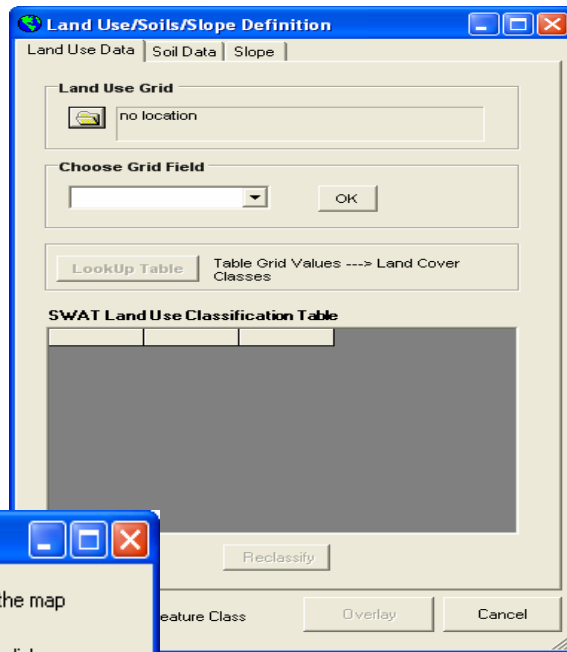
Ln 1, Col 1

- Next select HSU Analysis – Land Use/Soils/Slope Definition

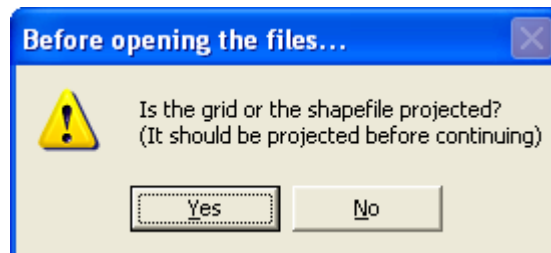


- Follow steps on the screen.
- Click the button on the Land Use Grid.

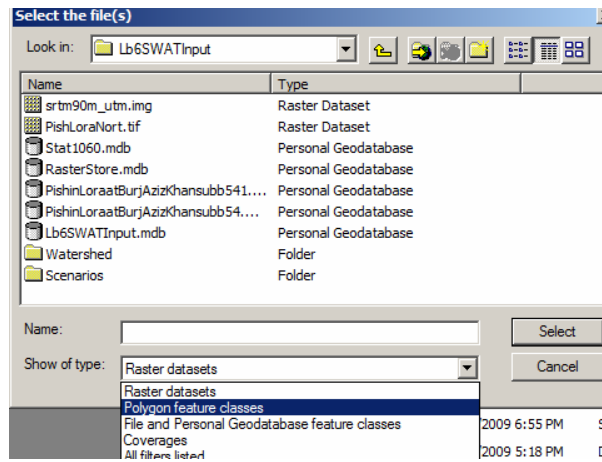
Next you may download from the disk (from your folder) or you may download from the ArcMap, if you added such layers.



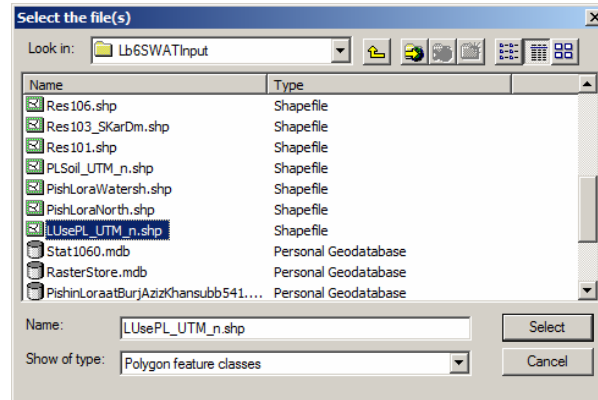
- Check projection.
- Click “Yes”, if projected.



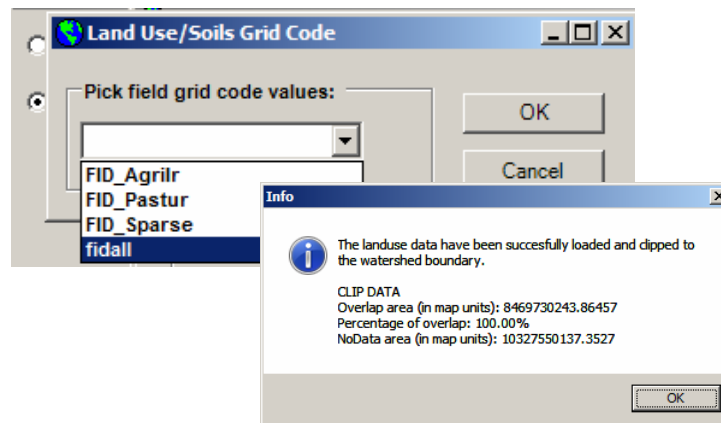
- Select Polygon feature classes (Shapefile)



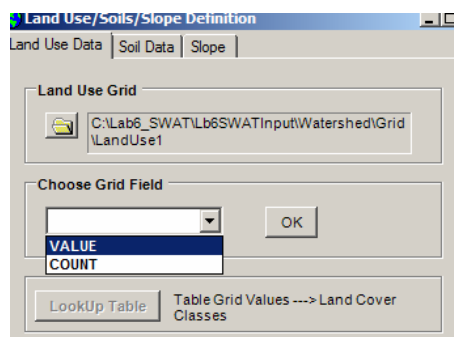
- Select LUsePL_UTM_n.shp.



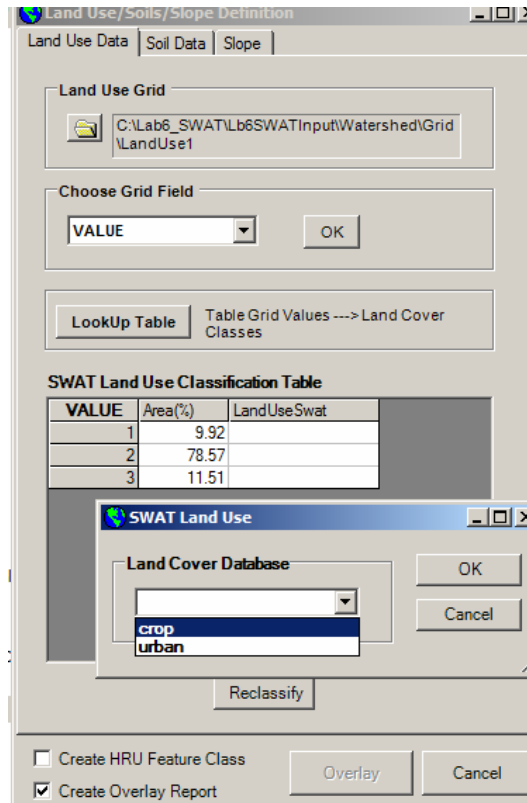
- Choose fidall
- Click "Ok"



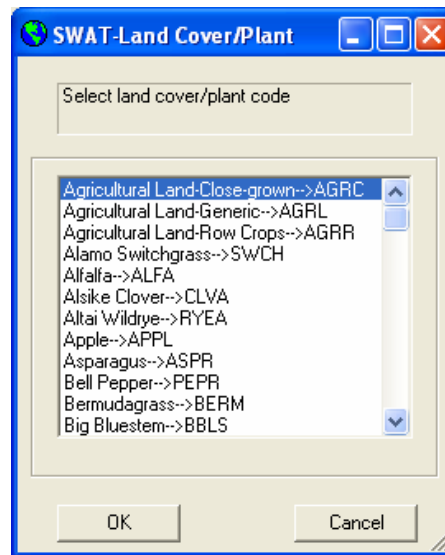
- Choose VALUE



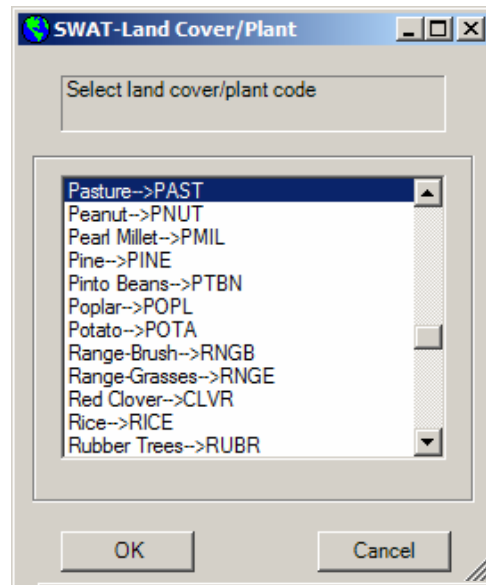
- Click on the place beneath of “LandUseSwat”, on the empty cell box, on line 1 of the SWAT Land Use Classification Table, with left mouse button
- Select on the Land Cover Database –crop



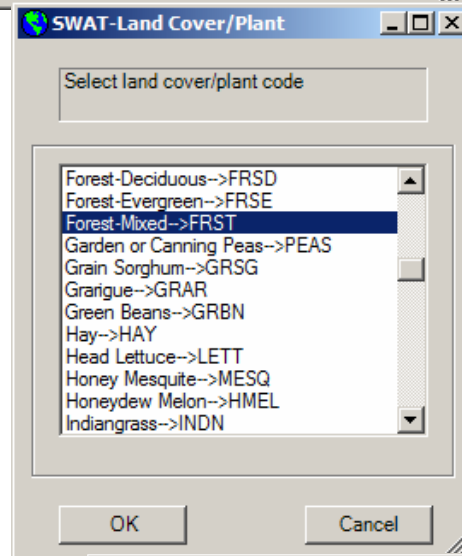
- Select Agricultural Land Close-grown-AGRC



- Do same actions for VALUE # 2, but choose PASTURE



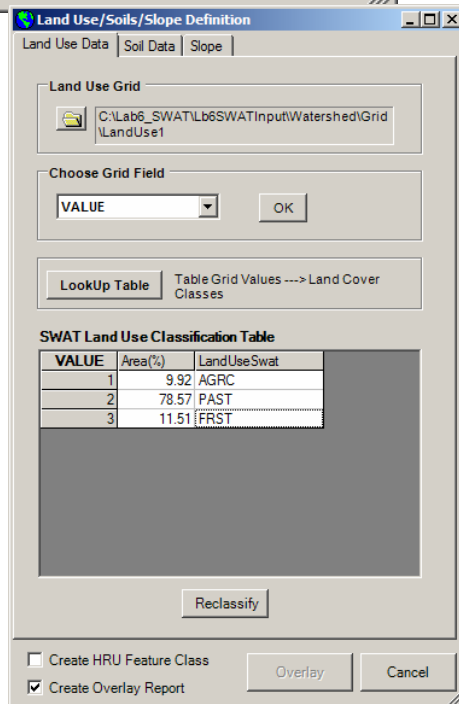
- Do same actions for VALUE # 3, but choose Forest-Mixed – FRST



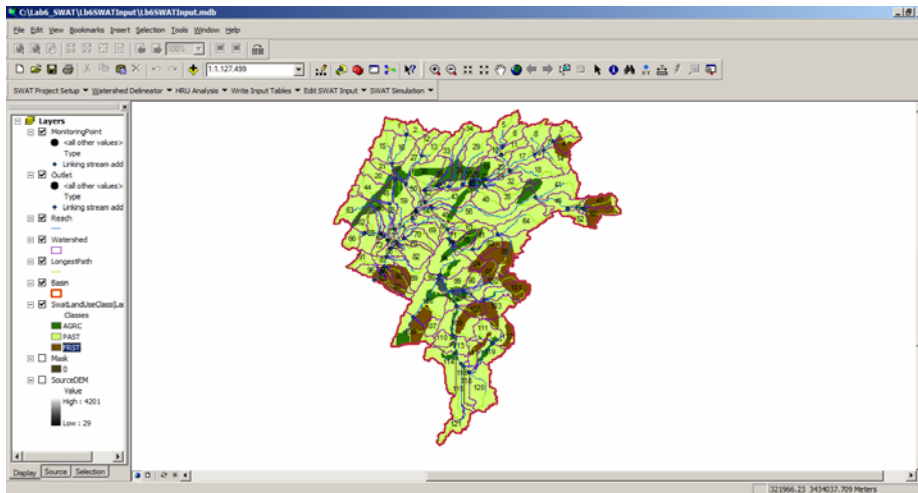
Comments:

Your LandUseSwat should be similar to the data as it shown on the right image.

- Click – Reclassify.



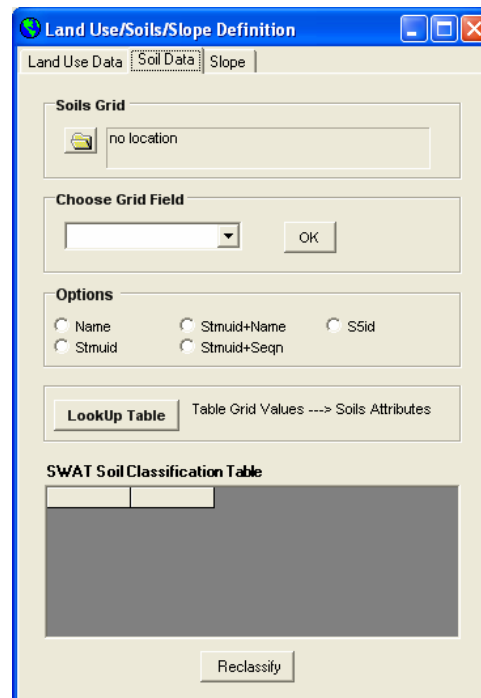
Your Land Use map should look like this image



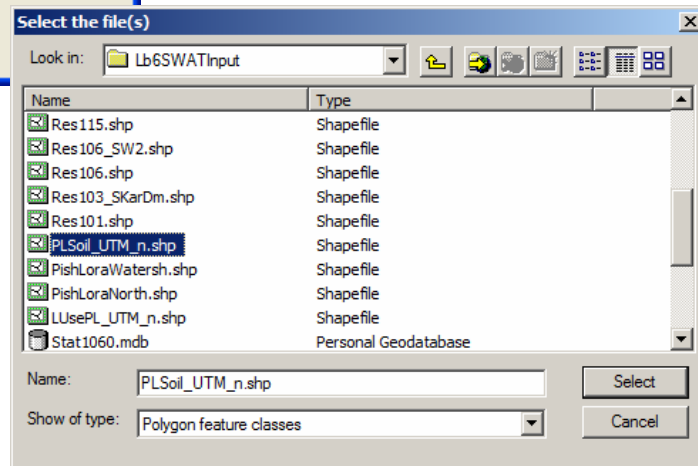
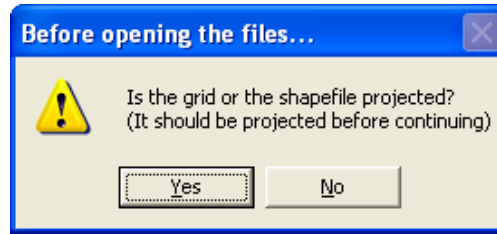
- Change Symbology in Properties and make land use map with name of the region, watershed, scale, legend, North arrow.

- Next select Soil Data

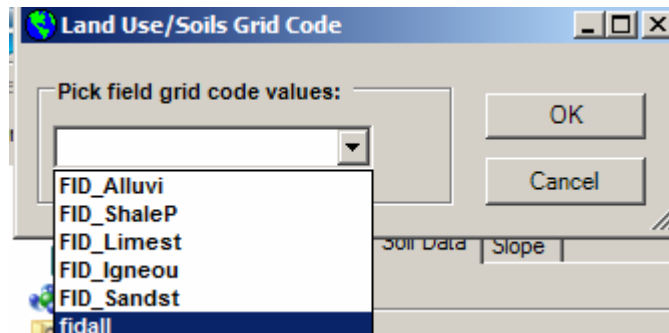
(You may download from the disk (from your folder) or you may download from the ArcMap, if you added such layers)



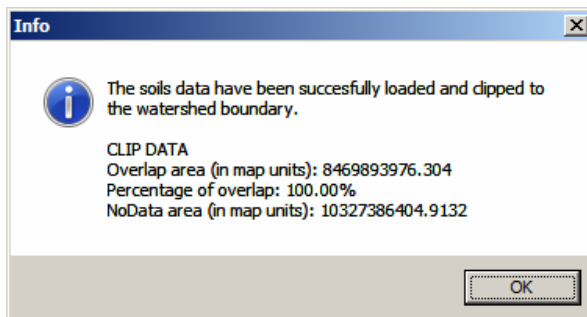
- Check projection and click “yes”, if it is projected



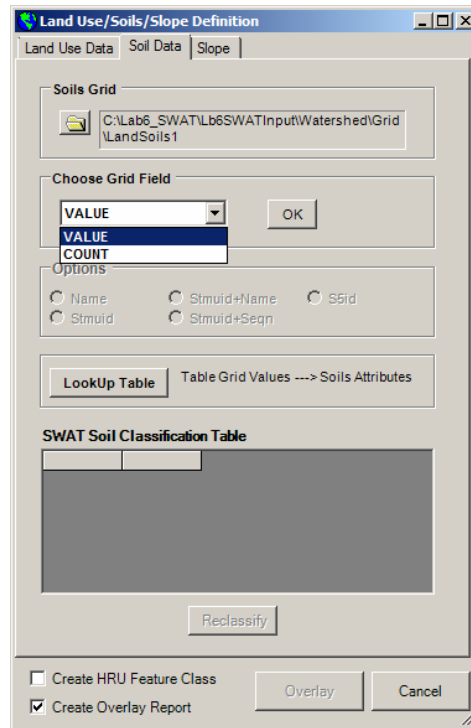
- In the “Show of type:” use Polygon feature classes.
- Select PLSoil_UTM_n.shp.



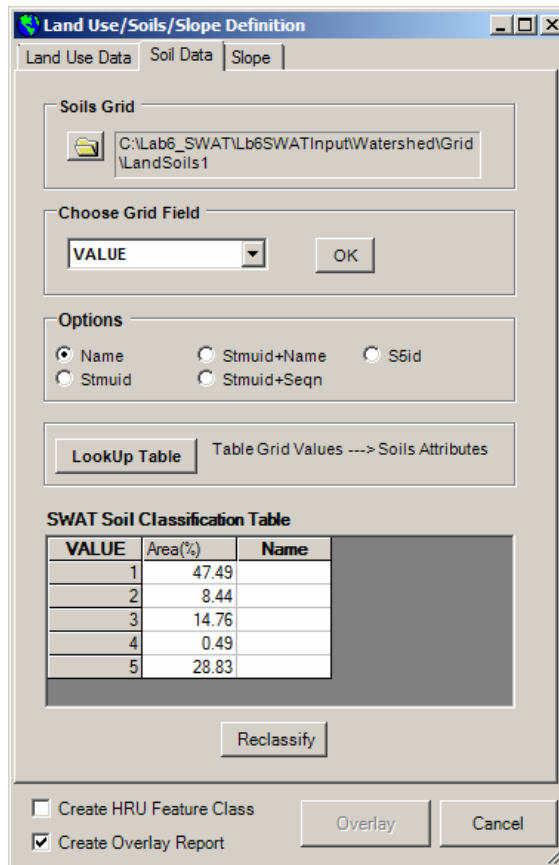
- Choose fidall.



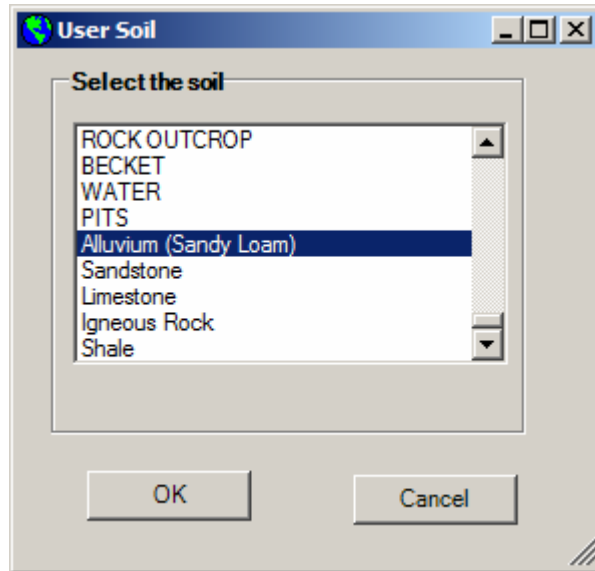
- Next “Choose Grid Field”
“VALUE”



- In “Options”
select
“Name”



- Double-click on the boxes beneath Name and enter these names for the following value fields:
 - Alluvium (Sandy Loam)
 - Shale
 - Limestone
 - Igneous Rock
 - Sandstone

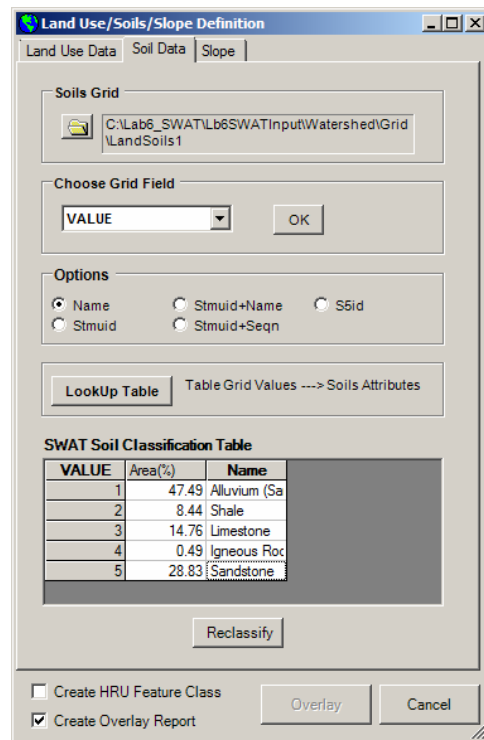


Comments:

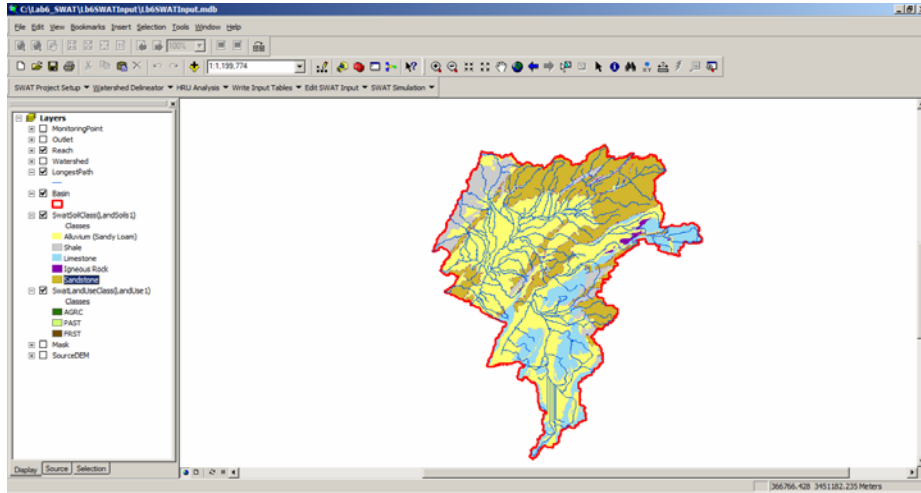
Be sure that you select the correct area and order that is shown above:

Biggest Area for Alluvium, smallest area igneous rock, otherwise, if you select wrong rock types with wrong area, your model will be incorrect.

- Click on “Reclassify”



Soil Classification should look like this image



- Change Symbology in Properties and make Soil map with name of the region, watershed, scale, legend, North arrow.

- Move to Slope
- Select multiple Slope

“Number of Slope Classes” is 3

Put 1 for current slop Class Upper 3

Put 2 for current slop Class Upper 10

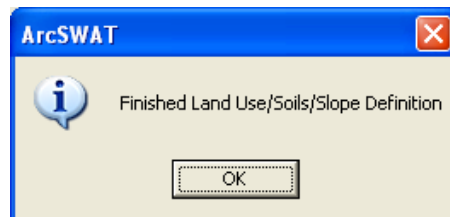
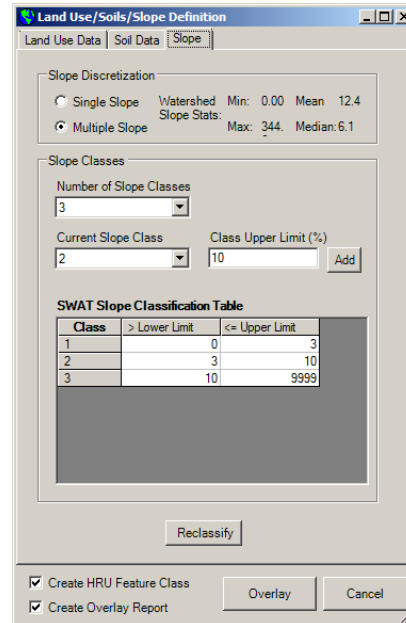
Ranges:

0-3

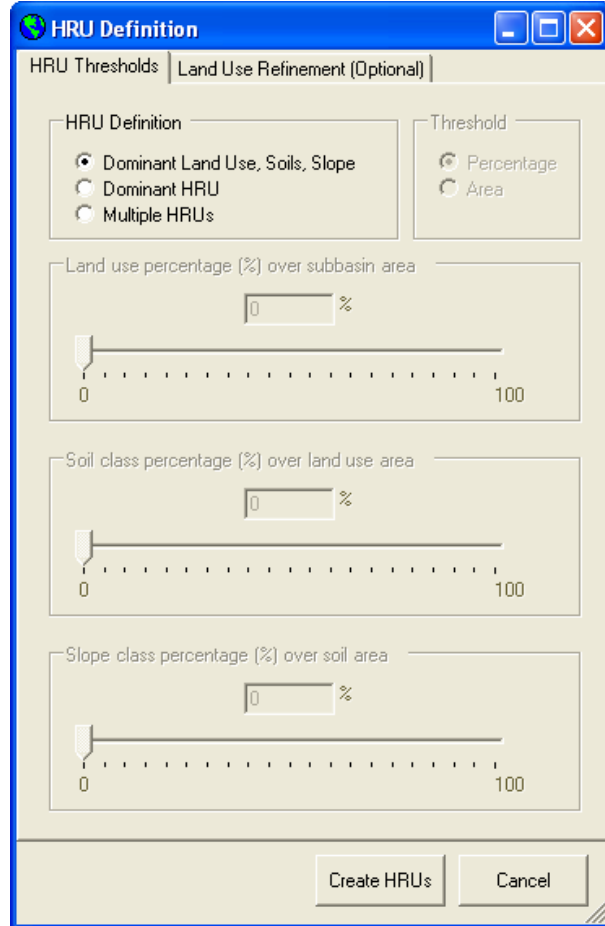
3-10

10-9999

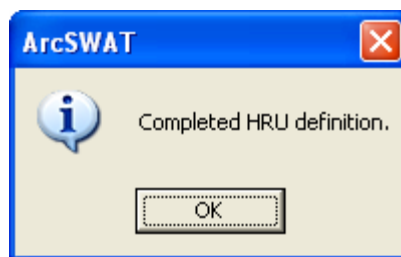
- Reclassify.
- Mark Create HRU Feature Class.
- Click “Overlay”.



- Select “Dominant Land Use, Soil, Slope” In HRU (Hydrologic Response Units) Analysis.



- Click Create HRUs.



- Review Reports.

LandUseSoilsReport - Notepad

Detailed LANDUSE/SOIL/SLOPE distribution SWAT model class Date: 3/24/2010 12:00:00 AM Time: 18:17:44.1934709

		Area [ha]	Area[acres]		
watershed		846990.8859	2092956.8287		
Number of Subbasins:	121				
		Area [ha]	Area[acres]	%wat. Area	
LANDUSE:	Agricultural Land-Close-grown --> AGRC	84010.0570	207593.0513	9.92	
	Pasture --> PAST	665515.3793	1644521.7779	78.57	
	Forest-Mixed --> FRST	97465.4497	240841.9995	11.51	
SOILS:	Alluvium (Sandy Loam)	402206.7625	993873.0206	47.49	
	Igneous Rock	4112.0109	10160.9845	0.49	
	Limestone	125033.4126	308963.8143	14.76	
	Sandstone	244150.7394	603308.6846	28.83	
	Shale	71487.9605	176650.3247	8.44	
SLOPE:	0-3	271702.3287	671390.0394	32.08	
	10-9999	326203.4048	806064.9233	38.51	
	3-10	249085.1525	615501.8660	29.41	
		Area [ha]	Area[acres]	%wat. Area	%Sub. Area
SUBBASIN #	1	5859.3886	14478.8423	0.69	
LANDUSE:	Pasture --> PAST	5859.5225	14479.1730	0.69	100.00
SOILS:	Alluvium (Sandy Loam)	3786.7713	9357.3012	0.45	64.63
	Shale	2072.7512	5121.8718	0.24	35.37
SLOPE:					

Ln 1, Col 1

HRU_LandUseSoilsReport - Notepad

SWAT model simulation Date: 3/24/2010 12:00:00 AM Time: 00:00:00

DOMINANT Landuse/soil OPTION

Number of HRUs: 121

Number of Subbasins: 121

		Area [ha]	Area[acres]		
watershed		846990.8859	2092956.8287		
		Area [ha]	Area[acres]	%wat. Area	
LANDUSE:	Pasture --> PAST	745640.5060	1842514.9724	88.03	
	Forest-Mixed --> FRST	84294.6694	208296.3428	9.95	
	Agricultural Land-Close-grown --> AGRC	17055.7105	42145.5135	2.01	
SOILS:	Alluvium (Sandy Loam)	475223.7304	1174301.5990	56.11	
	Shale	80363.6024	198582.4798	9.49	
	Sandstone	218713.0483	540450.8779	25.82	
	Limestone	72690.5049	179621.8720	8.58	
SLOPE:	3-10	113811.1628	281233.0739	13.44	
	10-9999	382129.9304	944262.1645	45.12	
	0-3	351049.7927	867461.5902	41.45	
		Area [ha]	Area[acres]	%wat. Area	%Sub. Area
SUBBASIN #	1	5859.3886	14478.8423	0.69	
LANDUSE:	Pasture --> PAST	5859.3886	14478.8423	0.69	100.00
SOILS:	Alluvium (Sandy Loam)	5859.3886	14478.8423	0.69	100.00

Ln 34, Col 1

SourceDEM

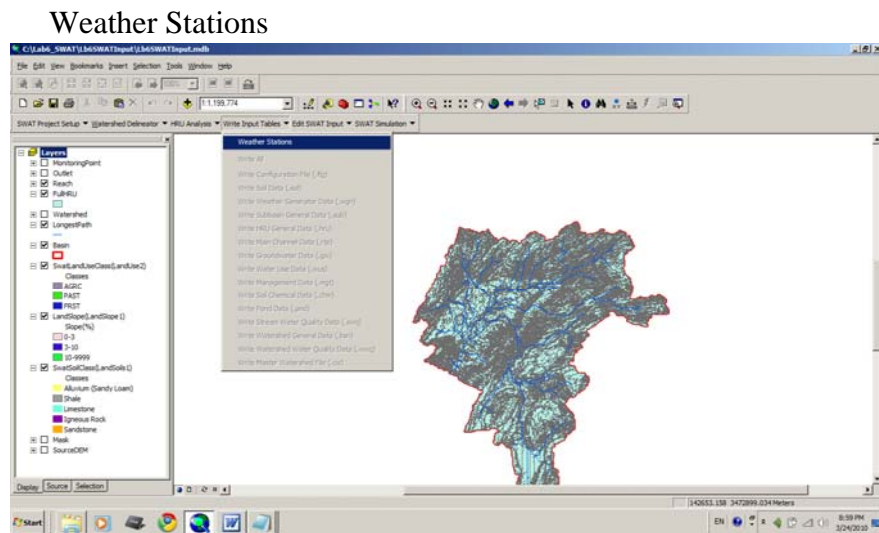
Display Source Selection

142653.158 3472899.034 Meters

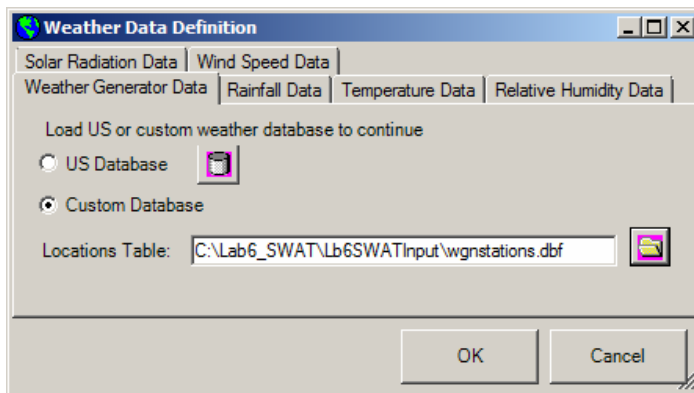
EN 8:56 PM 3/24/2010

- Compare HRU and subbasins.

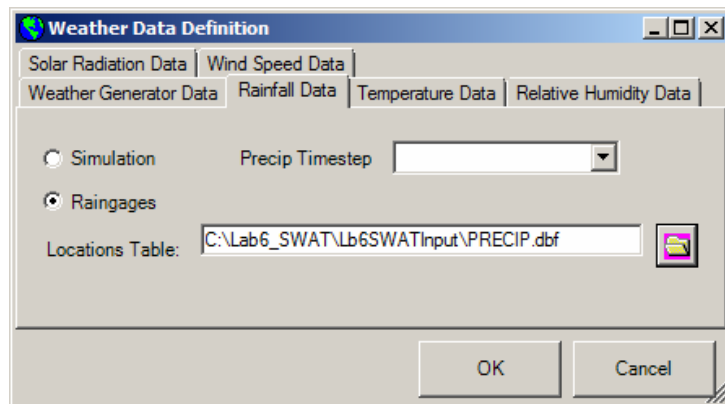
- Select Write Input Tables.



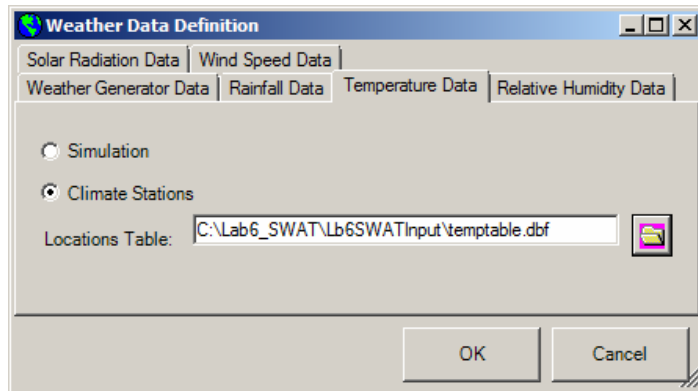
- Select Weather Generator Data – file wgnstations.dbf



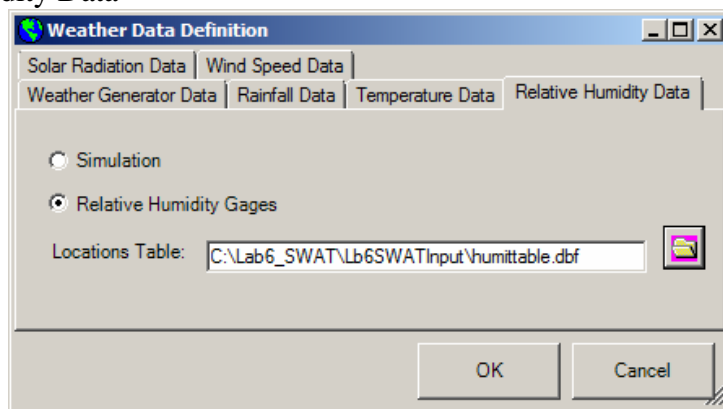
- Rainfall Data



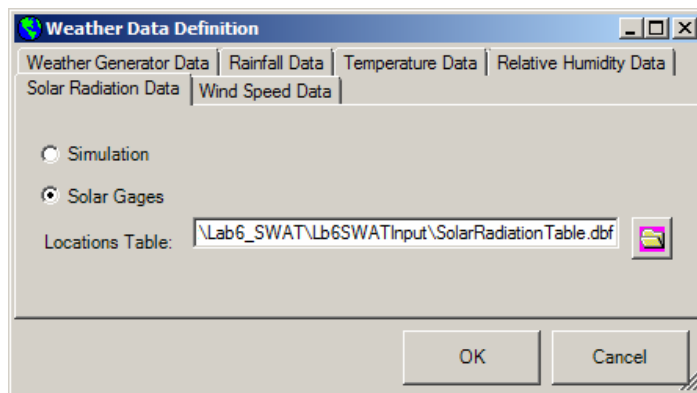
- Temperature Data



- Relative Humidity Data

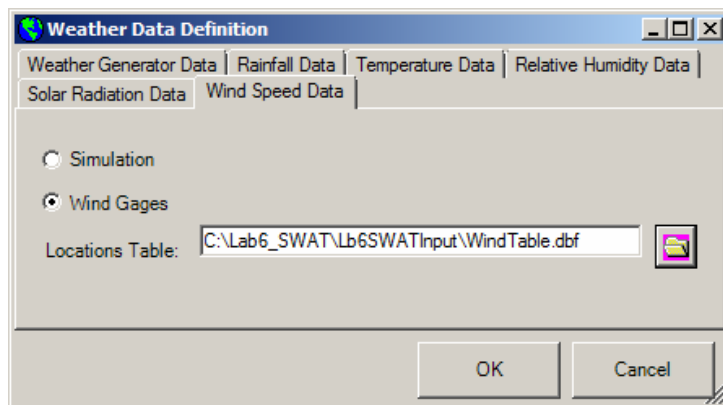


- Solar Radiation Data



- Wind Speed Data

- Click "Ok"



So, all your Input...Weather Stations for each variable should be the following files:

Rainfall Data: PRECIP.dbf

Temperature: temptable.dbf

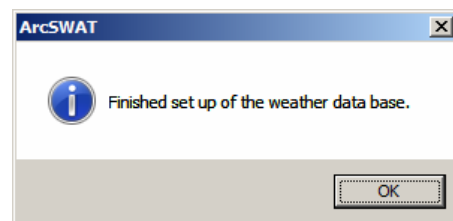
Relative Humidity: humitable.dbf

Solar Radiation: SolarRadiationTable.dbf

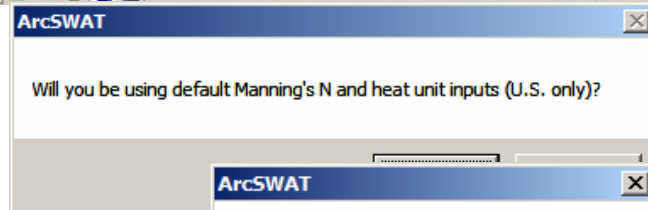
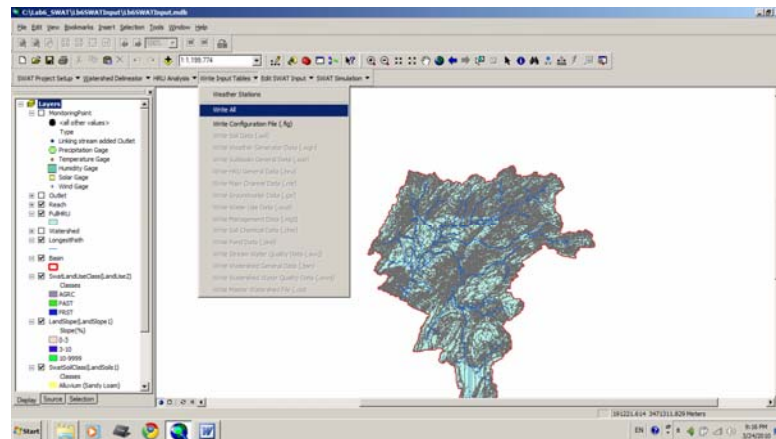
Wind Speed: WindTable.dbf

Weather Simulation:wgnstations.dbf

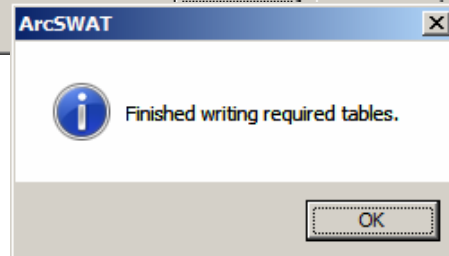
It will take some time to write all the data, you should receive this feedback:



- Next Write Input Tables / Weather stations.
- Click on Write All.



- Click "Yes".
- "OK".



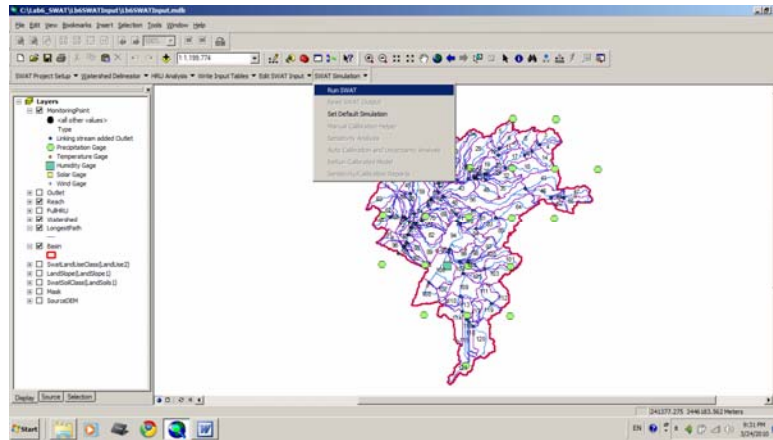
- Make maps of 1) HRU, 2) Numbered Subbasins, 3) Streams, 4) Meteorology Stations.
- Change Symbology in Properties and make maps with name of the region, watershed, scale, legend, North arrow.

Task 2

Run the model.

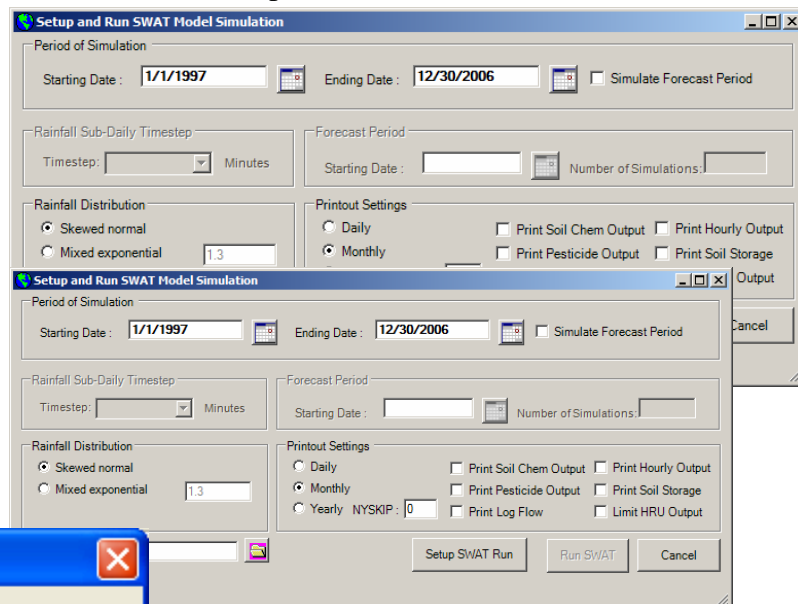
SWAT Simulation - Run SWAT

- Select Setup SWAT Run.



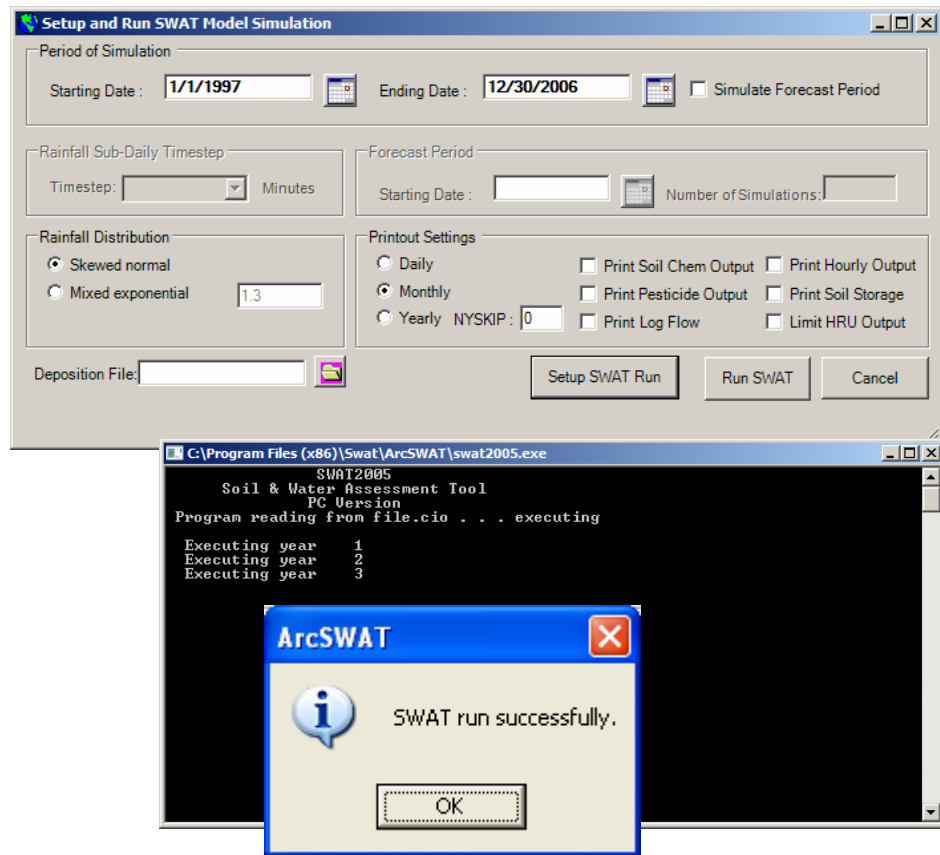
- Remove selection on Limit HRU Output.

- Click Setup SWAT Run.
- Click “Ok”

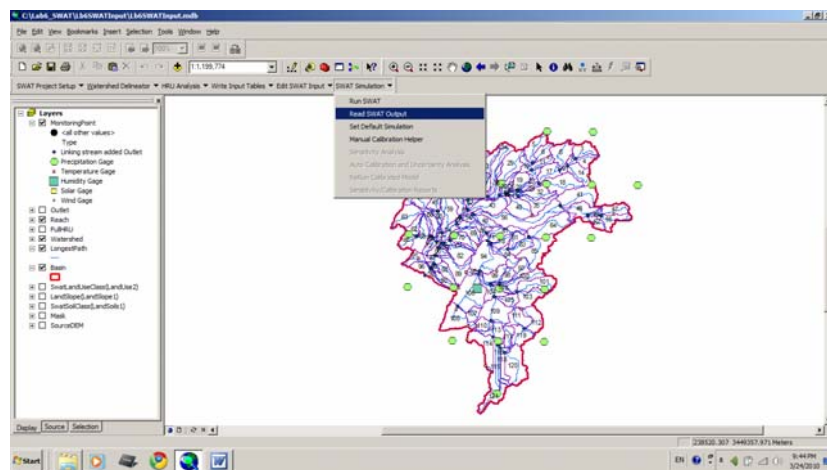


A new button will appear (Run SWAT)

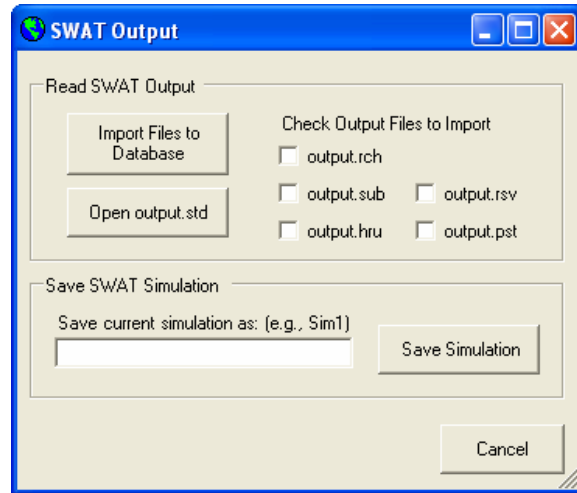
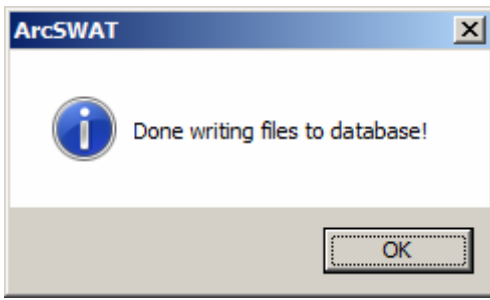
- Click “Run SWAT”.



- Read SWAT Output.

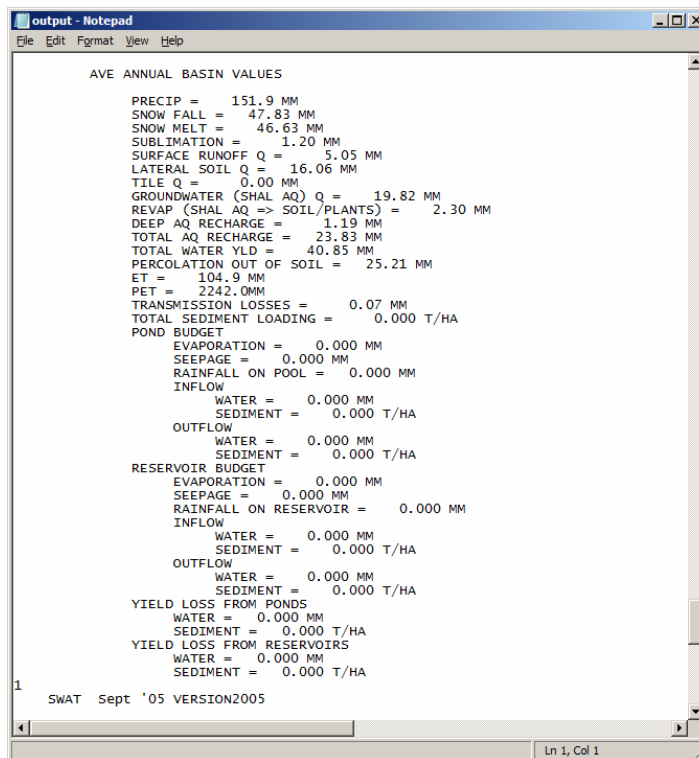


- Click on “Import Files to Database”.

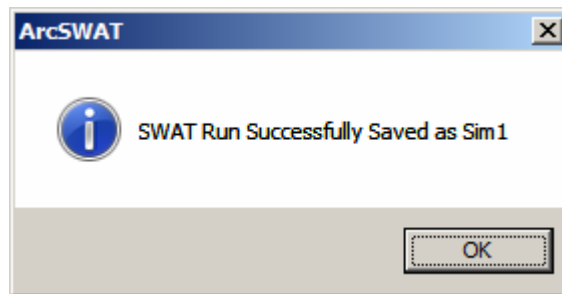
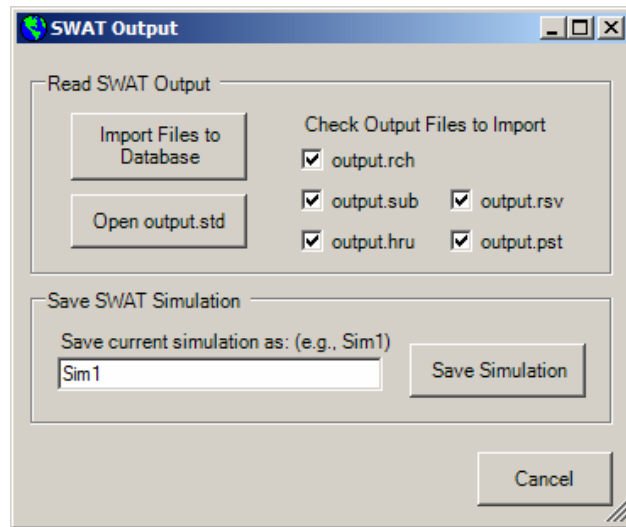


- Click on “Open output”.

These are data which you are going to work on for the calibration against discharge flow; your data may look differently, but should be close to this data.



- Select ALL parameters.
- Save your simulation
(Be consistent and save each times your simulation with increasing number.)



You may run your model many times during your model calibration.

Appendix B

Calibration of Hydrological Model

Calibration is very time consuming and you will have to run your model many times before getting the reasonable level for coefficient of determination and coefficient of efficiency. Two statistical measures, coefficient of determination (r^2) and coefficient of efficiency (E) (Nash and Sutcliffe, 1970) will be used to quantify the achieved levels of calibration and to evaluate the overall performance of the model. The coefficient of determination is obtained from the regression of the simulated values versus the observed values. The Nash-Sutcliffe coefficient of efficiency is defined by:

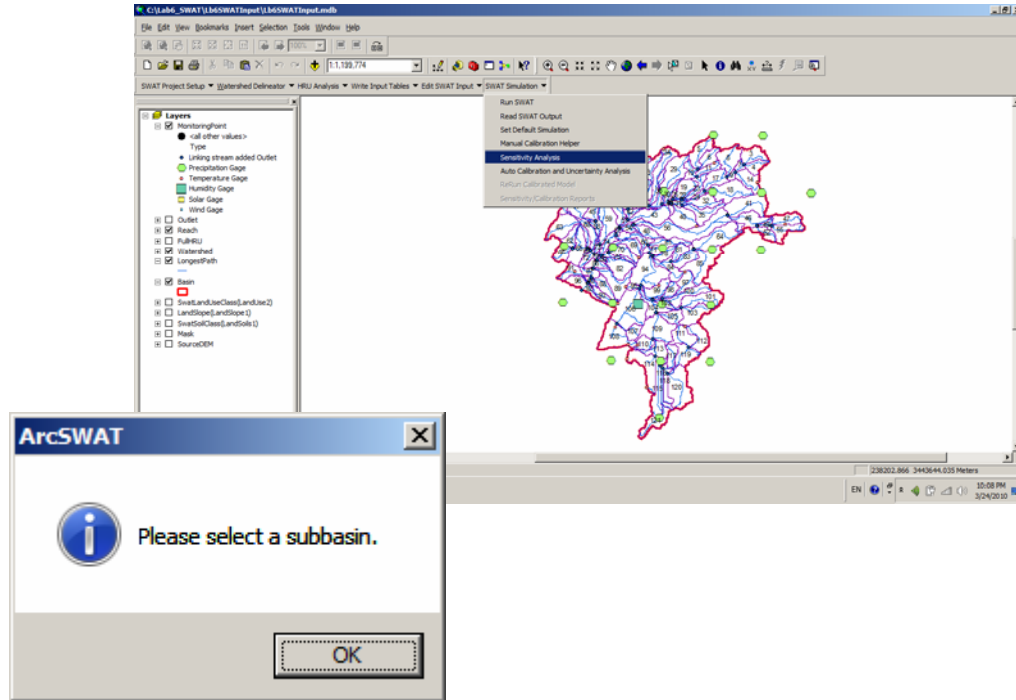
$$E = 1.0 - \frac{\sum_{i=1}^n (S_i - O_i)^2}{\sum_{i=1}^n (O_i - \bar{O})^2}$$

Where S_i and O_i are the simulated and observed monthly flows for each month i , \bar{O} is the mean of the observed monthly flows, and n is the total number of months over the simulation period.

SWAT is a semi-distributed continuous watershed simulator that computes long-term water flow over large basins using daily time steps. Major model components include: flow generation, stream routing, pond/reservoir routing, erosion/sedimentation, plant growth, nutrients, pesticides, and land management. In SWAT, a large-scale watershed can be divided into a number of subbasins, which are further subdivided into small groups called HRUs that possess unique land cover, soil, and management attributes. The water balance of each HRU is calculated through four water storage bodies: snow, soil profile, shallow aquifer, and deep aquifer. Flows generated from each HRU in a subbasin are then summed and routed through channels, ponds and/or reservoirs to the outlets of the watershed. The

detailed descriptions of formulation used in modeling hydrologic processes in HRUs/subbasins and routing can be found in SWAT tutorials.

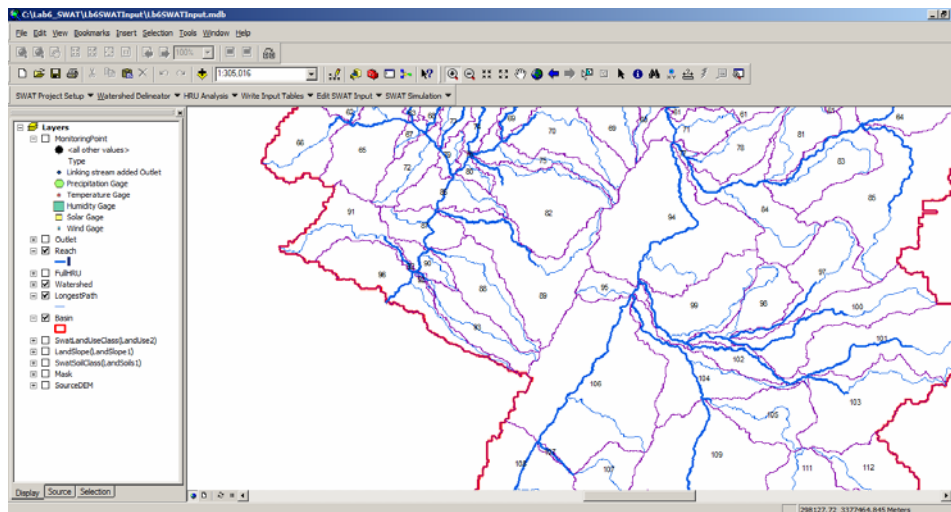
For calibration purposes you have to identify the most sensitive parameters.



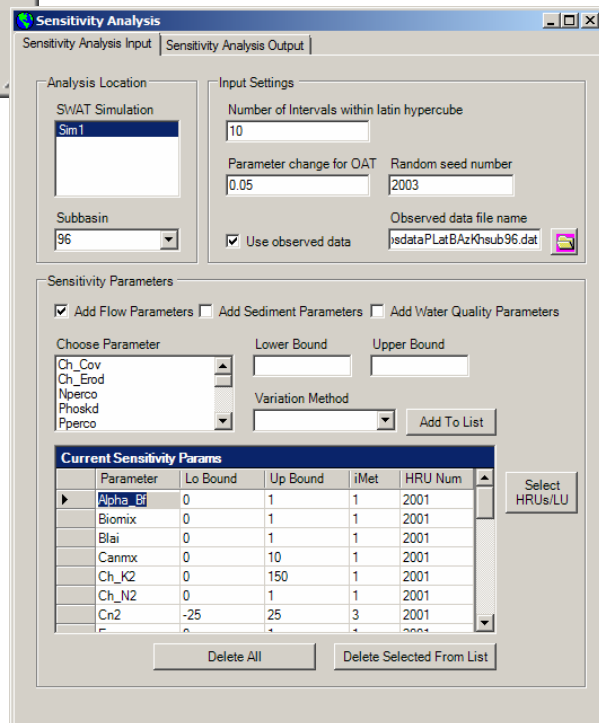
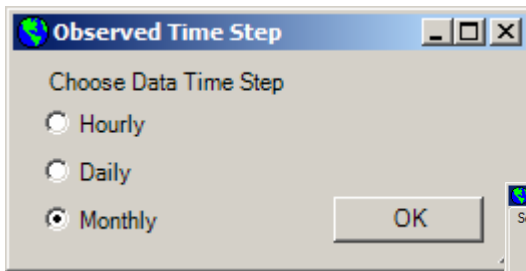
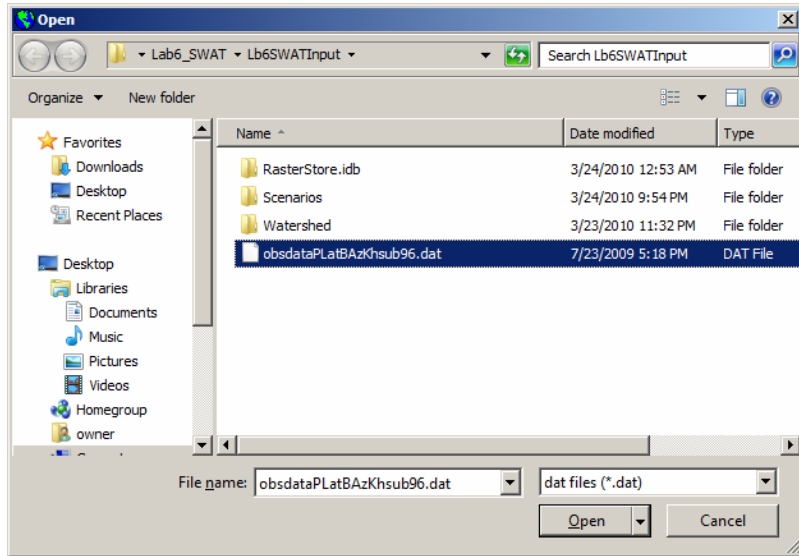
- Zoom and find out discharge outlet sub basin number

We have field discharge gauge measurement in this outlet.

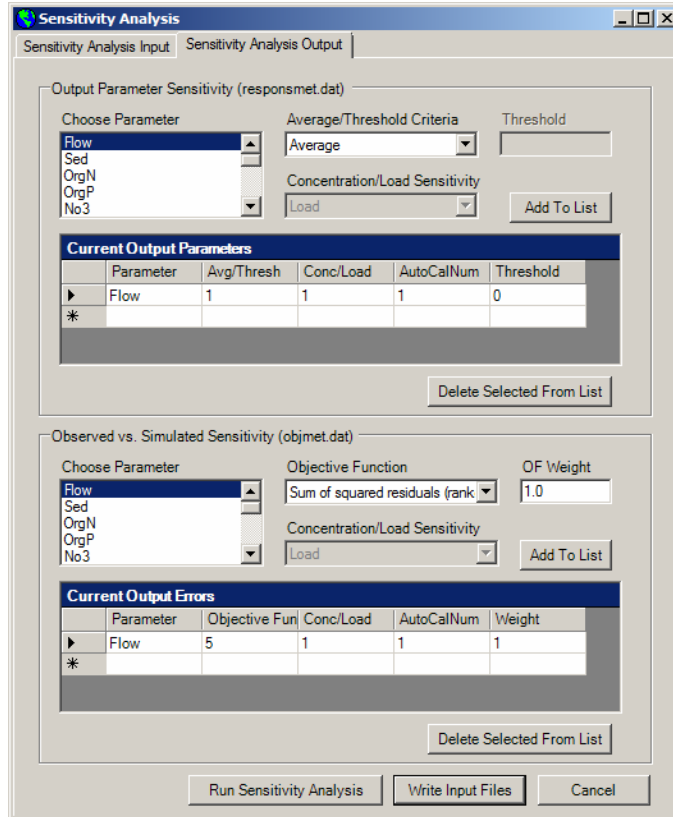
You will have to calibrate your model against this discharge gauge data.



- Make Input in Sensitivity Analysis.

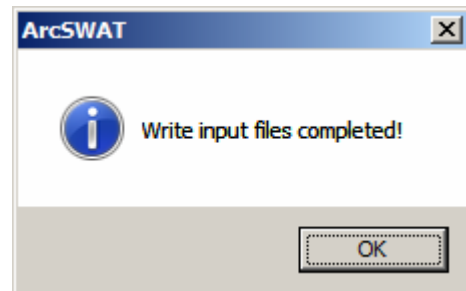


- Select Output in Sensitivity Analysis similarly that is shown on the print screen.

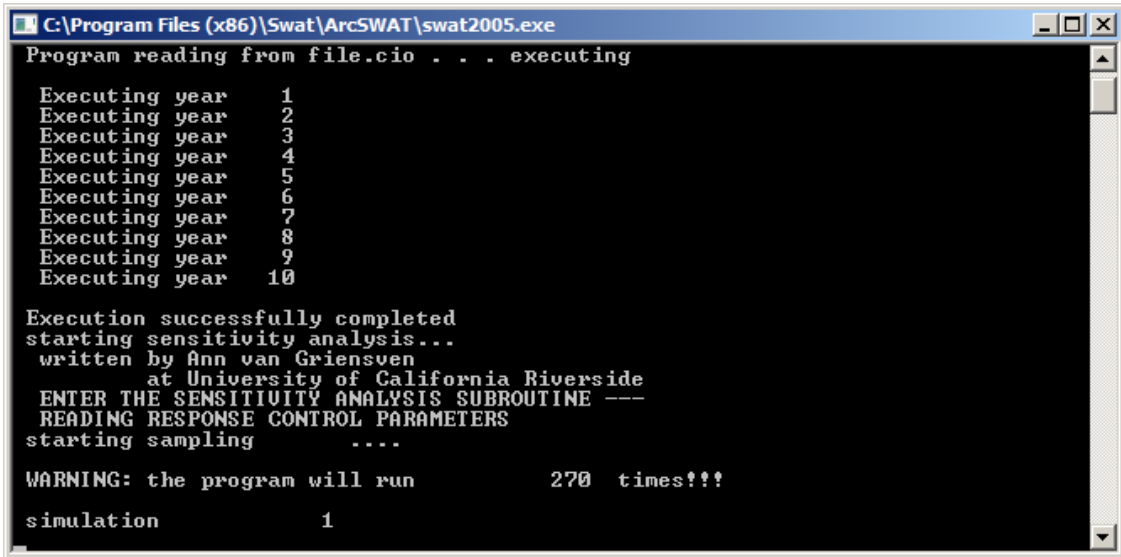


- Click on “Write Input Files”.

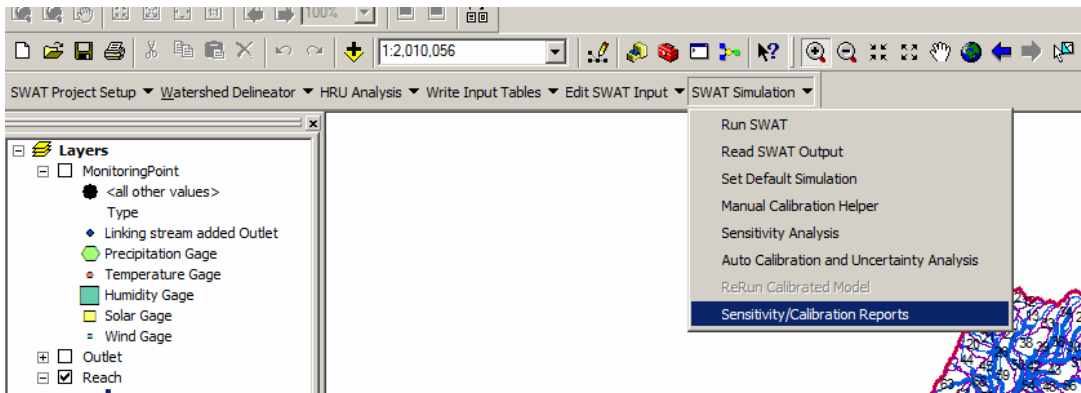
- Click on “Run Sensitivity Analysis”.



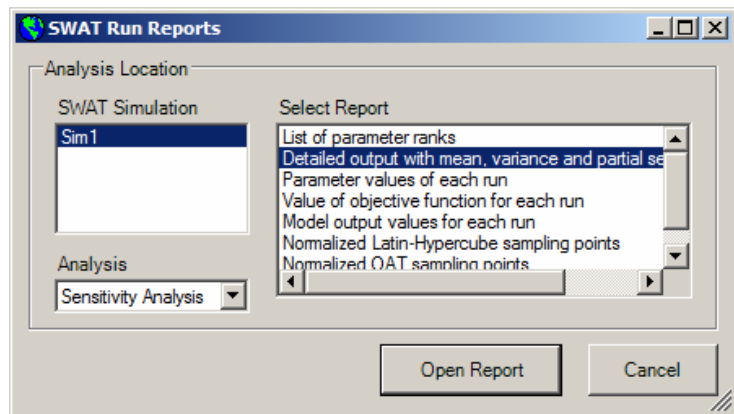
This operation may take many hours, 4-5 hours; you may keep it working overnight by itself.



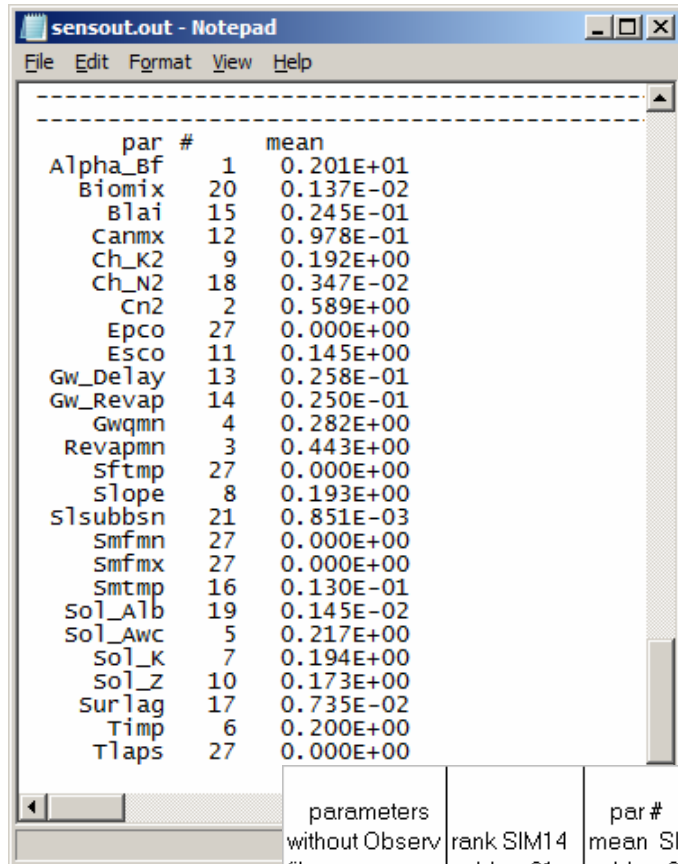
- When your long sensitivity operation is done, review results.



- Open and Review all of them.



- Prepare report of all these parameters and definitions; make table in EXCEL of these parameters.



parameters without Observ file	rank SIM14 subbas21	par # mean SIM14 subbas21
Gwqmn	1	0.204000
Alpha_Bf	2	0.107000
Esc0	3	0.098300
Sol_Z	4	0.078500
Sol_Awc	5	0.066900
Blai	6	0.066700
Timp	7	0.048100
Slope	8	0.043400
Sol_K	9	0.042200
Smtmp	10	0.026300
Ch_K2	11	0.019500
Gw_Revap	12	0.016500
Cn2	13	0.013700
Canmx	14	0.010200
Epc0	15	0.009210
Gw_Delay	16	0.003370
Ch_N2	17	0.002940
Surlag	18	0.002290
Revapmn	19	0.001880
Biomix	20	0.000997
Slsubbsn	21	0.000218
Sol_Alb	22	0.000115
Sftmp	27	0.000000
Smfmn	27	0.000000
Smfmx	27	0.000000
Tlaps	27	0.000000

Something similar should be in your table.

Appendix C

Using ACCESS and EXCEL for Data Management and Data Review

Analyze your data and review parameters, which you can modify for your model.

Based on several studies in Balochistan, Pakistan (TCI with WASA for QWSEIP in 2002-2004 years) that studied the ground water availability and productivity of the identified targeted hard rock / limestone aquifers as well as their interaction with the existing alluvial aquifer of Quetta Valley, the hydraulic conductivity ranged from 28.8 mm/hour - 540 mm/hour for alluvial aquifers and for hard rocks in the ranges 0.72 mm/hour - 72 mm/hour (TCI et al., 2004).

Your calibration parameters of hydraulic conductivities have to be in these ranges.

Your model may have different ranges of parameters compared to the following parameters.

Below is example of a hydrologic model which I developed for the NEPL.

For the karstified limestone of Chiltan, Kirthar, Dungan formations we used conductivity of 20 mm/h, that is consistent with report ranges. Alluvial (40-100 mm/h), sandstone (28 mm/h), reservoir bottom conductivities (5 and 15 mm/hour) are also in the range on the TCI studies. Therefore, the extrapolation of PLB catchments-specific parameters should provide realistic output in the reasonable allowable ranges.

Parameter ^a	SWAT Default Range (Value)	Final Value	Definition
SFTMP	(-5 - 5 (1.0) ^{a,b}	-2.0	Snowfall Temperature (°C)
SNOCOVMX	0-500 (1.0) ^b	500.0	Minimum snow water content that corresponds to 100% snow cover, SNO ₁₀₀ (mm H ₂ O)
SNO50COV	0-1 (0.5) ^a	0.5	Fraction of snow volume represented by SNOCOVMX that corresponds to 50% snow cover
TIMP	0-1 (1.0) ^a	1	Snow pack temperature lag factor
SMTMP	(-5 - 5 (0.5) ^a	3.0	Snow melt base temperature (°C)
SMFMX	0-10 (4.5) ^c	10	Melt factor for snow on June 21 (mm H ₂ O/ °C-day)
SMFMN	0-10 (4.5) ^c	0.0	Melt factor for snow on December 21 (mm H ₂ O/ °C-day)
SOL_AWC	Varies ^a	Varies (0.01-1)	Available water capacity of the soil layer (mm/mm soil)
ESCO	0-1 (0.95) ^a	0.0	Soil Evaporation Compensation Factor
GWQMN	0-5000 (0) ^a	Varies (100-600)	Threshold depth of water in the shallow aquifer required for return flow to occur (mm H ₂ O)
REVAPMN	0-500 (1.0) ^a	500	Threshold depth of water in the shallow aquifer for "revap" to occur (mm H ₂ O)
GW_REVAP	0.2-1.0 (0.2) ^a	0.02	Groundwater "revap" coefficient
GW_DELAY	0-500 (31) ^e	0	Groundwater delay time (days)
ALPHA_BF	0-1 (.048) ^f	Varies (0.048, 1)	Baseflow alpha factor (days)
RCHRG_DP	0-1 (0.05) ^a	0.05	Deep aquifer percolation fraction
CH_K1	0-150 (0.50) ^g	100.0	Effective hydraulic conductivity in tributary channel alluvium (mm/hr)
CH_K2	0-150 (0.0) ^g	0.0	Effective hydraulic conductivity in main channel alluvium (mm/hr)
CH_N1	0-0.3 (0.014) ^h	Varies (0.014)	Manning's "n" value for the tributary channels
CH_N2	0-0.3 (0.014) ^h	Varies (0.014)	Manning's "n" value for the main channel
RES_K	0-150 (0.50) ⁱ	Varies (5, 15)	Hydraulic conductivity of the reservoir bottom (mm/hr)

- Review EXCEL files; you may use these files as examples for your calibration or you may develop your system and methodology to work with these parameters.
- EXCEL File 1_In_out has several worksheets. The Sensitivity worksheets represent range of parameters in this file.
- EXCEL File Range1SW worksheet represents changes in input parameters which were used for calibration and output data.
- EXCEL File 2_out_graphs represents graphs, comparison of observed field and simulated discharge data

In your calculations use the following:

- SWAT simulated ranges of discharge rate has to be multiplied by number of days per month to get monthly discharge rate.
- The observed field data, which we are using for hydrologic modeling, are from 1998 to 2005 years, but we run the model from 1997 to 2006. The reason for it is in additional one year is necessary for the “heating” of model “engine”. At the same time the comparisons have to be for the same period of time. We compare the observed field data with simulated hydrologic data for the same period of 1998 to 2005 years.

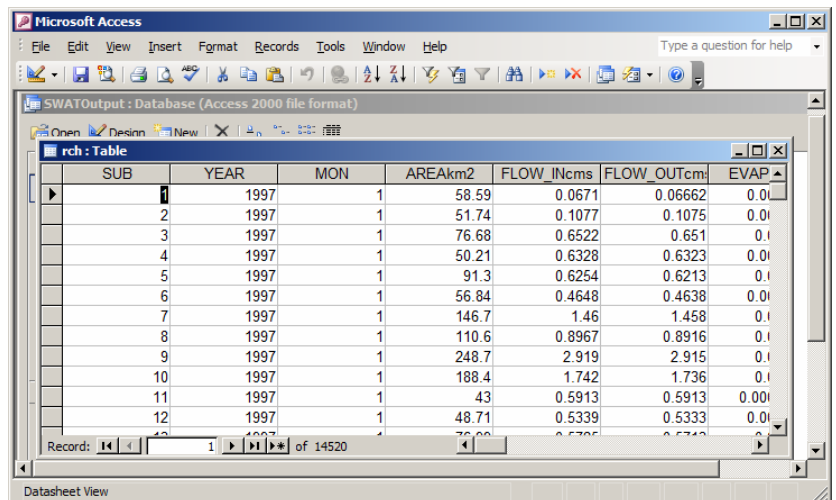
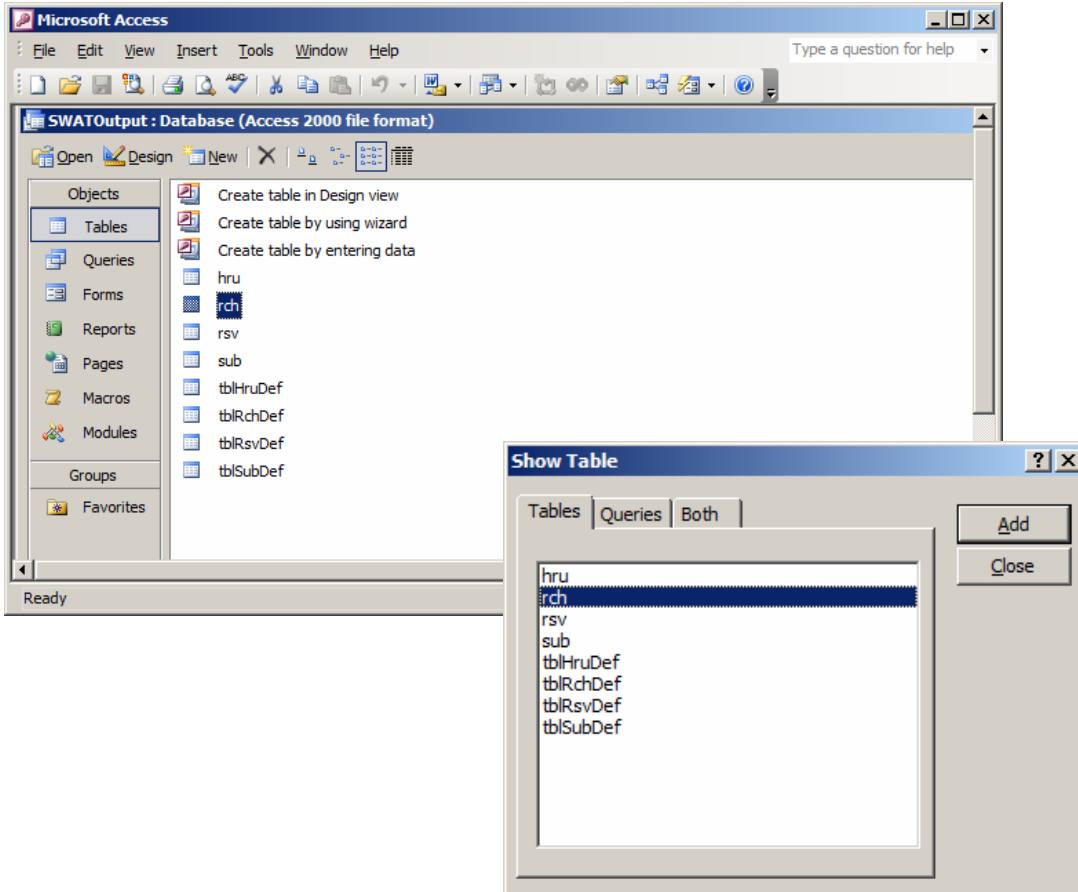
You will have to extract discharge rate data from SWAT by using ACCESS.

Open your output SWATOutput.mdb file for the simulation files, for example Sim1, by using ACCESS. This file should be in the SWAT simulated database folder \Scenarios\Sim1\TablesOut

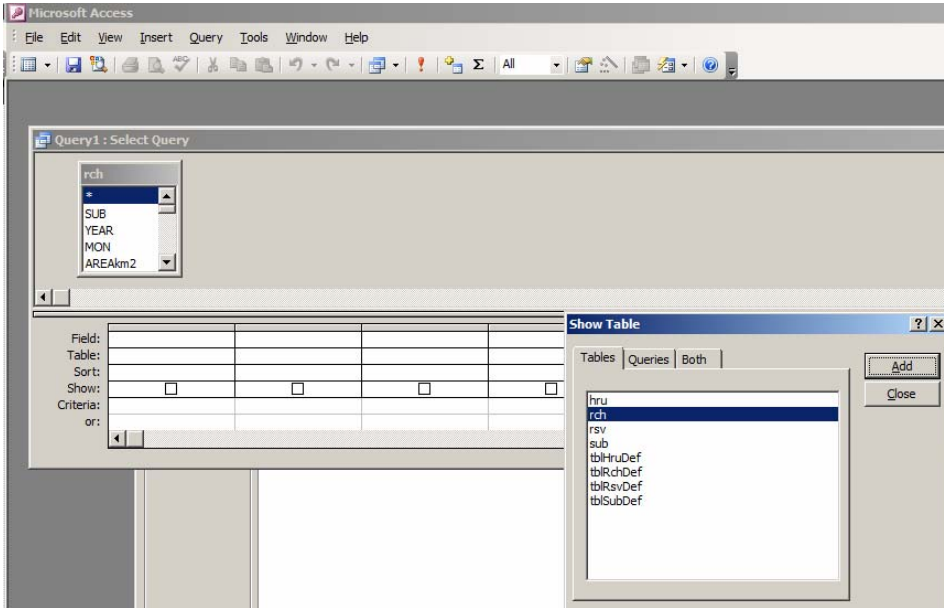
Extracted discharge rate data for the year 1998-2005 has to be put in the column Sim1, rate of file 2_out_graphs, then it will be shown in comparison with field

discharge data on graphs, with calculations of two coefficients of efficiency and determinations.

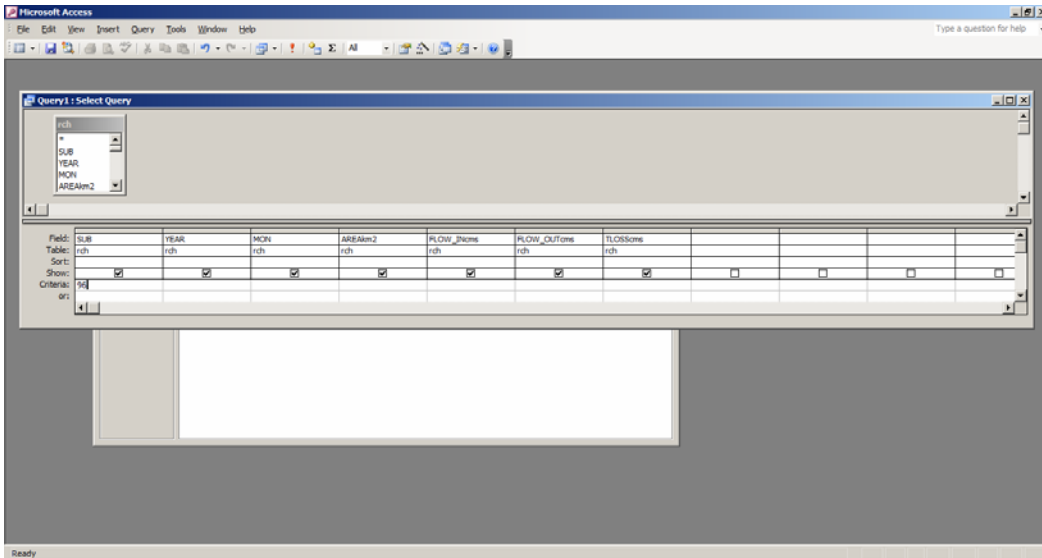
- Open in Access rch database from your file SWATOutput.mdb in folder \Scenarios\Sim1\TablesOut.
- Start Query.



- Add rch.



- Close show table.
- Fill Field columns as it shown below.



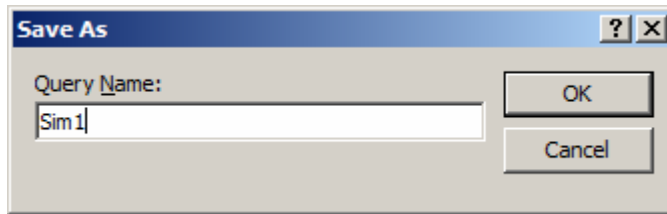
Criteria has to be with 96 (or you have to select another number which is consistent with observed field discharge sub basin, find out what is your sub basin with observed discharge from NEPL). So, you are comparing the observed field discharge with simulated modeling data.

- Click on Red exclamation mark to run query.

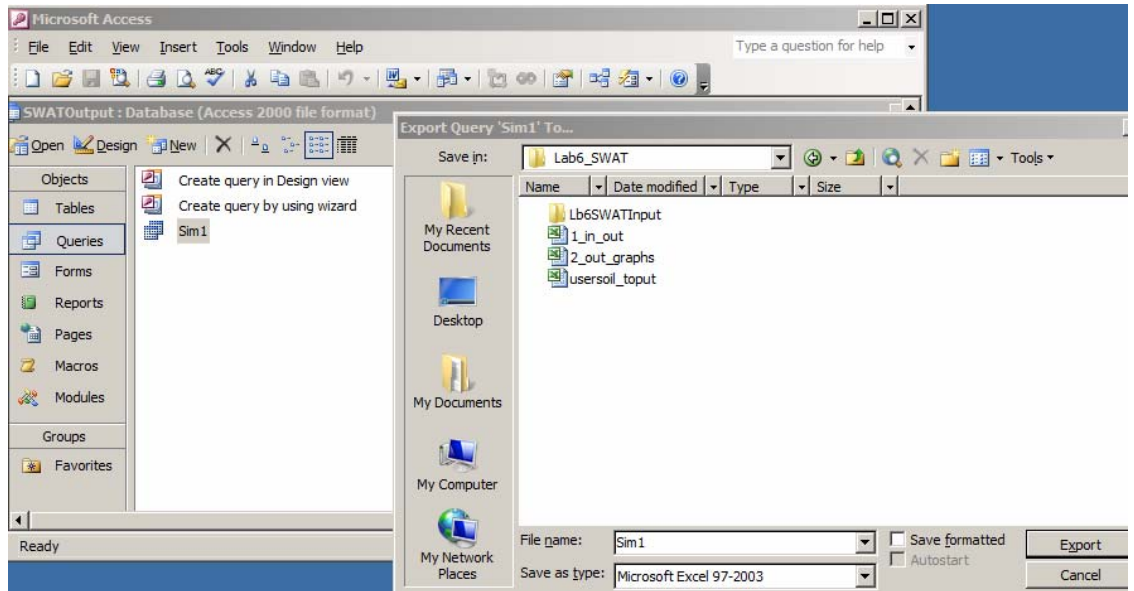
Your Query should look like this table

SUB	YEAR	MON	AREAk2	FLOW_INcms	FLOW_OUTcm	TLOSScms
96	1997	1	8470	30.87	30.82	
96	1997	2	8470	35.56	35.5	
96	1997	3	8470	35.55	35.46	
96	1997	4	8470	12.6	12.48	
96	1997	5	8470	0.7888	0.7139	
96	1997	6	8470	7.581E-07	0	
96	1997	7	8470	2.475	2.461	
96	1997	8	8470	13.52	13.37	
96	1997	9	8470	0.001528	0	
96	1997	10	8470	7.581E-07	0	
96	1997	11	8470	18.64	18.58	
96	1997	12	8470	43.13	43.07	
96	1998	1	8470	49.72	49.67	
96	1998	2	8470	39.47	39.41	
96	1998	3	8470	32.95	32.86	
96	1998	4	8470	9.128	8.99	

- Save your query.



- Export your Query in your folder in Excel format.



- Close ACCESS and open folder where you saved your EXCEL file.
- Open EXCEL file and copy FLOW_OUT data from 1998 to 2005

	A	B	C	D	E	F
1	SUB	YEAR	MON	AREAKm2	FLOW_INk	FLOW_OUTc
2	96	1997	1	8470	30.87	30.82
3	96	1997	2	8470	35.56	35.5
4	96	1997	3	8470	35.55	35.46
5	96	1997	4	8470	12.6	12.48
6	96	1997	5	8470	0.7888	0.7139
7	96	1997	6	8470	7.58E-07	0
8	96	1997	7	8470	2.475	2.461
9	96	1997	8	8470	13.52	13.37
10	96	1997	9	8470	0.001528	0
11	96	1997	10	8470	7.58E-07	0
12	96	1997	11	8470	18.64	18.58
13	96	1997	12	8470	43.13	43.07
14	96	1998	1	8470	49.72	49.67
15	96	1998	2	8470	39.47	39.41
16	96	1998	3	8470	32.95	32.86
17	96	1998	4	8470	9.128	8.99
18	96	1998	5	8470	2.481	2.405
19	96	1998	6	8470	0.4283	0.3999
20	96	1998	7	8470	1.562	1.508
21	96	1998	8	8470	0.000104	0
22	96	1998	9	8470	0.6847	0.65
23	96	1998	10	8470	7.58E-07	0
24	96	1998	11	8470	7.58E-07	0
25	96	1998	12	8470	7.58E-07	0
26	96	1999	1	8470	2.089	2.067

	A	B	C	D	E	F
86	96	2004	1	8470	0.1927	0.1706
87	96	2004	2	8470	6.298	6.235
88	96	2004	3	8470	2.72E-05	0
89	96	2004	4	8470	9.86E-05	0
90	96	2004	5	8470	0.000406	0
91	96	2004	6	8470	0.000141	0
92	96	2004	7	8470	6.57E-06	0
93	96	2004	8	8470	7.58E-07	0
94	96	2004	9	8470	7.58E-07	0
95	96	2004	10	8470	0.06262	0.0493
96	96	2004	11	8470	0.6451	0.6245
97	96	2004	12	8470	3.008	2.981
98	96	2005	1	8470	19.13	19.08
99	96	2005	2	8470	95.39	95.33
100	96	2005	3	8470	128.3	128.2
101	96	2005	4	8470	71.51	71.39
102	96	2005	5	8470	26.24	26.07
103	96	2005	6	8470	1.987	1.816
104	96	2005	7	8470	0.04412	0
105	96	2005	8	8470	0.01252	0
106	96	2005	9	8470	0.00467	0
107	96	2005	10	8470	0.001751	0
108	96	2005	11	8470	0.01401	0.003834
109	96	2005	12	8470	0.000253	0
110	96	2006	1	8470	18.82	18.77
111	96	2006	2	8470	25.03	24.97

- Open EXCEL File 1_In_out.

PARAMETER	MAX	MIN	SIMdefault	sim1, without reserv	without reserv	sim3
Alpha_Bf	1	0	0.048			1
Revapmn	500	0	1			1
Gw_Revap	0.2	0.02	0.02		0.02	
Ch_K2 (.rte)	500	-0.01	0			
Ch_K1 (SUB) transmission loss control	300	0	0.5		100	
Ch_N1	300	0	0.014			
Ch_N2	0.3	-0.01				
Sol_K	2000	0				
Slope	1	0	single slope			
Gw_Delay	50	0	31		0	
Timp (snow pack factor in .bsn)	1	0	1			
TLAPS (temp lapse rate in .sub) not is use			Temp/Elevation			
Cn2	98	35	ABCDC			
Surlag (.bsn)	20	1	4			
Sol_ZMX	3000	0				
Alluvium (Sandy Loam)						
Sandstone						
Limestone						
Igneous rock						
Shale						
Sol_Z1-Z2	3000	0				
Alluvium (Sandy Loam)						
Sandstone						
Limestone						
Igneous rock						
Shale						
Ch_N2	0.3	-0.01	0.014			
Blai						
Canmx	10	0	0			
Smtmp (snowmelt temp in .bsn)	5	0	0.5			3
Sfsubsn	150	10				
Sftmp (snowfall temp-re) in .bsn	5	-5	1			-2
Sol_Alb						
Smfmn (melt factor in December) in .bsn	10	0	4.5			0
Smfmx (melt factor in June) in .bsn	10	0	4.5			10
Esco (Evapor factor, .bsu .hru)	1	0	0.95			1
Tlaps	50	0				
Temperature table						
Sol_Avc	1	0	0.05			
SNOCVMX	500	0	1			500
SN05COV	1	0	0.5			0.5

- Review these parameters.

You may change these parameters to calibrate your model.

Your parameters have to be in the required ranges. All physical soil parameters have to be in the range of specific soil type and based on the previous findings by researchers. Review *Handbook of Hydrology* by David R. Maidment and SWAT tutorials to get more data.